

OPTIMAL ATTITUDE STABILIZATION AND CONTROL OF SPACECRAFT BY SOLAR RADIATION PRESSURE

By

RAPUR VENKATACHALAM

ME
1980 TH
D ME/1980/D
VEN
OPT



DEPARTMENT OF MECHANICAL ENGINEERING

INDIAN INSTITUTE OF TECHNOLOGY, KANPUR

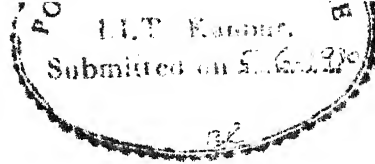
MAY, 1980

OPTIMAL ATTITUDE STABILIZATION AND CONTROL OF SPACECRAFT BY SOLAR RADIATION PRESSURE

**A Thesis Submitted
In Partial Fulfilment of the Requirements
for the Degree of
DOCTOR OF PHILOSOPHY**

**By
RAPUR VENKATACHALAM**

**to the
DEPARTMENT OF MECHANICAL ENGINEERING
INDIAN INSTITUTE OF TECHNOLOGY, KANPUR
MAY, 1980**



i

CERTIFICATE

This is to certify that, the thesis entitled "Optimal Attitude Stabilization and Control of Spacecraft by Solar Radiation Pressure" by Mr. R. Venkatachalam is a record of work carried out under my supervision and has not been submitted elsewhere for a degree.

A handwritten signature in cursive script, appearing to read "K. C. Pande", with a horizontal line underneath.

Dr. K.C. Pande
Assistant Professor
Department of Mechanical Engineering
I.I.T. Kanpur-16.

ACKNOWLEDGEMENT

I wish to express my profound gratitude to Dr. K.C. Pande who introduced me to this field, and provided me with constant inspiration and guidance during the preparation of the thesis. I am greatly indebted to him for the invaluable encouragement and help given throughout my course of study. My association with him has been fruitful as well as memorable.

I also wish to thank my friends, Mr. K.S. Ramakrishna and Mr. N. Gopinath, who helped me in proof-reading the thesis.

The investigation reported in the thesis was supported, in part, by the Indian Space Research Organization; Project No. ISRO/ME(KCP)/77-81/21.

R. VENKATACHALAM

C. KANPUR
AL LIBRARY

A 65900

PR 1981

ME-1980-D-VEN-OPT

SYNOPSIS

OPTIMAL ATTITUDE STABILIZATION AND CONTROL OF SPACECRAFT BY
SOLAR RADIATION PRESSURE

A Thesis Submitted
In Partial Fulfilment of the Requirements
for the Degree of
DOCTOR OF PHILOSOPHY

by

Rapur Venkatachalam

to the
Department of Mechanical Engineering
Indian Institute of Technology, Kanpur
May, 1980

Attitude control of high altitude spacecraft by means of solar radiation pressure is investigated. The objective is to develop solar pressure attitude control systems that are mechanically simple to implement and yet offer desirable control characteristics. A solar controller consisting of two highly reflective lightweight control surfaces rotatable about body-fixed axes is proposed for a variety of spacecraft missions. Such a configuration represents the minimum hardware implementation as at least two control surfaces are required to achieve the solar torque reversals. Spacecraft missions demanding earth-pointing attitude, inertially-fixed orientation and large-angle attitude maneuvers in presence of gravity-gradient torques are considered. Control laws directly governing the rotations of the two control surfaces are synthesized to meet the mission requirements and their validity is established for all times of the year.

The problem of stabilizing the pitch attitude of an unsymmetrical earth-pointing spacecraft is formulated first. Although the pitch dynamics is relatively simple, the solar radiation torque generated by the controller turns out to be a rather complicated transcendental function of the pitch attitude, control surface rotations and the time. To make the control synthesis mathematically tractable, linearization of the governing nonlinear equation of motion for small amplitude pitch motion and control surface excursions is undertaken. A piecewise linear feedback control law with constant gains is proposed for the differential rotation of the control surfaces. The system stability as a function of the attitude error and rate gains is established using Floquet theory. The approach is next extended to examine the potential of the controller in achieving three-axis stabilization of unsymmetrical earth-pointing spacecraft. Optimal control theory is employed to synthesize a feedback control law with periodic time-varying gains for the differential control surface rotation leading to an asymptotically stable system. Suboptimal control strategies involving gain scheduling a few times per year are suggested which lead to considerable reduction of the associated computational requirements.

Applications of the two-surface solar controller for missions demanding stabilization along arbitrary inertially-fixed

attitudes are considered next. The inertial pointing problems are characterized by the need to provide nominal controls countering the time-varying gravity gradient disturbances. For pitch stabilization, both the nominal and feedback control laws governing the differential control surface rotation are synthesized analytically. The stability properties of the system are shown, through certain transformations, to be governed by the classical Mathieu equation. The investigation is then extended to the problem of imparting inertially-fixed orientations to the symmetry axis of an axisymmetric spacecraft. For this more complex problem, a numerical approach is followed. Nominal control laws for the individual control surface rotations are developed and the governing equations of motion linearized in the neighbourhood of the desired inertial attitude. Minimization of a quadratic performance index then results in an optimal feedback control law for the differential control surface rotation assuring asymptotic stability for the system. Suboptimal control policies promising computational reductions during system implementation are explored.

Finally, the feasibility of achieving large-angle attitude maneuvers of the spacecraft symmetry axis is investigated. The attitude transitions being unrestricted, the full nonlinear equations of motion in the gravity-gradient field are treated for the synthesis. The problem is formulated as a minimum time

transfer problem with terminal state constraints. A gradient procedure is developed to determine the optimal open-loop strategy governing the differential control surface rotation for the specified maneuver. The transfer strategy is then coupled with the appropriate nominal and feedback control policies required for stabilization along the inertially-fixed terminal orientation.

The control system performance is analyzed through simulations of the complete nonlinear equations of motion in both earth-pointing as well as inertially-fixed modes of stabilization. The loss of solar control during the earth's shadow passage by the spacecraft is also modelled. Disturbances representing micrometeorite impacts and initial attitude misalignments are introduced. The results indicate a moderately sized controller to be capable of achieving control times of the order of a fraction of an orbit.

The thesis establishes the effectiveness of a mechanically simple two-surface solar pressure control system in stabilizing the spacecraft along earth-pointing as well as inertially-fixed attitudes. The analysis demonstrates the capability of the controller in stabilizing the spacecraft even along gravitationally unstable equilibria. Its ability to achieve stabilization along arbitrary inertially-fixed orientations opens new vistas for the concept of solar

pressure attitude control. The feasibility of accomplishing large-angle attitude maneuvers adds versatility to the concept, enabling the spacecraft to undertake diverse missions. The approach is semipassive in character as no mass expulsion schemes are involved and only a small power consumption is envisaged to rotate the control surfaces. This promises a long operational life-span for the spacecraft.

TABLE OF CONTENTS

Chapter		Page
1.	INTRODUCTION	1
	1.1 Preliminary Remarks	1
	1.2 Literature Review	3
	1.3 Purpose and Scope of the Investigation	8
2.	PITCH ATTITUDE STABILIZATION OF EARTH-POINTING SPACECRAFT	13
	2.1 Problem Formulation	13
	2.2 Control Synthesis	19
	2.3 System Stability and Performance	22
	2.4 Concluding Remarks	29
3.	THREE-AXIS ATTITUDE STABILIZATION OF EARTH-POINTING SPACECRAFT	31
	3.1 Formulation of the Problem	32
	3.2 Control Synthesis	38
	3.3 Computational Procedure	42
	3.4 Results and Discussion	45
	3.5 Concluding Remarks	53

Chapter		Page
4.	PITCH STABILIZATION OF SPACECRAFT IN AN INERTIALLY-FIXED ATTITUDE	55
	4.1 Problem Formulation and Control Synthesis	56
	4.2 Stability Analysis	64
	4.3 System Performance	70
	4.4 Concluding Remarks	74
5.	STABILIZATION OF SPACECRAFT SYMMETRY AXIS ALONG AN INERTIALLY-FIXED ATTITUDE	75
	5.1 Formulation of the Problem	75
	5.2 Control Synthesis	82
	5.3 Computational Procedure	85
	5.4 Results and Discussion	88
	5.5 Concluding Remarks	101
6.	LARGE-ANGLE ATTITUDE MANEUVERS OF SPACECRAFT SYMMETRY AXIS	102
	6.1 Problem Formulation and Control Synthesis	102
	6.2 Gradient Technique	107
	6.3 Computational Procedure :	112
	6.4 Results and Discussion	113
	6.5 Concluding Remarks	123

Chapter	Page
7. CLOSING COMMENTS	124
7.1 Summary of the Conclusions	124
7.2 Recommendations for Future Work	126
BIBLIOGRAPHY	128
APPENDIX A	132
APPENDIX B	135
APPENDIX C	137

LIST OF FIGURES

Figure		Page
1.1	Plan of study	12
2.1	Geometry of orbital and attitude motion	14
2.2	Radiation forces acting on control plate P_i	16
2.3	Stability charts for a dumbbell satellite nominally oriented along the (a) local vertical (b) local horizontal	24
2.4	Attitude responses and control histories with gains $\mu = 0.1$ and $\nu = 1.0$	27
2.5	Attitude responses and control histories with gains $\mu = 1.0$ and $\nu = 1.0$	28
3.1	(a) Geometry of orbital motion (b) Geometry of attitude motion	33
3.2	Solar controller configuration	34
3.3	Roll, yaw and pitch attitude gains for different values of ϕ	46
3.4	Roll, yaw and pitch attitude rate gains for different values of ϕ	47
3.5	Attitude response and control history subsequent to initial position disturbance, $\phi = 45^\circ, 90^\circ$	49
3.6	Attitude response and control history subsequent to initial impulsive disturbance, $\phi = 45^\circ, 90^\circ$	50
3.7	Attitude response and control history subsequent to initial impulsive disturbance, $\phi = 0$	51
4.1	Geometry of orbital and attitude motion	57

Figure

Page

4.2	(a) Variation of optimal δ_e and $ D $ with ζ (b) Typical comparison of the approximate and exact nominal control $\delta_o(\theta)$	61
4.3	Stability charts for (a) $q = 0.3$ (b) 0.6	68
4.4	(a) Stability chart for $q = 1.5$ (b) Stability chart for $q = 3.0$ showing the rectangular bound on the representative point for $i = 23.5^\circ$, $C = 5$, $\mu = 0.25$, $v = 0.6$	69
4.5	Typical system response (a) $K = 0.5$, (b) $K = 1.0$	73
5.1	(a) Geometry of orbital motion (b) Geometry of attitude motion	76
5.2	Solar controller configuration	78
5.3	Typical system gain histories for $\phi = 0$ and 45° ($\alpha_{1e} = 30^\circ$, $\alpha_{2e} = 20^\circ$)	89
5.4	Typical system gain histories for $\phi = 90^\circ$ and 135° ($\alpha_{1e} = 30^\circ$, $\alpha_{2e} = 20^\circ$)	90
5.5	Attitude responses and control histories for stabilization along $\alpha_{1e} = 30^\circ$, $\alpha_{2e} = 20^\circ$ ($\phi = 45^\circ$)	91
5.6	Attitude responses and control histories for stabilization along $\alpha_{1e} = 30^\circ$, $\alpha_{2e} = 20^\circ$ ($\phi = 90^\circ$)	92
5.7	Attitude responses and control histories for stabilization along $\alpha_{1e} = 30^\circ$, $\alpha_{2e} = 20^\circ$ ($\phi = 135^\circ$)	93
5.8	Attitude responses and control histories for stabilization along $\alpha_{1e} = -30^\circ$, $\alpha_{2e} = 50^\circ$ ($\phi = 45^\circ$)	94

Figure		Page
5.9	Attitude responses and control histories for stabilization along $\alpha_{1e} = 30^\circ$, $\alpha_{2e} = 20^\circ$, showing the earth's shadow effect ($\phi = 0$)	96
5.10	Suboptimal system response for $\phi = 30^\circ$ obtained using feedback gains corresponding to $\phi = 45^\circ$	98
5.11	Suboptimal system response for $\phi = 60^\circ$ obtained using feedback gains corresponding to $\phi = 45^\circ$	99
5.12	Suboptimal system response for $\phi = 90^\circ$ obtained using feedback gains corresponding to $\phi = 45^\circ$	100
6.1	Typical convergence to the optimal solution for the maneuver $\alpha_{10} = -10^\circ$, $\alpha_{20} = -10^\circ$ to $\alpha_{1f} = 25^\circ$, $\alpha_{2f} = 30^\circ$	115
6.2	Optimal trajectories and control histories obtained with different ramp type guesses for the control	116
6.3	Optimal trajectory and control history obtained with the initial guess $u_0(\theta) = 0$	118
6.4	Optimal trajectories and control histories obtained with different initial guesses for the final time	119
6.5	System response and control required for large-angle maneuver followed by inertially-fixed attitude stabilization	121
6.6	System response and control required for large-angle maneuver followed by inertially-fixed attitude stabilization	122
C-1	Geometry of the earth's shadow	138

LIST OF SYMBOLS

A, ϵ	control surfaces area and moment arm, respectively
C	solar parameter
\tilde{C}	$2 \rho p A \epsilon / \Omega^2$, Equation (3.12)
F	feedback gain matrix
F_j	elements of F (Chapter 3) $j = \gamma, \gamma', \beta, \beta', \lambda, \lambda'$
F_k	elements of F (Chapter 5) $k = \alpha_1, \alpha_1', \alpha_2, \alpha_2'$
\bar{F}_i	solar force acting on the control surface P_i , $i = 1, 2$
$\bar{I}, \bar{J}, \bar{K}$	unit vectors along X, Y, Z axes, respectively
I	inertia parameter, I_x/I_y (Chapters 5 and 6)
I_x, I_y, I_z	principal moments of inertia of the spacecraft
K	inertia parameter, $(I_z - I_y)/I_x$ (Chapters 2 and 4)
K_1, K_2	satellite shape parameters, $K_1 = (I_z - I_x)/I_y$ and $K_2 = (I_x - I_y)/I_z$
N	ascending node
NN'	line of nodes
O	center of the earth
P_i	control surface, $i = 1, 2$
R	radius of circular orbit
R_E	radius of the earth
S	satellite center of mass
X, Y, Z	inertial coordinate system with X along the orbit normal and YZ defining the orbit plane

\bar{e}	unit vector along the earth-sun line, $e_x \bar{i} + e_y \bar{j} + e_z \bar{k}$
i	orbit inclination from the ecliptic plane
$\bar{i}, \bar{j}, \bar{k}$	unit vectors along spacecraft principal axes x, y, z , respectively
\bar{n}_i	unit normal to the control surface P_i , $i = 1, 2$
p	solar radiation pressure, $4.65 \times 10^{-6} \text{ N/m}^2$
q	parameter defined in Equation (4.17c)
r_x, r_y, r_z	components of unit vector along the local vertical
\bar{s}_i	unit vector along the direction of reflection
t	time
$u(\theta)$	control variable
$u_0(\theta)$	initial guess for open-loop control
$u_{\text{opt}}(\theta)$	optimal open loop control
$\bar{x}(\theta)$	state vector
x, y, z	principal axes of the satellite
x_i, y_i, z_i	coordinates parallel to X, Y, Z , respectively, with its origin at S
x'_i, y'_i, z'_i	intermediate coordinate system (Chapter 5)
x_0, y_0, z_0	rotating orbital coordinate system with y_0 along local vertical, z_0 tangent to the orbit and x_0 perpendicular to the orbit plane
$x_1, y_1, z_1;$ x_2, y_2, z_2	intermediate coordinate systems (Chapter 3)
Ψ	angle between \bar{e} and \bar{R} (Appendix C)
Ω	orbital angular velocity

α	pitch attitude angle measured from the line of nodes
α_e	desired inertially-fixed pitch attitude
$\tilde{\alpha}$	pitch attitude deviation from the desired orientation, $\alpha - \alpha_e$
α_1, α_2	attitude angles defining the symmetry axis orientation relative to the inertial reference frame
α_{1e}, α_{2e}	desired inertial orientation of the symmetry axis (Chapter 5)
$\tilde{\alpha}_1, \tilde{\alpha}_2$	deviations from the desired orientation, $(\alpha_1 - \alpha_{1e}), (\alpha_2 - \alpha_{2e})$, respectively
α_{10}, α_{20}	initial specified symmetry axis orientation
α_{1f}, α_{2f}	final desired inertial orientation of symmetry axis (Chapter 6)
γ, β, λ	roll, yaw and pitch attitude angles of earth-oriented spacecraft, respectively
δ_i	rotation of the control surface P_i , $i = 1, 2$
δ_e	'off' position of control surfaces
$\tilde{\delta}_i$	rotation of control surface P_i about the 'off' position δ_e , $(\delta_i - \delta_e)$, $i = 1, 2$
$\tilde{\delta}$	equal and opposite rotations of control surfaces about δ_e , $\tilde{\delta} = \tilde{\delta}_1 = -\tilde{\delta}_2$
δ_o, δ_{io}	nominal controls, $i = 1, 2$
$\zeta(\phi)$	$- \arctan (\tan \phi \cos i) \quad (\text{Chapter 2})$ $- \arctan (\tan \phi \cos i) + \lambda_p \quad (\text{Chapter 3})$ $- \arctan (\tan \phi \cos i) + \alpha_e \quad (\text{Chapter 4})$ <p>with the arctan function lying in the same quadrant as ϕ</p>
η	$\theta + \zeta$

θ	orbital angle
θ_f	final time
$(\theta_f)_0$	initial guess for θ_f
$(\theta_f)_{opt}$	optimal θ_f
λ_p	location of the control surface rotation axis from the y-axis (Chapter 3)
$\bar{\lambda}, \bar{p}, \bar{R}_i, \bar{v}$	Lagrange multiplier vectors
μ, v	feedback gains
$\tilde{\mu}, \tilde{v}$	$2C \sigma \mu$ and $2C \sigma v$ (Chapter 2)
	$2C \sigma D \mu$ and $2C \sigma D v$ (Chapter 4)
μ_E	power of the earth as a center of force
ξ_i	angle of incidence, $i = 1, 2$
ρ	reflectivity of the control surfaces
$\sigma(\phi)$	$1 - \sin^2 \phi \sin^2 i$
τ	time constant, transmissibility of control surfaces
ϕ	solar aspect angle
$\phi(\bar{x}(\theta_f), \theta_f)$	measure of terminal error
$\bar{\psi}$	constraints on final states
ψ_i	components of $\bar{\psi}$, $i = 1, 2, 3, 4$
(\cdot)	d/dt
$(\cdot)'$	$d/d\theta$
k_0, k'_0	initial conditions, $k = \tilde{\alpha}, \tilde{\alpha}_1, \tilde{\alpha}_2, \gamma, \beta, \lambda$

1. INTRODUCTION

1.1 Preliminary Remarks

The general motion of a space vehicle consists of the translation of its center of mass and the rotational motion about the center of mass. The former describes the orbital motion of the vehicle and the latter is referred to as its attitude motion.

The attitude dynamics of a satellite is subject to a variety of environmental influences. These are : the gravity-gradient effect, the earth's magnetic field, aerodynamic forces, radiation pressure due to the earth's radiation and albedo at low altitudes (< 800 km), and direct solar radiation pressure at high altitudes. Attitude motion may also be excited due to encounters with micrometeorites. On the other hand, successful operation of a vast majority of space missions demands that the spacecraft maintain a preferred orientation in space. For example, communications, weather, military, earth-resources applications, etc., require the spacecraft to continually point towards the earth. Missions involving scientific and astronomical observations may demand the satellite to maintain an inertially-fixed pointing. The capability to accomplish attitude maneuvers between any two specified spatial orientations may also be desired in certain applications. An effective attitude control system is hence necessary to achieve the mission objectives.

1. INTRODUCTION

1.1 Preliminary Remarks

The general motion of a space vehicle consists of the translation of its center of mass and the rotational motion about the center of mass. The former describes the orbital motion of the vehicle and the latter is referred to as its attitude motion.

The attitude dynamics of a satellite is subject to a variety of environmental influences. These are : the gravity-gradient effect, the earth's magnetic field, aerodynamic forces, radiation pressure due to the earth's radiation and albedo at low altitudes (< 800 km), and direct solar radiation pressure at high altitudes. Attitude motion may also be excited due to encounters with micrometeorites. On the other hand, successful operation of a vast majority of space missions demands that the spacecraft maintain a preferred orientation in space. For example, communications, weather, military, earth-resources applications, etc., require the spacecraft to continually point towards the earth. Missions involving scientific and astronomical observations may demand the satellite to maintain an inertially-fixed pointing. The capability to accomplish attitude maneuvers between any two specified spatial orientations may also be desired in certain applications. An effective attitude control system is hence necessary to achieve the mission objectives.

Several methods are available for attitude control which involve the use of active control elements, spin-stabilization technique and the utilization of environmental forces. Active stabilization procedures involve mass expulsion schemes and/or components requiring a large amount of energy which is an expensive commodity aboard a spacecraft. The advantage of the technique lies in the ability to achieve any orientation with a very high degree of accuracy. However, the large energy consumption leads to a reduced operational life-time for the satellite. Spin-stabilization relies on the inherent tendency of a spinning body to maintain a fixed attitude in torque-free space. The method does not involve any energy consumption. Its pointing accuracy, however, is limited as it deteriorates due to the effect of external disturbances. Combinations of the active methods and spin-stabilization are commonly employed in the form of momentum bias or dual-spin configurations.

Methods of attitude control based on the utilization of the environmental forces are either completely passive or involve very small energy consumption. The gravity-gradient stabilization technique is based on designing the satellite mass distribution such that the earth-pointing orientation of the satellite represents a stable configuration in the gravity-gradient field. Although the procedure involves no energy consumption, low pointing accuracy and very slow rates of

attitude correction are achieved. The exploitation of the aerodynamic forces, the earth's magnetic field and solar radiation pressure involve the introduction of suitable control elements which may be operated with very little electrical power to generate attitude control torques. For example, movable aerodynamic surfaces may be employed at low altitudes to intercept the relative free-molecular flow. Onboard electromagnets are used to generate control torques through interaction with the earth's magnetic field over a range of orbital altitudes. For high altitude spacecraft, control surfaces are employed to intercept the incident solar radiation to develop control moments about the satellite center of mass. These methods promise high pointing accuracies with an increased operational life-span for the spacecraft.

This thesis deals with the utilization of solar radiation pressure for the attitude control of high altitude spacecraft. The development and analysis of solar pressure attitude control systems for a variety of spacecraft missions forms the main objective of the work.

1.2 Literature Review

Most of the early researches in the utilization of solar radiation pressure for attitude control relate to the problem of maintaining a sun-pointing spacecraft attitude. Sohn¹ (1959) considered solar pressure attitude control of an interplanetary

spacecraft using a weathervane type tail surface. This enables the spacecraft to maintain a nominally fixed orientation relative to the satellite-sun line. The author also mentioned the idea of including rate sensors for solar damping of undesirable oscillations about the nominal orientation. Frye and Stearns² (1959) presented a general survey concerning the utilization of gravity-gradient, aerodynamic and solar radiation torques for attitude stabilization and also provided a brief description of sensors and control devices. The authors proposed a trailing cone system to intercept the direct solar radiation to derive control torques tending to align the cone axis with the sun-line. The concept of introducing small servo driven solar control surfaces, called 'Solarons', to achieve attitude damping was also mentioned. Newton³ (1960) suggested the possibility of generating corrective radiation torques by designing spherical satellites with one-half of the surface having reflective properties and the other half absorptive properties. With the reflecting half nominally facing the sun, a stabilizing radiation torque is achieved. Hibbard⁴ (1961) proposed a reflector-collector configuration for providing focussed radiation pressure with a view to achieve onboard weight savings. Merrick et al.^{5,6} (1966, 68) considered the damping of attitude oscillations by providing relative motion between a pair of connected bodies. Acord and Nicklas⁷ (1964) evolved a passive stabilizer capable of providing attitude damping

through a thermo-mechanical phase lag arrangement.

The problem of aligning the spin-axis of a spinning spacecraft towards the sun was investigated by Ule⁸ (1963). The author suggested the use of windmill type mirror-arrays and corner mirror-arrays for producing restoring precession torques. A mechanism for spin rate control involving a pair of flat surfaces with one side reflective and the other side absorbent was proposed. The angle of attack of the spin rate control surfaces could be governed either by remote control or by centrifugal forces. A passive solar damping approach where a structural element provides a phase shift between the solar restoring torque and attitude motion was suggested by Carrel and Limburg⁹ (1965). Further development of various mechanisms along similar lines was done by Peterson¹⁰ (1966), Colombo¹¹ (1966) and Harrington¹² (1966). The use of a grated solar sail for attitude control of sun-pointing spinning spacecraft was studied by Falcovitz¹³ (1966). For the same problem, Crocker¹⁴ (1970) proposed two body mounted differentially coated solar surfaces for precession control and a pair of spring mounted solar paddles for spin rate control. Pande¹⁵ (1976) considered semipassive spin-axis orientation control by means of two rotatable control surfaces. The concept enables the spin-axis to attain any arbitrary pointing in space.

The above mentioned studies represent rather simplified situations as a torque-free environment is assumed throughout.

Solar pressure attitude control of satellites under more realistic dynamic conditions was examined by Mallach¹⁶ (1966). The author suggested the possibility of achieving solar damping of the librations of satellites in the gravity-gradient field and presented a simplified analysis using averaged radiation torques. Modi and Flanagan¹⁷ (1971) examined the planar attitude control of a gravity-gradient system in an ecliptic orbit using the radiation pressure to provide the damping torque. Modi and Tschann^{18,19} (1971,73) extended the analysis by the introduction of a displacement and velocity sensitive controller. Practical feasibility of the system was considered through an arrangement involving an unfurlable membrane whose effective area could be judiciously governed. Modi and Kumar^{20,21} (1971,74) studied planar as well as coupled libration control through the use of solar surfaces which may be translated relative to the spacecraft body to govern the solar control torques.

A more practical approach, employing highly reflective control surfaces rotatable about body-fixed axes, was proposed by Modi and Pande²² (1973) for three-axis control of a dual-spin satellite. A large number of control surfaces were found necessary to achieve independent control of the roll, yaw and pitch torques. Unfortunately, the solar torque components turn out to be extremely complicated, coupled, transcendental functions of the control surface rotations and the orbital

angle. Therefore, a coupled system of transcendental equations must be solved continuously to determine the required control surface rotations. This limits the applicability of the method to spacecraft having a sophisticated onboard computational capability. Modi and Pande²³ (1974) also developed a simpler model involving four independently rotatable control surfaces for three-axis control of axisymmetric spacecraft. Bang-bang control laws directly specifying the control surface rotations as functions of the attitude errors and rates were suggested. This not only led to computational simplifications but also improved the rates of attitude correction for large errors. However, an undesirable chatter behaviour was observed in the small error regime. The analyses investigated the applicability of the technique in nonecliptic orbits of arbitrary inclination and suggested modifications to the control laws to reduce the eccentricity induced steady state errors. Pande et al.²⁴ (1974) investigated the minimum time pitch control problem for a gravity-oriented satellite. The authors also recognized the possibility of using solar pressure control in conjunction with magnetic²⁵ (1974) and aerodynamic²⁶ (1974) modes of control.

There have been two experiments to date to examine the practical performance of solar pressure attitude control systems. The first relates to the flight of Mariner IV spacecraft^{27,28} (1966, 69) which was equipped with four solar

vanes attached to the tips of the solar panels. The vanes were designed to passively stabilize the spacecraft so as to align its roll axis along the sun-line. A small amount of damping⁷ was also provided by the passive solar vane actuator. Unfortunately, one of the vanes proved to be inoperative during the early portion of the mission. Subsequently, a power transient aboard the spacecraft caused reactivation of the solar vane. The solar pressure experiment, conducted on depletion of the attitude control gas, showed the solar vanes to be capable of maintaining the spacecraft roll axis within 1° of the sun-line in conjunction with nutation damping provided by gyros. A recent experiment²⁹ (1979) conducted by the European space Agency established the effectiveness of the method for geostationary communications satellites. The solar panels of OTS-2 spacecraft were rotated differentially to generate control torques about the roll and yaw axes. A ground commanded discontinuous mode of control was used for the solar panel rotation during the experiment. For a period of six days, all the spacecraft thrusters were completely disabled and its attitude was controlled successfully entirely by solar radiation pressure.

1.3 Purpose and Scope of the Investigation

From the foregoing, it is apparent that most practical solar controller configurations proposed for earth-pointing

spacecraft involve a number of rotatable control surfaces. Clearly, it would be of interest to simplify the hardware implementation through the minimization of the number of control surfaces. Moreover, the continuous feedback control laws developed for the solar torque components require extensive onboard computational capability to determine the commanded control surface rotations. On the other hand, control strategies directly specifying feedback relations for the control surface rotations are limited to a discontinuous mode of operation leading to an unsatisfactory performance in the small error region. Hence, there is a need to develop continuous control laws that directly govern the control surface rotations as functions of the attitude errors and rates.

The literature review also indicates that utilization of solar pressure for attitude control has been limited to either sun-oriented or earth-pointing spacecraft. Its application for attaining space-oriented attitudes, unfortunately, has remained unexplored. On the other hand, solar pressure stabilization of satellites along an inertially-fixed attitude would represent an inexpensive technique for long-life applications such as astronomical observations. Furthermore, it would be of interest to develop solar controllers capable of achieving arbitrary large-angle attitude maneuvers in space. Such a system would add versatility to the spacecraft and enable it to undertake diverse missions through an entirely semipassive approach.

The thesis makes an attempt at developing solar pressure control systems meeting the above mentioned objectives. Controller configurations consisting of two highly reflective lightweight control surfaces rotatable about body-fixed axes are proposed for the different pointing objectives. Such configurations represent the minimum hardware implementation as at least two control surfaces are required to achieve the control torque reversals.

The problem of stabilizing the pitch attitude of an unsymmetrical earth-pointing spacecraft is analyzed first. A piecewise linear feedback control law with constant gains is proposed for the differential rotation of the control surfaces. The system stability and performance are analyzed as functions of the attitude error and rate gains.

Next, the approach is extended to develop a solar control system for three-axis stabilization of unsymmetrical earth-pointing spacecraft. Optimal control theory is employed to synthesize a feedback control law for the differential control surface rotation leading to an asymptotically stable system. Suboptimal control strategies are suggested which promise considerable reduction of the computational requirements during the system implementation.

This is followed by an investigation of missions demanding an inertially-fixed attitude. The inertial pointing problems

are characterized by the need to provide nominal controls countering the time-varying gravity-gradient disturbances. For pitch stabilization, both the nominal and feedback control laws governing the differential control surface rotation are synthesized analytically. The influence of system gains and parameters on its stability and response characteristics is established.

The study is then extended to the problem of imparting inertially-fixed orientations to the symmetry axis of an axisymmetric spacecraft. For this more complex problem, a numerical approach is followed. Nominal control laws for the individual control surface rotations are developed and linear optimal control theory is applied for the control synthesis in the neighbourhood of the desired inertial orientation. Again, the possibility of employing suboptimal control policies with reduced computational requirements is explored.

Finally, the feasibility of achieving large-angle attitude maneuvers of the spacecraft symmetry axis is investigated. The problem is formulated as a minimum time transfer problem with terminal state constraints. A gradient procedure is developed to determine the optimal open-loop strategy for the differential control surface rotation. The transfer strategy is then coupled with the appropriate nominal and feedback control policies required for stabilization along the inertially-fixed terminal orientation.

Figure 1.1 schematically represents the plan of study.

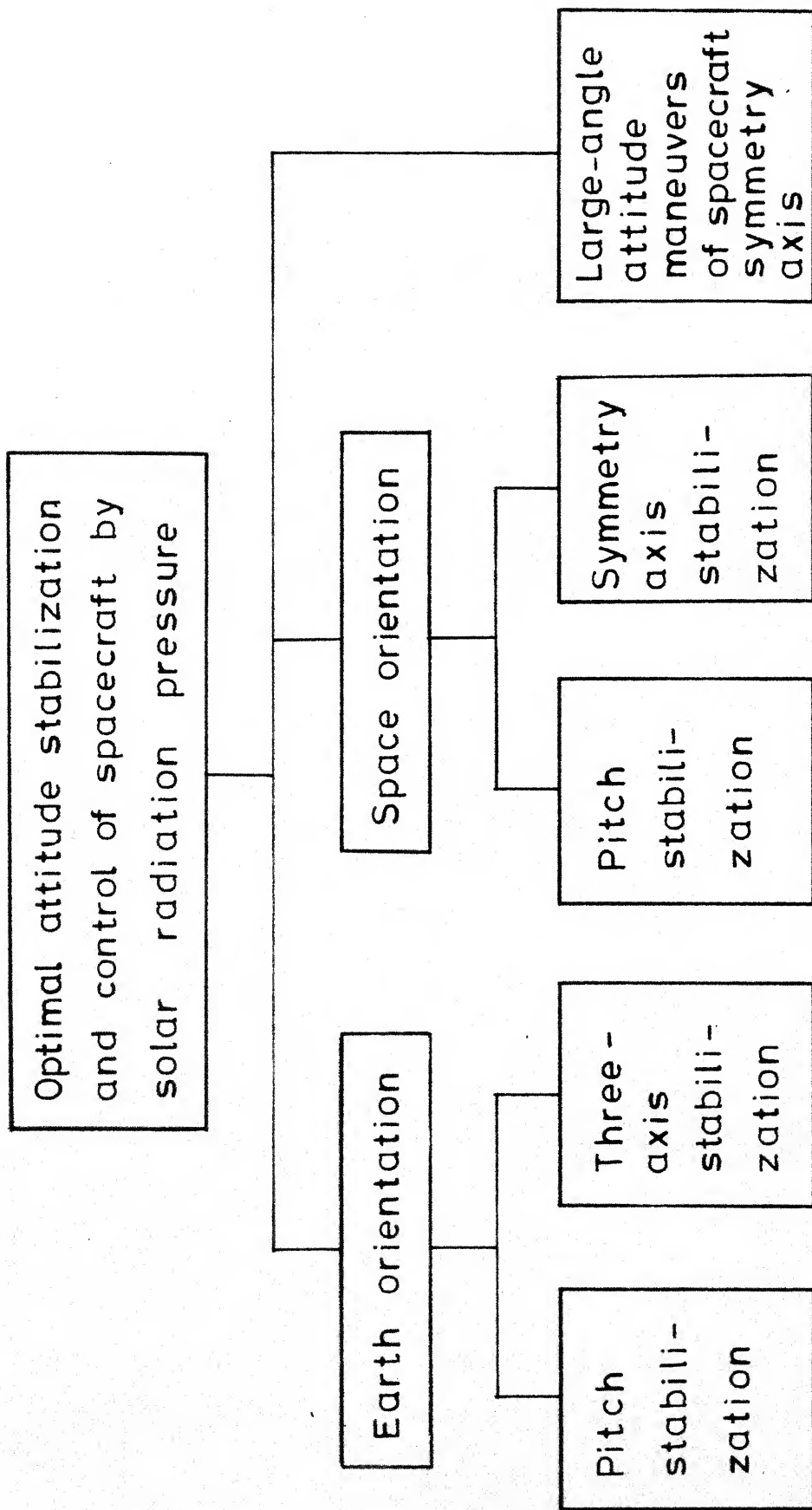


Fig. 1.1 Plan of study

2. PITCH ATTITUDE STABILIZATION OF EARTH-POINTING SPACECRAFT

This chapter presents the development of a solar controller for controlling the pitch attitude of an unsymmetrical earth-pointing satellite. A controller configuration involving two highly reflective rotatable control surfaces is proposed. The governing equation of motion is found to be nonlinear and nonautonomous in character, rendering it difficult to arrive at a suitable control strategy for the control surface rotations. A simple feedback control law, directly specifying the differential rotation of the control surfaces, is developed following linearization of the pitch equation. The stability of the control system is analyzed using Floquet theory and the validity of the control law is established for all times of the year. The system performance is studied through simulation of the full nonlinear equations of motion.

2.1 Problem Formulation

Figure 2.1 shows the geometry of the orbital and attitude motion of an unsymmetrical satellite with its center of mass S moving in a circular orbit about the earth's center O . The inertial frame of reference, X, Y, Z , is selected such that the Y -axis points towards the ascending node N , and YZ defines the plane of the orbit. The unit vector \bar{e} indicates the orientation of the earth-sun line. x_0, y_0, z_0 represent the rotating

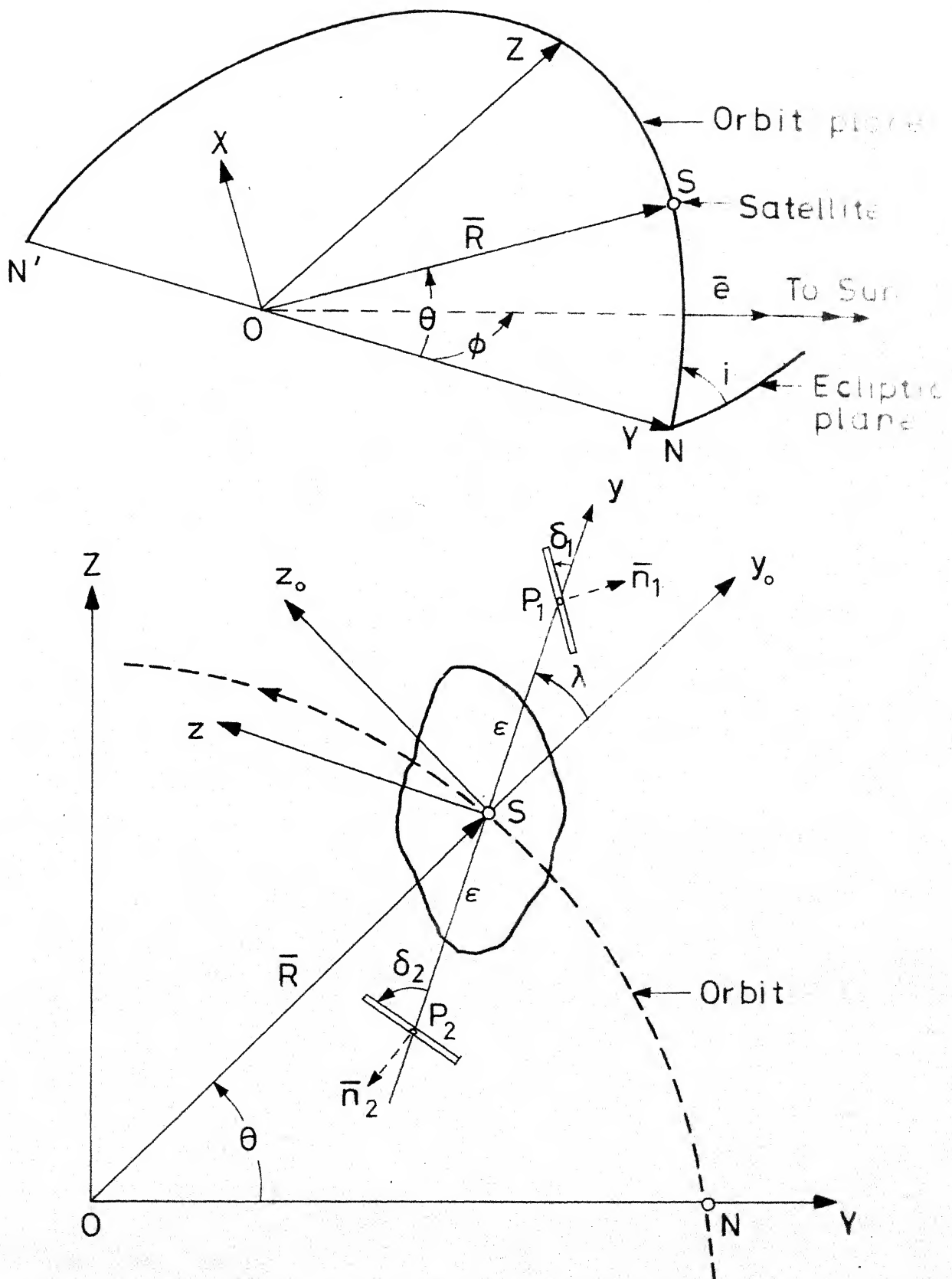


Fig.2.1 Geometry of orbital and attitude motion

orbital coordinate system with y_0 along the local vertical, z_0 tangent to the orbit in its plane and x_0 along the orbit normal. The spacecraft executes pitch attitude motion λ in the plane of the orbit.

The solar pressure controller consists of two identical, highly reflective, lightweight surfaces P_1 and P_2 which are permitted rotations δ_1 and δ_2 , respectively, from the y -axis. The center of pressure of each surface lies on the satellite y -axis (may be anywhere in yz -plane). This, along with the fact that the radiation force on a highly reflective surface is directed along the surface normal, ensures that only a pitch moment is produced by the controller.

The equation of pitch motion may be written as

$$(d/dt) [I_x(\dot{\lambda} + \dot{\theta})] = M_g + M_s \quad (2.1)$$

where M_g and M_s represent the gravitational and the solar torques about the pitch axis.

The gravitational torque component M_g is well known to be³⁰,

$$M_g = -3(I_z - I_y)\sin \lambda \cos \lambda \quad (2.2)$$

Figure 2.2 shows the components of the radiation force acting on the control plate P_i under specular reflection conditions. The resultant solar pressure force \bar{F}_i acting on the plate is given by

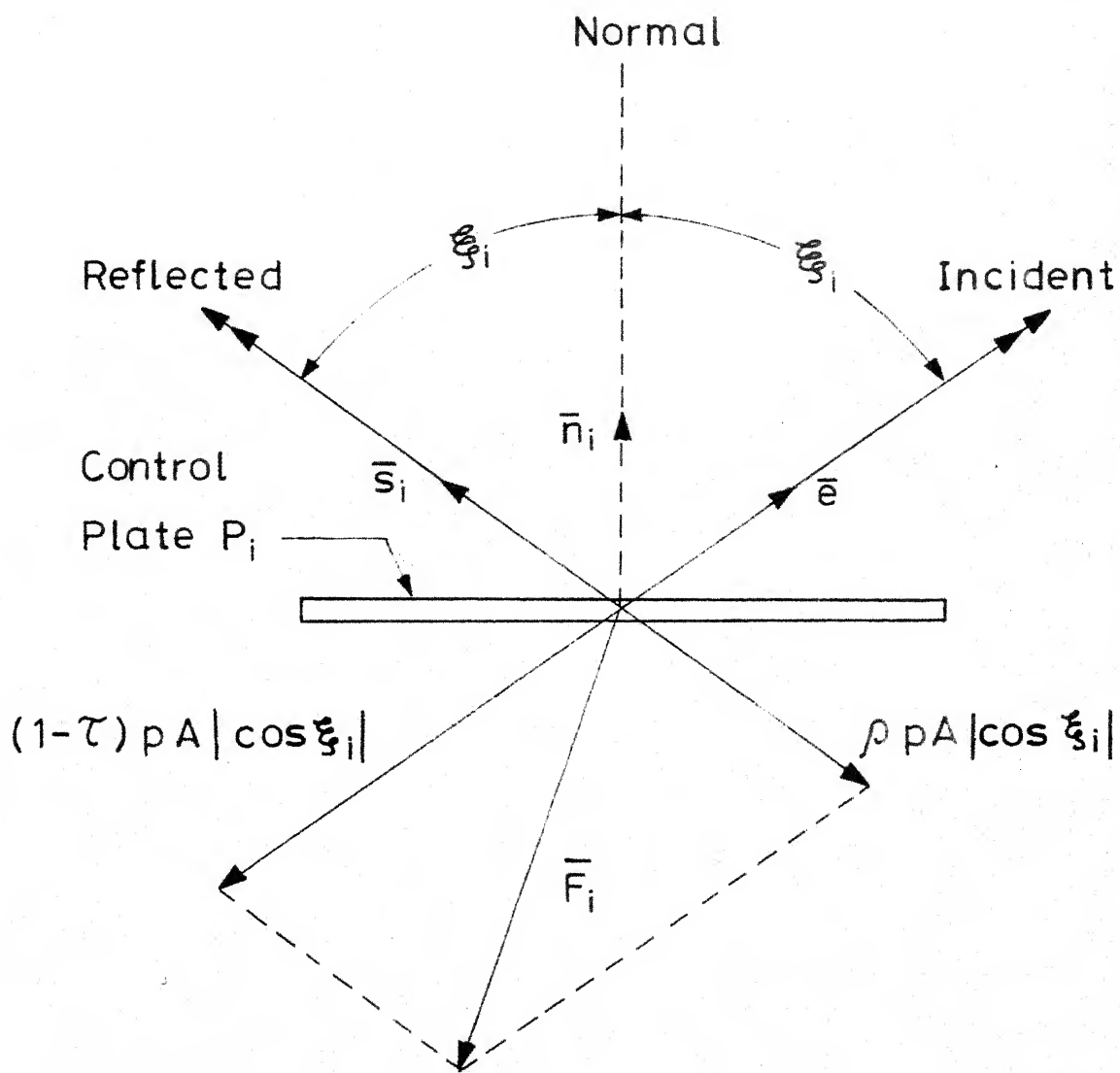


Fig. 2.2 Radiation forces acting on control plate P_i

$$\bar{F}_i = -pA |\cos \xi_i| [(1-\tau)\bar{e} + \rho \bar{s}_i] \quad (2.3)$$

Expressing \bar{s}_i in terms of \bar{e} and \bar{n}_i , and ignoring terms of order $(1-\tau-\rho)/2\rho$ compared to unity, which is justifiable for surfaces of high reflectivity, it simplifies to

$$\bar{F}_i = -2\rho pA |\cos \xi_i| \cos \xi_i \bar{n}_i \quad (2.4)$$

The angle of incidence ξ_i is obtained from

$$\cos \xi_i = \bar{e} \cdot \bar{n}_i \quad (2.5)$$

The unit vector along the sun-line may be expressed as

$$\bar{e} = e_x \bar{i} + e_y \bar{j} + e_z \bar{k} \quad (2.6)$$

where

$$e_x = -\sin \phi \sin i \quad (2.7a)$$

$$e_y = \cos \phi \cos(\theta + \lambda) + \sin \phi \cos i \sin(\theta + \lambda) \quad (2.7b)$$

$$e_z = -\cos \phi \sin(\theta + \lambda) + \sin \phi \cos i \cos(\theta + \lambda) \quad (2.7c)$$

The unit normal to plate P_i is given by

$$\bar{n}_i = \sin \delta_i \bar{j} - \cos \delta_i \bar{k} \quad (2.8)$$

Substitution of Equations (2.6) and (2.8) in Equation (2.5) gives

$$\cos \xi_i = (1 - \sin^2 \phi \sin^2 i)^{\frac{1}{2}} \sin(\theta + \zeta + \lambda + \delta_i) \quad (2.9)$$

where

$$\zeta(\phi) = -\arctan(\tan \phi \cos i) \quad (2.10)$$

The solar pressure moment acting on the spacecraft then becomes

$$\bar{M}_s = \epsilon \bar{J} \times \bar{F}_1 - \epsilon \bar{J} \times \bar{F}_2 \quad (2.11)$$

$$= 2 \rho_p A \epsilon (|\cos \xi_1| \cos \xi_1 \cos \delta_1 - |\cos \xi_2| \cos \xi_2 \cos \delta_2) \bar{I} \quad (2.12)$$

Substituting for M_g and M_s from Equations (2.2) and (2.12) in Equation (2.1), and changing the independent variable from t to θ through the relation $\theta = \Omega t$, the governing pitch equation takes the form

$$\lambda'' + 3K \sin \lambda \cos \lambda = \tilde{M}_s \quad (2.13)$$

where

$$\begin{aligned} \tilde{M}_s = C \sigma [& |\sin(\theta + \zeta + \lambda + \delta_1)| \sin(\theta + \zeta + \lambda + \delta_1) \cos \delta_1 \\ & - |\sin(\theta + \zeta + \lambda + \delta_2)| \sin(\theta + \zeta + \lambda + \delta_2) \cos \delta_2] \end{aligned} \quad (2.14)$$

Here, the function $\sigma(\phi)$ is given by

$$\sigma(\phi) = 1 - \sin^2 \phi \sin^2 i \quad (2.15)$$

and the solar parameter C , characterizing the controller size is defined as

$$C = 2 \rho_p A \epsilon / I_x \Omega^2 \quad (2.16)$$

As ϕ varies by 2π radians in a year, both $\sigma(\phi)$ and $\zeta(\phi)$ represent extremely slow variables compared to the orbital angle θ . Therefore, they remain practically constant over a number of the satellite orbits. In the analysis to follow, the solar aspect angle ϕ as well as other slow variables such

as $\sigma(\phi)$, $\zeta(\phi)$, etc., are treated as system parameters which acquire different values at different times of the year.

2.2 Control Synthesis

When the two control surfaces are parallel ($\delta_1 = \delta_2 = \delta_e$) the stable equilibrium position of the system corresponds to the alignment of the minimum moment of inertia axis along the local vertical, i.e., $\lambda = 0, \pi$ with $K > 0$. Consequently, a control law of the form

$$\tilde{M}_s(\delta_1, \delta_2, \lambda, \theta) = -\mu \lambda' - \nu \lambda \quad (2.17)$$

where μ , ν represent constant positive gain factors, leads to asymptotic stability of the pitch motion. However, its implementation would require continuous solution of the transcendental Equation (2.14) to determine the δ_1 , δ_2 values required to generate the commanded torque. Also, as this would mean solving one equation for the two unknowns, a suitable constraint between them must be specified.

In order to bypass the computational difficulty, a simplification of the torque expression is presently undertaken. It is assumed that the control surface excursions from their 'off' positions are small. Replacing δ_1 by $(\delta_e + \tilde{\delta}_1)$, δ_2 by $(\delta_e + \tilde{\delta}_2)$, and retaining only the linear terms in $\tilde{\delta}_1$ and $\tilde{\delta}_2$, the solar torque expression (2.14) reduces to

$$\begin{aligned} \tilde{M}_S = C \sigma (\tilde{\delta}_1 - \tilde{\delta}_2) & |\sin(\theta + \zeta + \lambda + \delta_e)| \\ & \times [2 \cos(\theta + \zeta + \lambda + \delta_e) \cos \delta_e \\ & - \sin(\theta + \zeta + \lambda + \delta_e) \sin \delta_e] \end{aligned} \quad (2.18)$$

The simplified expression indicates that for small control surface rotations about the 'off' position δ_e , the radiation torque depends on the single control variable $(\tilde{\delta}_1 - \tilde{\delta}_2)$. This fact can be used to advantage during mechanization of the system as the two surfaces may be rotated in opposite directions by equal amounts employing a single drive arrangement.

Furthermore, the solar torque depends on the choice of δ_e in addition to its time-varying character. Maximization of the torque producing ability of a given controller, characterized by $|\tilde{M}_S / C(\tilde{\delta}_1 - \tilde{\delta}_2)|$, appears to be a suitable criterion for the selection of δ_e . This however, leads to a δ_e dependent on both θ and λ . On the other hand, it would be desirable to have a constant δ_e about which the control surfaces rotate. Hence, maximization of the average torque generating ability over a torque cycle,

$$\begin{aligned} |\tilde{M}_S / C(\tilde{\delta}_1 - \tilde{\delta}_2)|_{av} = (\sigma / \pi) \int_0^\pi & |\sin(\tilde{\theta} + \delta_e) \{2 \cos(\tilde{\theta} + \delta_e) \cos \delta_e \\ & - \sin(\tilde{\theta} + \delta_e) \sin \delta_e\}| d\tilde{\theta} \end{aligned} \quad (2.19)$$

is considered, where $\tilde{\theta} = (\theta + \zeta + \lambda)$ represents a dummy variable of integration.

It may be easily shown that the integral is a maximum for $\delta_e = n\pi$, minimum for $\delta_e = (2n+1)\pi/2$ where $n = 0, 1, 2, \dots$. Taking $\delta_e = 0$, letting $\delta_1 = \tilde{\delta}$, $\tilde{\delta}_2 = -\tilde{\delta}$ and substituting Equation (2.18) in Equation (2.13), the equation of motion takes the form

$$\lambda'' + 3K \sin \lambda \cos \lambda = 4C \sigma \tilde{\delta} |\sin(\theta + \zeta + \lambda)| \cos(\theta + \zeta + \lambda) \quad (2.20)$$

The control law for the variable $\tilde{\delta}$ should be so chosen that the controller introduces positive damping and restoring effects in the pitch dynamics of the satellite. The control system should also exhibit asymptotic stability for small amplitude motion over a range of system parameters. To meet these objectives, we consider the control law

$$\tilde{\delta} = -\operatorname{sgn}\{\cos(\theta + \zeta)\} (\mu \lambda' + \nu \lambda) \quad (2.21)$$

The dynamics of the controlled system is described by the differential equation resulting from the substitution of Equation (2.21) in Equation (2.20). For pitch motion near the equilibrium attitude, linearization in λ leads to

$$\lambda'' + (\tilde{\mu} |\sin 2\eta|) \lambda' + (\tilde{\nu} |\sin 2\eta| + 3K) \lambda = 0 \quad (2.22)$$

where $\tilde{\mu} = 2C \sigma \mu$, $\tilde{\nu} = 2C \sigma \nu$ and $\eta = (\theta + \zeta)$ is a new independent variable.

It is apparent that the damping and restoring torques introduced by the solar controller are time-varying in character. However, they remain nonnegative throughout. One

may, therefore, expect to find a range of combinations of the parameters $\tilde{\mu}$, $\tilde{\nu}$ and K leading to asymptotically stable operation.

2.3 System Stability and Performance

The time-varying coefficients in Equation (2.22) are periodic functions of η with a period of $\pi/2$. Hence, Floquet theory³¹ may be applied to determine the stability of the system.

Letting $x_1 = \lambda$, $x_2 = \lambda'$, $\bar{x} = (x_1, x_2)^T$, Equation (2.22) may be expressed in the form

$$\bar{x}' = M(\eta) \bar{x} \quad (2.23)$$

where

$$M(\eta) = \begin{bmatrix} 0 & 1 \\ -(\tilde{\nu} |\sin 2\eta| + 3K) & -\tilde{\mu} |\sin 2\eta| \end{bmatrix} \quad (2.24)$$

The stability analysis involves the examination of the characteristic multipliers of the system (2.23). These are the eigenvalues of the square matrix $Y(\pi/2)$ where $Y(\eta)$ satisfies the matrix differential equation

$$Y'(\eta) = M(\eta) Y(\eta) \quad (2.25)$$

and the initial conditions $Y(0) = I$, the unity matrix. The system is said to be asymptotically stable if, and only if, the

moduli of all characteristic multipliers are less than unity. It is unstable if any characteristic multiplier has a modulus greater than unity.

In the absence of a closed-form solution, the system (2.23) was integrated numerically over the period $\eta = 0$ to $\eta = \pi/2$ to obtain the stability information. The results of the analysis were summarized in the form of stability charts in the $\tilde{\mu}, \tilde{\nu}$ parameter space for different values of the satellite inertia parameter. The stability investigation extended over a large range of the controller gains. For a clearer appreciation of the resulting stability-instability patterns, the stability charts for a restricted range of $\tilde{\mu}, \tilde{\nu}$ are shown in Figure 2.3 for two extreme values of K .

It is apparent from Figure 2.3a that for a dumbbell configuration aligned nominally along the local vertical ($K = 1$), a wide range of parameters results in asymptotically stable motion. Instability occurs only for certain regions of small $\tilde{\mu}$ values. These small instability regions were found to appear repeatedly in a pattern as larger values of $\tilde{\nu}$, beyond those shown in the figure, were considered. The most adverse situation of a dumbbell configuration nominally aligned along the local horizontal direction ($K = -1$) is represented in Figure 2.3b. The instability region is significantly enlarged as the gravity torque now acts as a destabilizing influence.

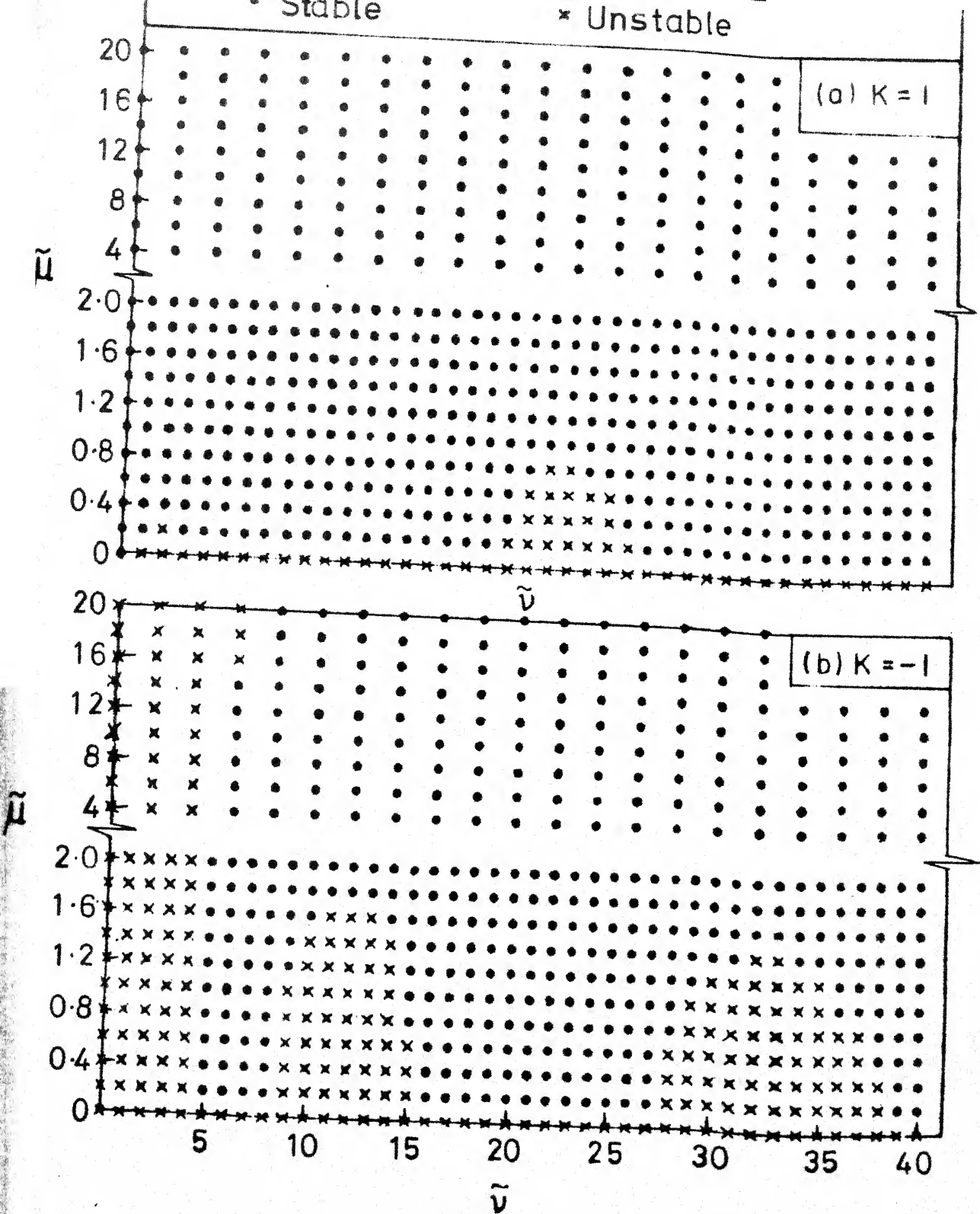


Fig. 2.3 Stability charts for a dumbbell satellite nominally oriented along the (a) local vertical (b) local horizontal

The appearance of instability near the $\tilde{\mu}$ axis indicates that a minimum amount of restoring torque from the controller (minimum $\tilde{\nu}$) is essential to have stable operation. Also, for small $\tilde{\nu}$ values the instability region enlarges somewhat as $\tilde{\mu}$ is increased, suggesting that an increase in the time-varying damping torque may at times lead to instability. Nevertheless, the results establish the capability of the solar controller in achieving pitch stabilization along the inherently unstable gravitational equilibrium attitude. The stability analysis for intermediate values of the inertia parameter showed similar stability-instability regions with the general trend of increasing stable regions as K increased from -1 to $+1$ in the physically possible range of $-1 \leq K \leq 1$.

Note that $\tilde{\mu}$ and $\tilde{\nu}$ would vary slowly as the time of the year changes. Their variation is relatively small for satellite orbits having a low inclination from the ecliptic plane. Hence, it would be desirable to select the gains $\tilde{\mu}$, $\tilde{\nu}$ so that the system operating point lies well within the stable region of the stability chart. This would ensure asymptotically stable operation throughout the year.

Another feature characterizing the controller's performance would be the speed of attitude correction it is capable of. The largest "system time constant", which provides an estimate of the time taken to reduce the amplitude or the amplitude envelope by a factor $1/e$, may be taken as an

approximate measure of the controller's speed of response.

The largest time constant is given by

$$\tau = - (\pi/2) / \ln |\rho_i|_{\max} \quad (2.26)$$

where $|\rho_i|_{\max}$ is the largest of the moduli of the characteristic multipliers. The dependence of τ on the controller gains and inertia parameter was found to be quite complicated. Generally, τ decreased with increase in $\tilde{\mu}$, $\tilde{\nu}$ and K . Time constants of the order of a few orbital degrees ($\approx 15 - 20^\circ$) were found achievable within the parameter range $0 < \tilde{\mu}, \tilde{\nu} < 50$.

The full nonlinear equations of motion (2.13) were integrated in conjunction with the control law (2.21) for different values of the controller gains and initial conditions to study the system response. Typical responses obtained are presented in Figures 2.4 and 2.5. These show the attitude responses and the control histories subsequent to an initial position error and an impulsive disturbance. The response is observed to be of a damped oscillatory character with $\mu = 0.1$ and $\nu = 1.0$ (Figure 2.4). When the parameter μ is increased to 1.0, with ν remaining the same, the response is found to be of an over damped nature (Figure 2.5). This characteristic of the present nonautonomous system appears to be quite similar to a second order system with constant coefficients.

$C = 10$	$K = 0.5$	$\zeta = 0$
$\delta_e = 0$	$\mu = 0.1$	$\nu = 1.0$

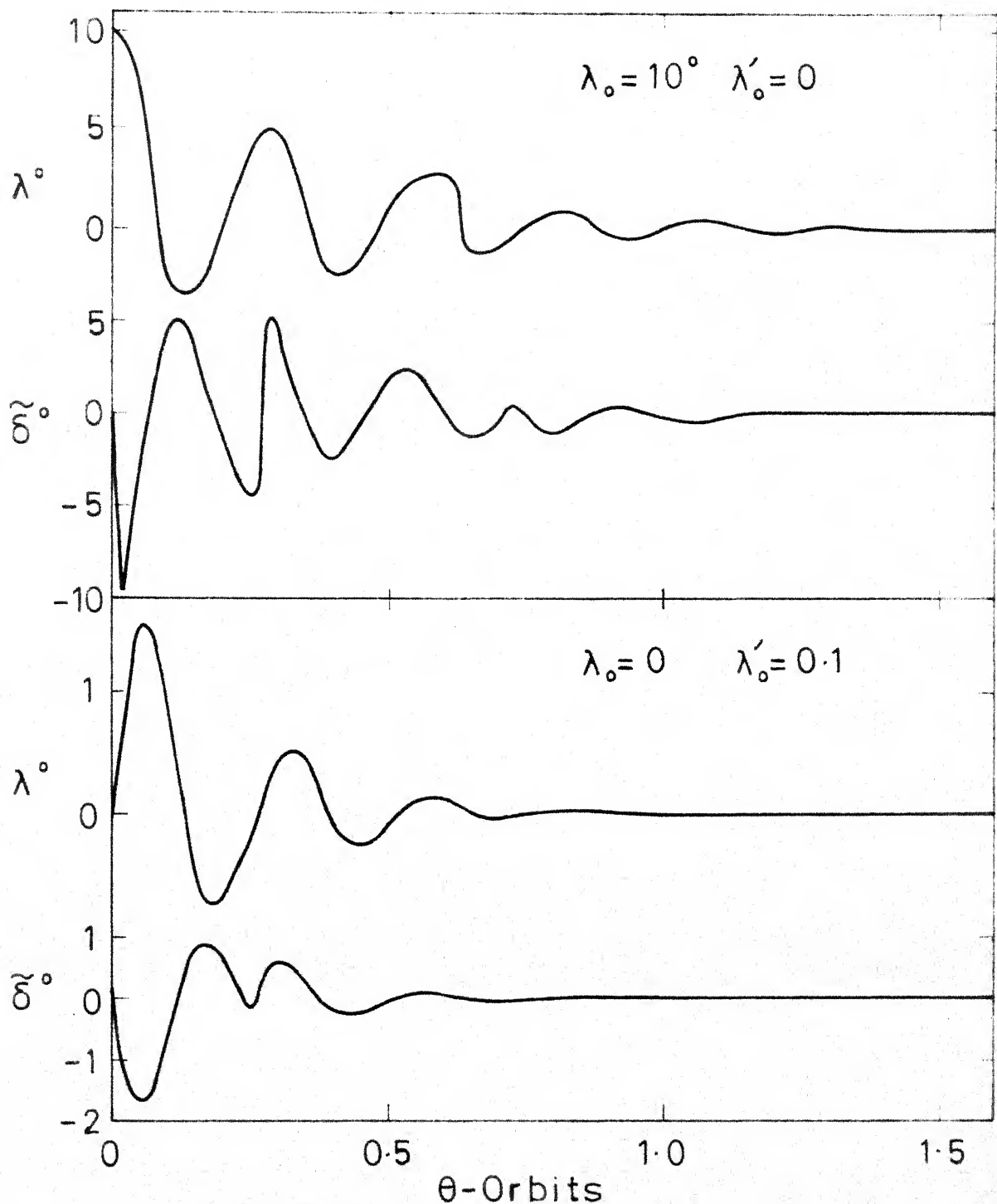


Fig. 2.4 Attitude responses and control histories with gains $\mu = 0.1$ and $\nu = 1.0$

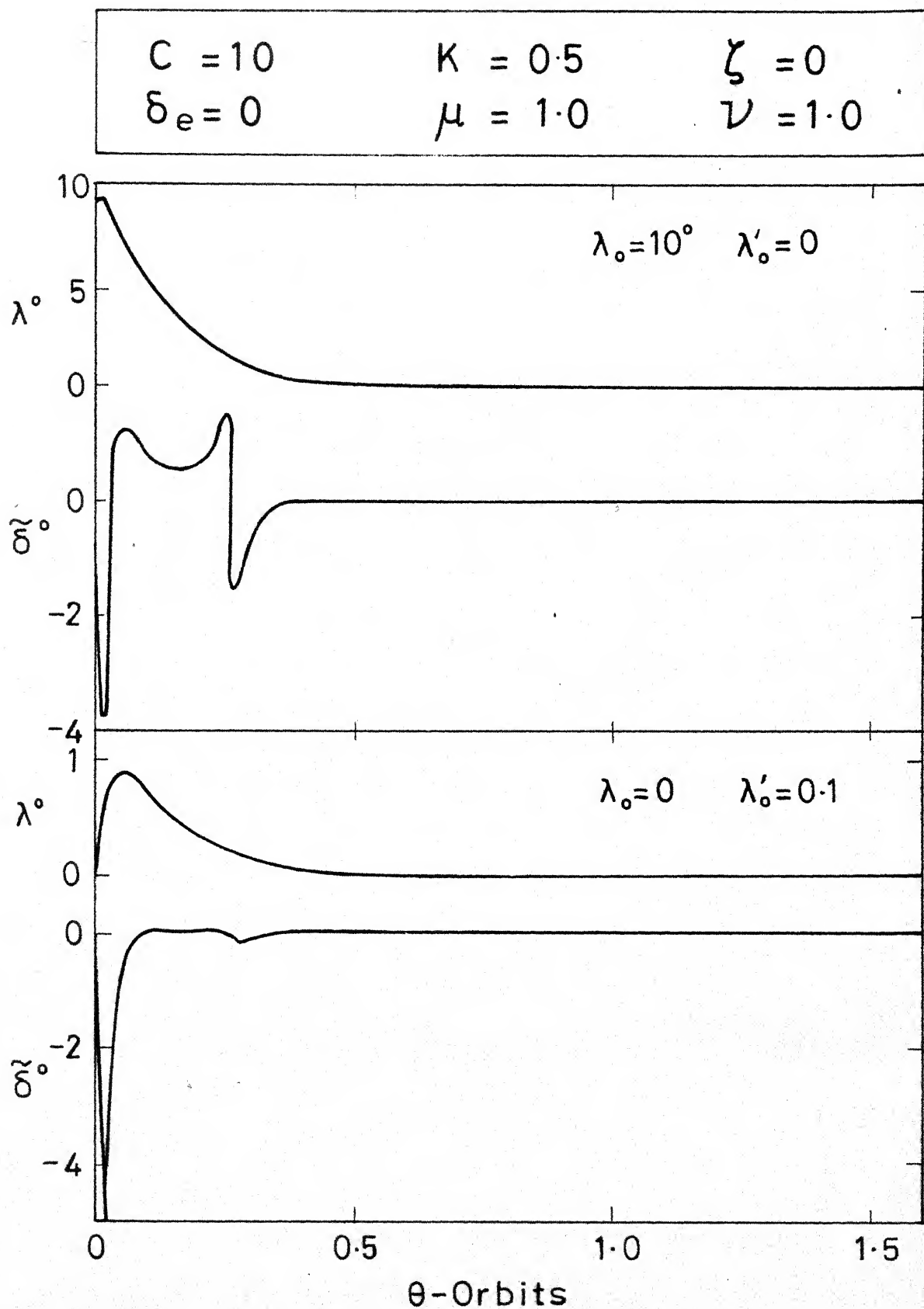


Fig. 2.5 Attitude responses and control histories with gains $\mu=1.0$ and $\nu=1.0$

The results exhibit time constants ranging from about 50° to 150° of the orbit. These, of course, are due to the very small values of the gains employed. Considerable reductions in the settling times were found possible with the use of increased μ and ν values. It may be noted here that the impulsive disturbance $\lambda'_0 = 0.1$ represents a much greater value than is likely to occur due to micrometeorite impacts³². Consequently, much smaller settling times would be expected in reality. The typical system response presented may be better appreciated with a numerical example. The solar parameter value $C \approx 10$ is achieved for a spacecraft having $I_x = 500 \text{ Kg-m}^2$ in the geostationary orbit with a control surface area $A = 1\text{m}^2$ and moment arm $\epsilon = 3\text{m}$.

2.4 Concluding Remarks

The conclusions based on the present study may be summarized as follows :

- (i) The analysis shows that it is possible to design a mechanically simple solar pressure control system for pitch control of earth-pointing satellites. The suggested control law for the control surface rotations is also very simple to realize.
- (ii) The controller is capable of stabilizing the spacecraft pitch attitude along gravitationally stable as well as unstable orientations.

- (iii) The control system assures asymptotically stable operation over a wide range of system parameters.
- (iv) The controller appears to be useful for applications wherein control times of the order of a few degrees of the orbit may be acceptable, such as, long-life scientific missions.

3. THREE-AXIS ATTITUDE STABILIZATION OF EARTH-POINTING SPACECRAFT

The previous analysis suggests that it should be possible to modify the controller geometry to generate solar control torques about three mutually perpendicular body-fixed axes. The two-surface controller may then be utilized for three-dimensional attitude control of earth-pointing spacecraft. The development and analysis of a three-axis attitude control system using only a single pair of rotatable control surfaces forms the objective of this chapter. The equations governing roll, yaw and pitch degrees of freedom are formulated for a triaxial spacecraft moving in a circular orbit of arbitrary inclination from the ecliptic plane. Optimal control theory is applied to synthesize a feedback control law for the differential control surface rotation which promises asymptotically stable system operation. The optimal control law involves the implementation of periodic time-varying gains. Suboptimal control strategies promising considerable reduction of the associated computational requirements are explored. Numerical results are presented which establish the effectiveness of the control system in stabilizing the spacecraft attitude even under severe gravity-gradient conditions and external disturbances.

3.1 Formulation of the Problem

Figure 3.1a shows the geometry of the orbital motion of an unsymmetrical satellite with its center of mass S moving in a circular orbit about the earth's center O . The rotational motion of the spacecraft about its center of mass may be conveniently specified by a set of finite rotations indicated in Figure 3.1b. The rotations performed in the sequence, γ about the z_0 -axis, β about the y_1 -axis and λ about x_2 -axis, bring the orbital coordinates x_0, y_0, z_0 into coincidence with the satellite principal axes x, y, z . The rotations are referred to as the roll (γ), yaw (β) and pitch (λ) angles, respectively.

The proposed solar controller configuration is indicated in Figure 3.2. It consists of two highly reflective lightweight surfaces P_1 and P_2 with their center line $P_1 P_2$ located at an angle λ_p from the y -axis in the yz -plane. The surfaces intercept the solar radiation pressure resulting in a torque about the satellite center of mass. The solar radiation torque may be controlled by rotating the control surfaces about their body-fixed axes by angles δ_1 and δ_2 as shown in the figure.

The dynamical equations governing the attitude motion may be derived using the classical Lagrangian approach. The kinetic and the potential energies associated with the rotational motion of the spacecraft in the gravity-gradient field are found to be :

$$T = (1/2)(I_x \omega_x^2 + I_y \omega_y^2 + I_z \omega_z^2) \quad (3.1)$$

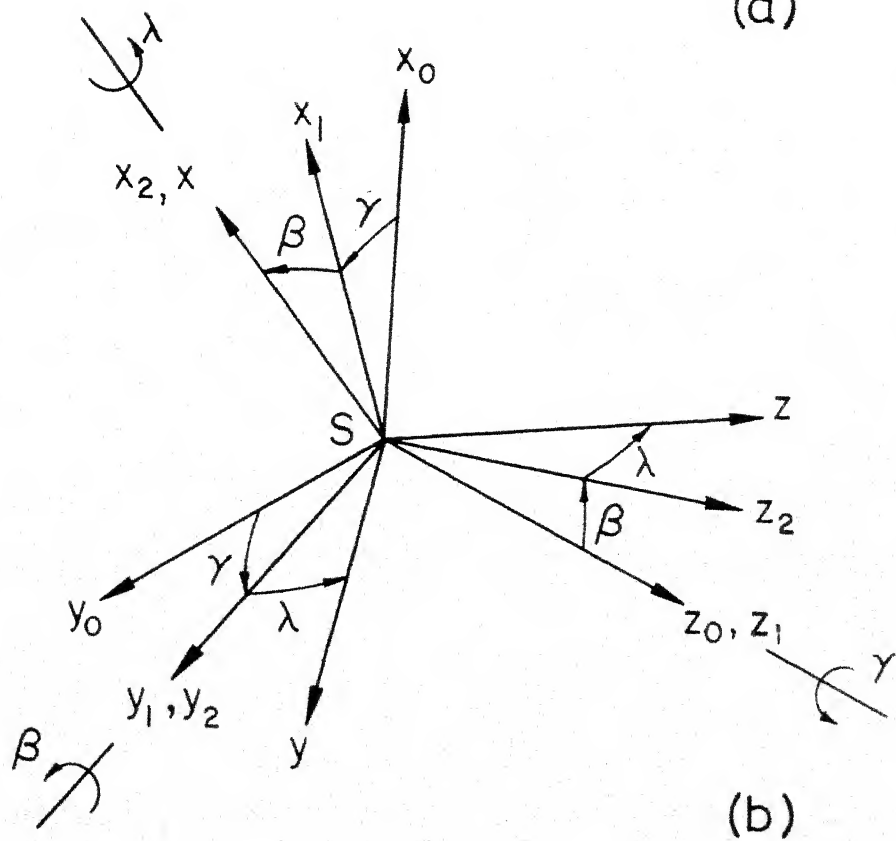
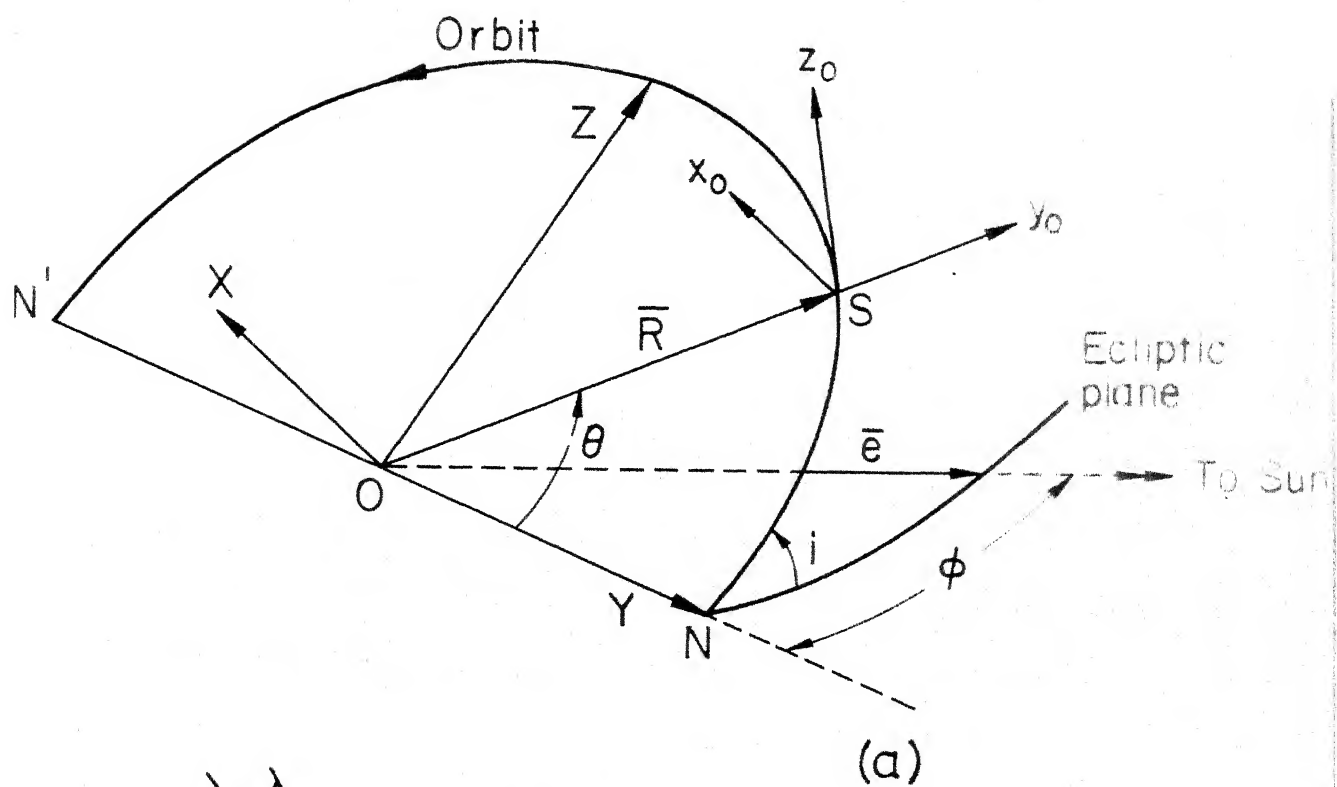


Fig. 3.1 (a) Geometry of orbital motion
(b) Geometry of attitude motion

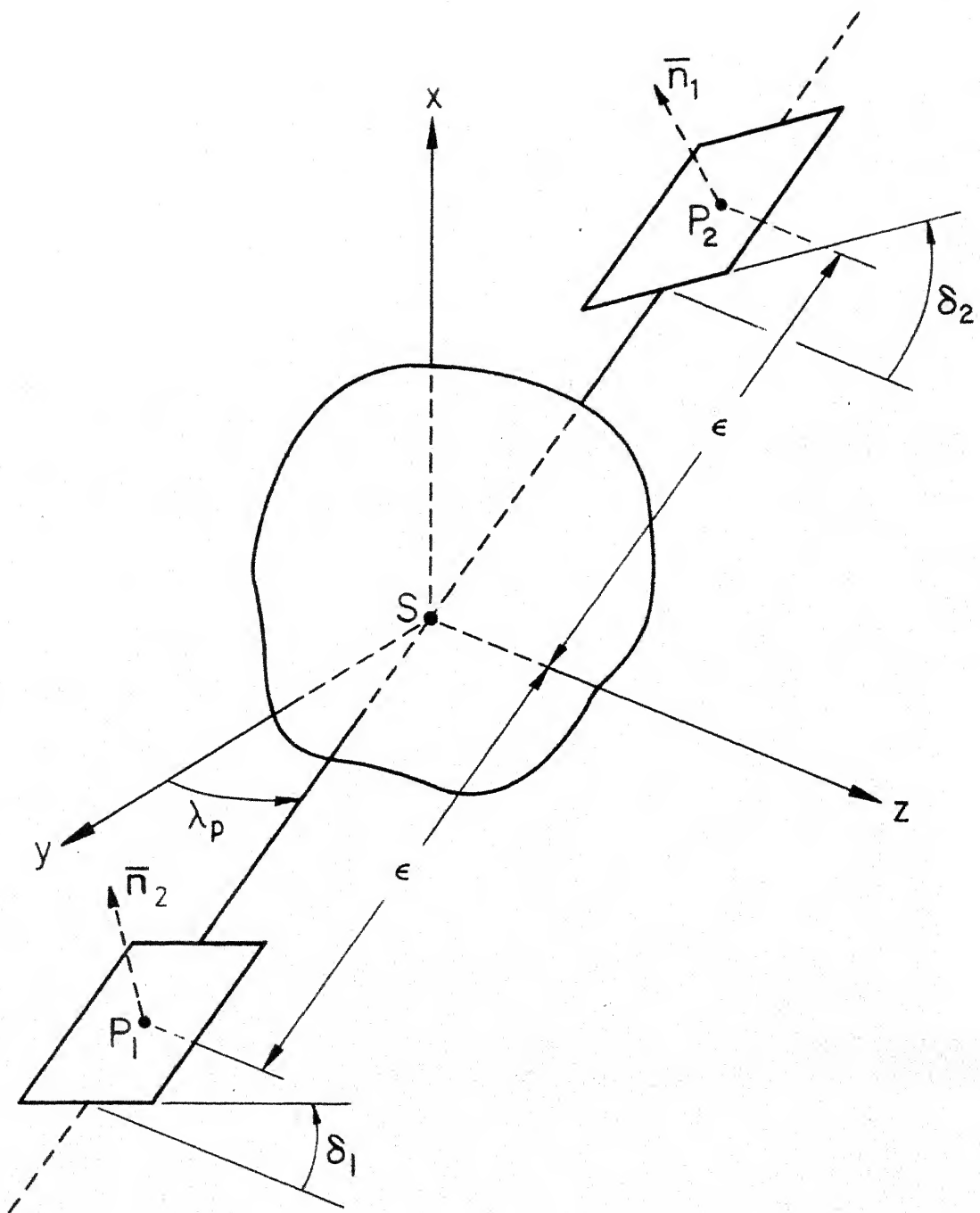


Fig. 3-2 Solar controller configuration

where

$$\omega_x = \dot{\theta} \cos \gamma \cos \beta - \dot{\gamma} \sin \beta + \dot{\lambda} \quad (3.2a)$$

$$\omega_y = (\dot{\beta} - \dot{\theta} \sin \gamma) \cos \lambda + (\dot{\theta} \cos \gamma \sin \beta + \dot{\gamma} \cos \beta) \sin \lambda \quad (3.2b)$$

$$\omega_z = -(\dot{\beta} - \dot{\theta} \sin \gamma) \sin \lambda + (\dot{\theta} \cos \gamma \sin \beta + \dot{\gamma} \cos \beta) \cos \lambda \quad (3.2c)$$

and

$$\begin{aligned} V = & -(\mu_E/4 R^3) [(2I_x - I_y - I_z)(1 - 3 \sin^2 \gamma \cos^2 \beta) \\ & + 3(I_y - I_z) \{ (\sin^2 \gamma \sin^2 \beta - \cos^2 \gamma) \cos 2\lambda \\ & - (\sin 2\gamma \sin \beta) \sin 2\lambda \}] \end{aligned} \quad (3.3)$$

The equations of motion are then obtained from

$$(d/dt)(\partial L / \partial \dot{k}) - (\partial L / \partial k) = Q_k \quad (3.4)$$

$$k = \gamma, \beta, \lambda$$

where $L = (T - V)$ is the system Lagrangian and Q_k ($k = \gamma, \beta, \lambda$) denote the generalized forces due to solar radiation pressure.

The solar pressure torque about the satellite center of mass is given by

$$\begin{aligned} \bar{M}_s = & \epsilon (\cos \lambda_p \bar{j} + \sin \lambda_p \bar{k}) \times \bar{F}_1 \\ & - \epsilon (\cos \lambda_p \bar{j} + \sin \lambda_p \bar{k}) \times \bar{F}_2 \end{aligned} \quad (3.5)$$

where

$$\bar{F}_i = -2\rho pA |\cos \xi_i| \cos \xi_i \bar{n}_i, \quad i = 1, 2 \quad (3.6)$$

$$\begin{aligned}\bar{n}_i &= (\cos \delta_i) \bar{i} + (\sin \lambda_p \sin \delta_i) \bar{j} \\ &\quad - (\cos \lambda_p \sin \delta_i) \bar{k}, \quad i = 1, 2\end{aligned}\quad (3.7)$$

Using the principle of virtual work, the generalized forces are obtained as :

$$Q_Y = (2\rho p A \epsilon) [h_1 \cos \beta \cos(\lambda + \lambda_p) - h_2 \sin \beta] \quad (3.8a)$$

$$Q_\beta = -(2\rho p A \epsilon) h_2 \sin(\lambda + \lambda_p) \quad (3.8b)$$

$$Q_\lambda = (2\rho p A \epsilon) h_1 \quad (3.8c)$$

Here, the quantities h_1 and h_2 are defined to be

$$h_1 = |\cos \xi_1| \cos \xi_1 \cos \delta_1 - |\cos \xi_2| \cos \xi_2 \cos \delta_2 \quad (3.9a)$$

$$h_2 = |\cos \xi_1| \cos \xi_1 \sin \delta_1 - |\cos \xi_2| \cos \xi_2 \sin \delta_2 \quad (3.9b)$$

where

$$\begin{aligned}\cos \xi_i &= e_x \cos \delta_i + (e_y \sin \lambda_p - e_z \cos \lambda_p) \sin \delta_i, \\ (i &= 1, 2)\end{aligned}\quad (3.10)$$

and the earth-sun unit vector components e_x, e_y, e_z are given in Appendix A.

Substituting Equations (3.1), (3.3) and (3.8) in Equation (3.4), and nondimensionalizing the independent variable through the

relation $\theta = \Omega t$, the equations of attitude motion finally take the form :

$$\begin{aligned} & \{I_x \sin^2 \beta + (I_y \sin^2 \lambda + I_z \cos^2 \lambda) \cos^2 \beta\} \gamma'' \\ & + \{(I_y - I_z) \cos \beta \sin \lambda \cos \lambda\} \beta'' - \{I_x \sin \beta\} \lambda'' \\ & = f_\gamma + \tilde{C} \{h_1 \cos \beta \cos (\lambda + \lambda_p) - h_2 \sin \beta\} \end{aligned} \quad (3.11a)$$

$$\begin{aligned} & \{(I_y - I_z) \cos \beta \sin \lambda \cos \lambda\} \gamma'' + \{I_y \cos^2 \lambda + I_z \sin^2 \lambda\} \beta'' \\ & = f_\beta - \tilde{C} h_1 \sin (\lambda + \lambda_p) \end{aligned} \quad (3.11b)$$

$$- (I_x \sin \beta) \gamma'' + I_x \lambda'' = f_\lambda + \tilde{C} h_2 \quad (3.11c)$$

Here, the quantities f_k ($k = \gamma, \beta, \lambda$) are rather lengthy functions of the attitude angles and their derivatives. Their full forms are presented in Appendix A. The functions h_1, h_2 indicate the dependence of the radiation torque on the control surface rotations δ_1 and δ_2 . The parameter \tilde{C} characterizing the magnitude of the solar torque generated by the controller is given by

$$\tilde{C} = 2 \rho_p A \epsilon / \Omega^2 \quad (3.12)$$

The equations of motion consist of a sixth order, coupled, nonlinear, nonautonomous system of differential equations. Consequently, the selection of a suitable control policy for the control surface rotations δ_1, δ_2 is indeed formidable. Therefore, an approach based on the linearization of the

equations of motion about the system equilibrium configuration is presently considered.

3.2 Control Synthesis

An inspection of Equations (3.11) indicates that the system possesses the equilibrium configuration :

$$\gamma = \beta = \lambda = 0 \quad (3.13a)$$

$$\delta_1 = \delta_2 = \delta_e \text{ (arbitrary)} \quad (3.13b)$$

Physically, this implies that when the two control surfaces are parallel and no external disturbances act on the satellite, the body-fixed principal axes, x, y, z , would remain aligned with the orbital coordinates, x_o, y_o, z_o , respectively. This corresponds to the nominal earth-pointing attitude of the spacecraft. The objective of the solar controller is to maintain the earth orientation of the satellite in presence of external disturbances. For small amplitude motion near the equilibrium position, the governing equations may be simplified through linearization. Substituting $\delta_1 = \delta_e + \tilde{\delta}_1$, $\delta_2 = \delta_e + \tilde{\delta}_2$ and linearizing in $\tilde{\delta}_1, \tilde{\delta}_2, \gamma, \beta, \lambda$, Equations (3.11) take the form :

$$\gamma'' - (K_2 - 1) \beta' + 4K_2 \gamma = (\bar{C}/I_z) g_1(\theta, \phi, \delta_e) \cos \lambda_p (\tilde{\delta}_1 - \tilde{\delta}_2) \quad (3.14a)$$

$$\beta'' - (K_1 + 1) \gamma' - K_1 \beta = -(\bar{C}/I_y) g_1(\theta, \phi, \delta_e) \sin \lambda_p (\tilde{\delta}_1 - \tilde{\delta}_2) \quad (3.14b)$$

$$\lambda'' + 3 [(K_1 + K_2)/(1 + K_1 K_2)] \lambda = (\tilde{C}/I_x) g_2(\theta, \phi, \delta_e)(\tilde{\delta}_1 - \tilde{\delta}_2) \quad (3.14c)$$

where

$$g_1(\theta, \phi, \delta_e) = (1/2) |b| [3a \sin 2\delta_e + 2 \sqrt{1-a^2} (\cos^2 \delta_e + \cos 2\delta_e) \sin(\theta + \zeta)] \quad (3.15a)$$

$$g_2(\theta, \phi, \delta_e) = (1/2) |b| [2a(\sin^2 \delta_e - \cos 2\delta_e) + 3 \sqrt{1-a^2} \sin 2\delta_e \sin(\theta + \zeta)] \quad (3.15b)$$

with

$$a = \sin \phi \sin i \quad (3.16a)$$

$$b = -a \cos \delta_e + \sqrt{1-a^2} \sin \delta_e \sin(\theta + \zeta) \quad (3.16b)$$

$$\zeta = \lambda_p - \tan^{-1} (\tan \phi \cos i) \quad (3.16c)$$

The linearized equations of motion reveal certain features of the dynamic structure of the system. For small control surface excursions about the 'off' position δ_e , the radiation torque depends only on the difference $(\tilde{\delta}_1 - \tilde{\delta}_2)$ between the two control surface rotations. Consequently, all the three degrees of freedom must be controlled by maneuvering the single variable $(\tilde{\delta}_1 - \tilde{\delta}_2)$. This may lead to somewhat complicated control synthesis. From a mechanization point of view, however, it appears advantageous as pointed out earlier.

Furthermore, the uncontrolled system exhibits a gyroscopically coupled roll-yaw (out-of-orbit-plane) motion

and an uncoupled pitch (in-orbit-plane) motion. Hence, to achieve a good overall performance, the controller should provide significant torque contributions in both these modes. Nondimensional measures of the solar torques controlling the roll-yaw and pitch motions per unit differential control surface rotation are given by

$$\tilde{M}_{\gamma\beta} = \sqrt{M_{\gamma}^2 + M_{\beta}^2} / \tilde{C} (\tilde{\delta}_1 - \tilde{\delta}_2) = g_1(\theta, \phi, \delta_e) \quad (3.17a)$$

$$\tilde{M}_{\lambda} = M_{\lambda} / \tilde{C} (\tilde{\delta}_1 - \tilde{\delta}_2) = g_2(\theta, \phi, \delta_e) \quad (3.17b)$$

For best performance, the 'off' position δ_e of the control surfaces should be selected such that both $|\tilde{M}_{\gamma\beta}|$ and $|\tilde{M}_{\lambda}|$ are as large as possible for all values of θ and ϕ . The optimum δ_e would obviously be a function of both θ and ϕ . On the other hand, it would be desirable from practical considerations to have a constant δ_e about which the control surfaces rotate. Acceptable constant values of δ_e may be obtained by requiring that the average values of both $|\tilde{M}_{\gamma\beta}|$ and $|\tilde{M}_{\lambda}|$ over an orbit be sufficiently high. Restricting attention to near ecliptic orbits ($i \leq 30^\circ$), the effect of ϕ on the magnitudes of g_1 and g_2 becomes relatively small. Analysis shows that most choices of δ_e , except very near $\delta_e = 0$ or 90° , lead to sufficiently high values of the average out-of-plane and in-plane solar torque components. Best results were obtained with $\delta_e \approx 30^\circ, 105^\circ$.

Optimal control theory is next applied to derive a feedback control law for the differential control surface rotation $(\tilde{\delta}_1 - \tilde{\delta}_2)$. This is rendered convenient by first expressing Equations (3.14) in the state variable form. Letting $x_1 = \gamma$, $x_2 = \gamma'$, $x_3 = \beta$, $x_4 = \beta'$, $x_5 = \lambda$, $x_6 = \lambda'$ and $u = (\tilde{\delta}_1 - \tilde{\delta}_2)$, they take the form,

$$\dot{\bar{x}}(\theta) = A\bar{x}(\theta) + B(\theta) \bar{u}(\theta) \quad (3.18)$$

where the matrices A and B are given by,

$$A = \begin{bmatrix} 0 & 1 & 0 & 0 & 0 & 0 \\ -4K_2 & 0 & 0 & K_2-1 & 0 & 0 \\ 0 & 0 & 0 & 1 & 0 & 0 \\ 0 & K_1+1 & K_1 & 0 & 0 & 0 \\ 0 & 0 & 0 & 0 & 0 & 1 \\ 0 & 0 & 0 & 0 & \frac{-3(K_1+K_2)}{1+K_1K_2} & 0 \end{bmatrix} \quad \text{and } B(\theta) = \begin{bmatrix} 0 \\ (\tilde{C}/I_z)g_1 \cos \lambda_1 \\ 0 \\ (\tilde{C}/I_y)g_1 \sin \lambda_p \\ 0 \\ (\tilde{C}/I_x)g_2 \end{bmatrix} \quad (3.19)$$

It is noticed that the constant A matrix depends on the satellite shape parameters K_1, K_2 which determine the stability of the uncontrolled satellite. The elements of the B matrix, on the other hand, are periodic functions of the orbital time θ .

In order to obtain a feedback control law which assures asymptotically stable operation of the system, we consider the minimization of the quadratic performance index³³

$$J = (1/2) \int_0^{\theta_f \rightarrow \infty} [\bar{x}^T(\theta) Q(\theta) \bar{x}(\theta) + \bar{u}^T(\theta) W(\theta) \bar{u}(\theta)] d\theta \quad (3.20)$$

where $Q(\theta)$ and $W(\theta)$ represent positive semidefinite and positive definite weighting matrices, respectively. The control law minimizing the index (3.20) is well known to be³⁴

$$\bar{u}(\theta) = F(\theta) \bar{x}(\theta) \quad (3.21)$$

where the gain matrix $F(\theta)$ is given by

$$F(\theta) = -W^{-1}(\theta) B^T(\theta) K(\theta) \quad (3.22)$$

Here, $K(\theta)$ represents the solution of the matrix-Riccati equation

$$\begin{aligned} K'(\theta) = & -K(\theta) A - A^T K(\theta) - Q(\theta) \\ & + K(\theta) B(\theta) W(\theta)^{-1} B^T(\theta) K(\theta) \end{aligned} \quad (3.23)$$

with boundary condition $K(\theta_f \rightarrow \infty) = 0$.

3.3 Computational Procedure

The attitude control performance of the system was evaluated for a specific satellite equipped with the solar controller. The data used and the computational procedure employed are summarized below :

- (i) A triaxial spacecraft in the geostationary orbit
($i = 23.5^\circ$) with the following inertia properties is considered: $I_x = 400$, $I_y = 275$, $I_z = 620 \text{ kg} - \text{m}^2$.

These inertia values lead to the shape parameters

$K_1 = 0.8$, $K_2 = 0.2$ which correspond to an unstable earth-pointing configuration in absence of the controller³⁵.

The inertia parameter values were so selected purposefully in order to examine the controller performance under adverse gravitational conditions.

The control surface areas, moment arms, the body location of the control surface rotation axes and their 'off' position are taken to be, $A = 1 \text{ m}^2$, $\epsilon = 3 \text{ m}$, $\lambda_p = 0$, $\delta_e = 105^\circ$, which result in the parameter $\tilde{C} = 4860 \text{ kg-m}^2$.

- (ii) The choice of weighting matrices $Q(\theta)$ and $W(\theta)$, is somewhat arbitrary. Presently, they are both taken to be identity matrices. This corresponds to assigning equal weights to the attitude error, attitude rate and the differential control surface rotation.
- (iii) A value of the solar aspect angle ϕ is selected next. This completes the parameter specification for the problem.
- (iv) The matrix-Riccati equation (3.23) is then solved backward in time with the boundary condition $K(\theta_f \rightarrow \infty) = 0$. In practice, $\theta_f = 10$ orbits was found to be sufficiently large for the solution $K(\theta)$ to reach a steady state periodic character with a period 2π .

(v) The associated 2π - periodic gain matrix,

$$F(\theta) = [F_Y \quad F_Y' \quad F_\beta \quad F_\beta' \quad F_\lambda \quad F_\lambda'] \quad (3.24)$$

is evaluated next from Equation (3.22). Fourier coefficients are fitted to the system feedback gains to facilitate their subsequent generation.

(vi) Finally, the full nonlinear Equations (3.11) governing the system dynamics are integrated to obtain the attitude response of the system. The simulation requires the control surface rotations δ_1, δ_2 measured from the yz-plane. Assuming the surfaces to be driven by equal amounts in opposite directions from the 'off' position δ_e , one obtains,

$$\delta_1 = \delta_e + u/2 \quad (3.25a)$$

$$\delta_2 = \delta_e - u/2 \quad (3.25b)$$

The possibility of loss of control during the eclipse of the satellite by the earth was also considered. For this purpose, the shadow criterion (Appendix C) was introduced during the evaluation of the attitude response.

(vii) For different values of ϕ , the steps (iv) to (vi) are repeated to evaluate the system performance at different times of the year. It is noted that replacing ϕ by $(\phi + \pi)$ and u by $-u$ leaves the governing Equations (3.11) unchanged. Hence, it is only necessary to vary ϕ over a half-year period.

3.4 Results and Discussion

Figures 3.3 and 3.4 present the system gains for different values of the solar aspect angle ϕ . The gains are plotted as functions of $\eta = (\theta + \zeta)$ for convenience. It is apparent that the nature of the pitch gains F_λ, F_λ' is quite different from that of the roll and yaw gains F_γ, F_γ' and F_β, F_β' . In particular, F_γ and F_β always maintain opposite signs while the corresponding rate gains F_γ' and F_β' always have the same sign. This behaviour appears to be due to the gyroscopic coupling between the roll and yaw degrees of freedom.

Although the gains have been computed for the satellite in the equatorial orbit, the gain histories shown for $\phi = 0$ have a much wider implication. Note that the governing system Equation (3.14), with η as the independent variable, remain the same in the situations $i = \text{arbitrary}, \phi = 0$ and $i = 0, \phi = \text{arbitrary}$. Consequently, the results shown for $\phi = 0$ also represent the gain histories required for a satellite in the ecliptic plane at all times of the year. In such a case, the gain histories show a skew-symmetric variation from their zero mean value which corresponds to the skew-symmetric nature of the functions $g_1(\theta), g_2(\theta)$ with the parameter $a = \sin \phi \sin i$ equalling zero.

As pointed out earlier Fourier series representation for the periodic gains was employed for evaluating the system

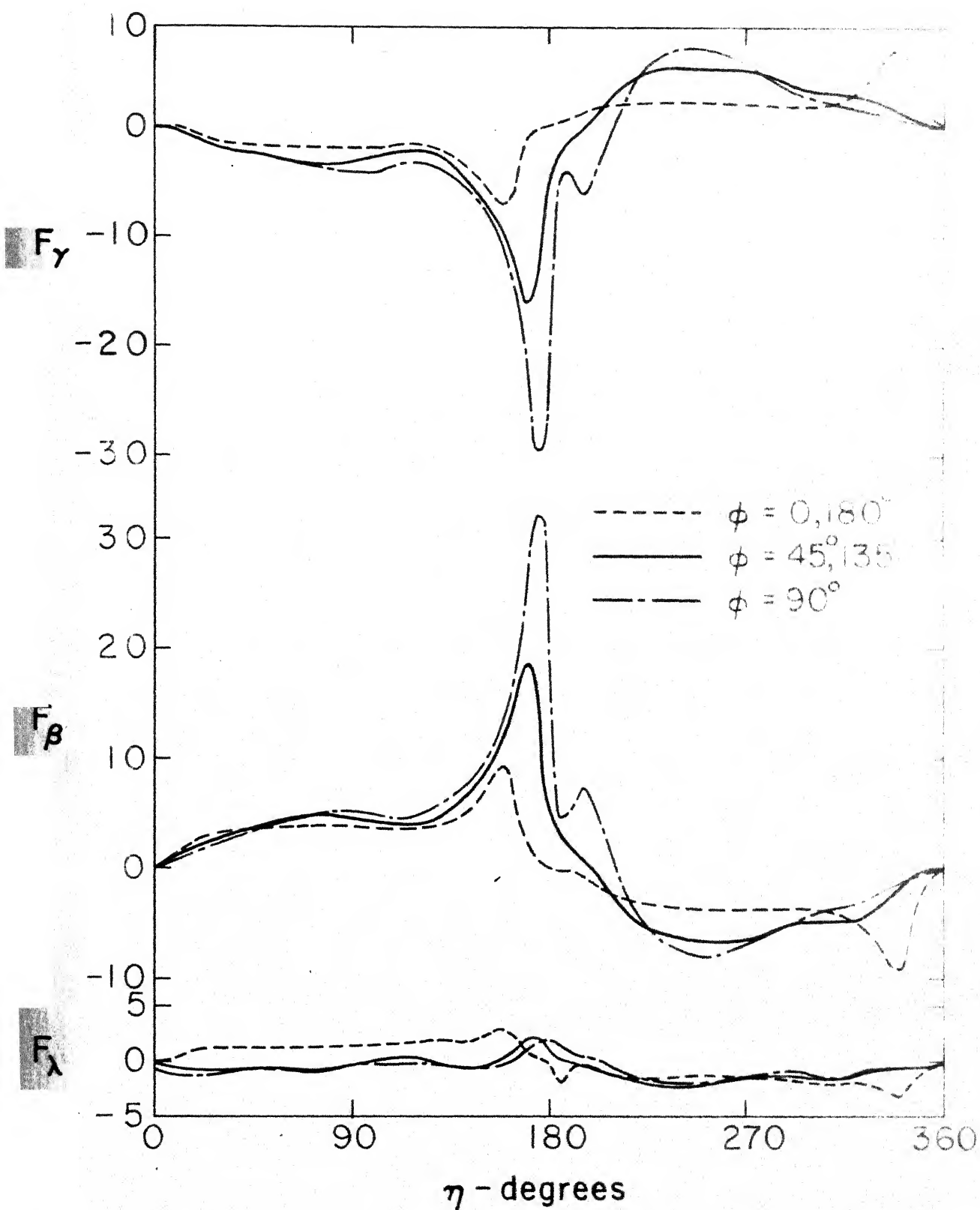


Fig. 3.3 Roll, yaw and pitch attitude gains for different values of ϕ

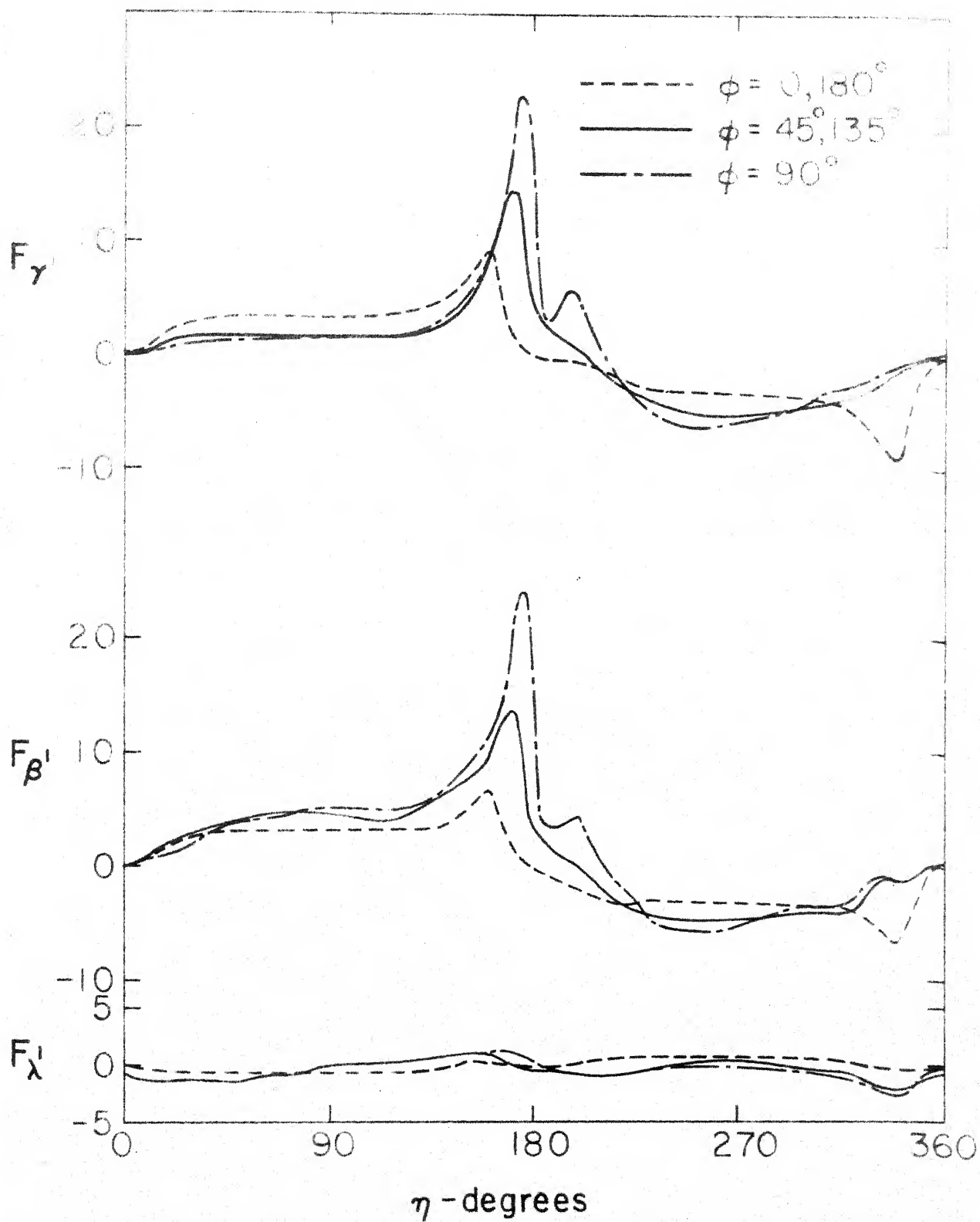


Fig. 3.4 Roll, yaw and pitch attitude rate gains for different values of ϕ

response. Fourier series truncated after five sine and cosine terms gave results with sufficient accuracy. Typical attitude response of the spacecraft following an initial misalignment of 10° about each of the roll, yaw and pitch axes is shown in Figure 3.5. The time-history of the differential control surface rotation u is also indicated. Complete correction about all the three axes is achieved within two orbits. The maximum control surface excursions from their mean position are also reasonably small. The responses shown for two different times of the year, $\phi = 45^\circ$ and $\phi = 90^\circ$, exhibit only local variations in their behaviour. The overall damping time remains practically the same.

Figure 3.6 shows the controller performance when the spacecraft is subjected to impulsive disturbances such as might result from micrometeorite impacts. It is apparent that the system is able to damp out the effect of simultaneous disturbances of 0.05 about each axis in slightly over two orbits. Again, the effect of ϕ is limited to local changes in the response character.

The geostationary orbit, for $\phi = 45^\circ$ and $\phi = 90^\circ$, happens to be entirely free from the earth's shadow. To evaluate its influence, the worst situation of $\phi = 0$ leading to the longest shadow passage is considered. Typical system responses, with and without the shadow effect, are shown in Figure 3.7. It is

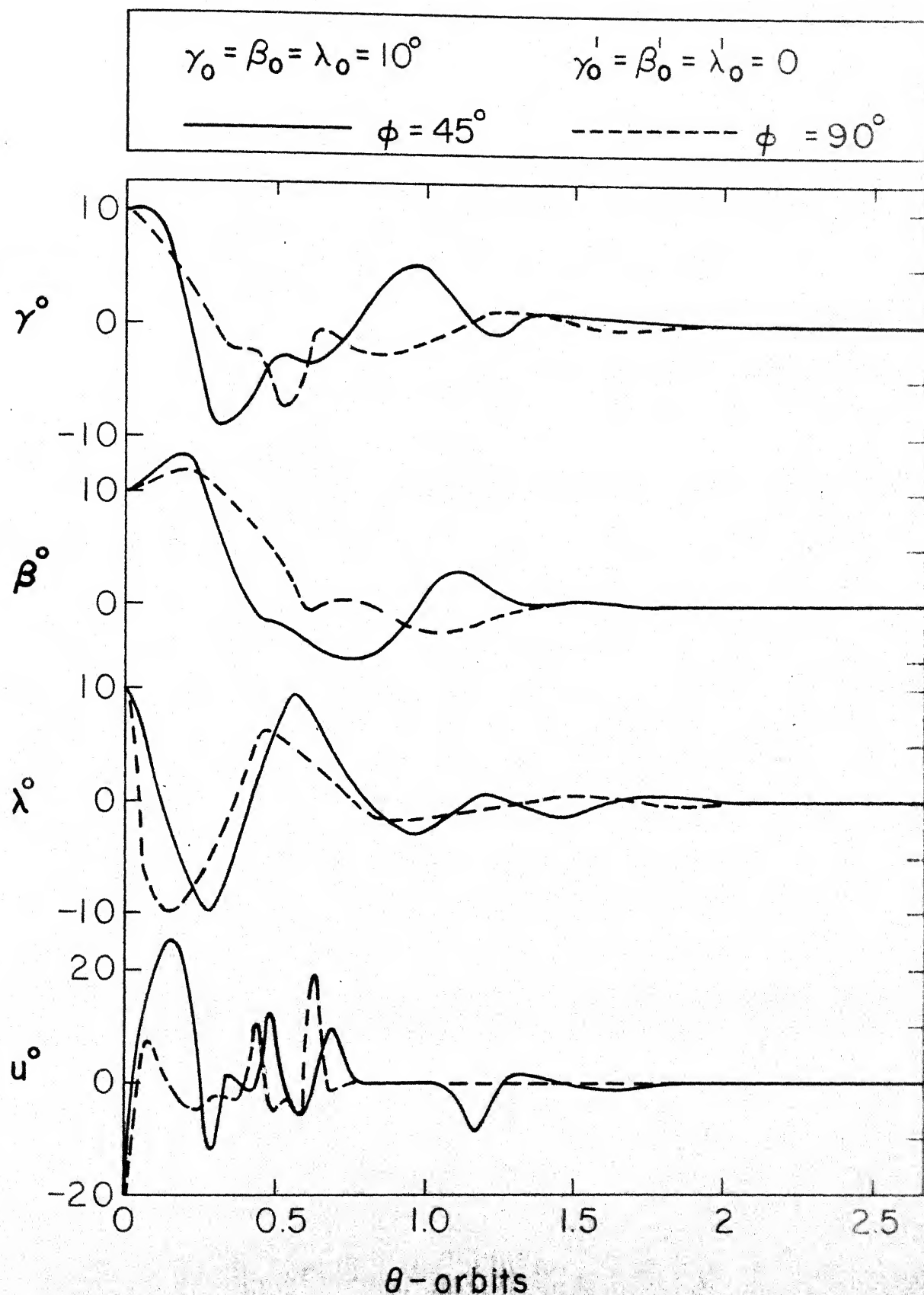


Fig. 3-5 Attitude response and control history subsequent to initial position disturbance, $\phi = 45^\circ, 90^\circ$

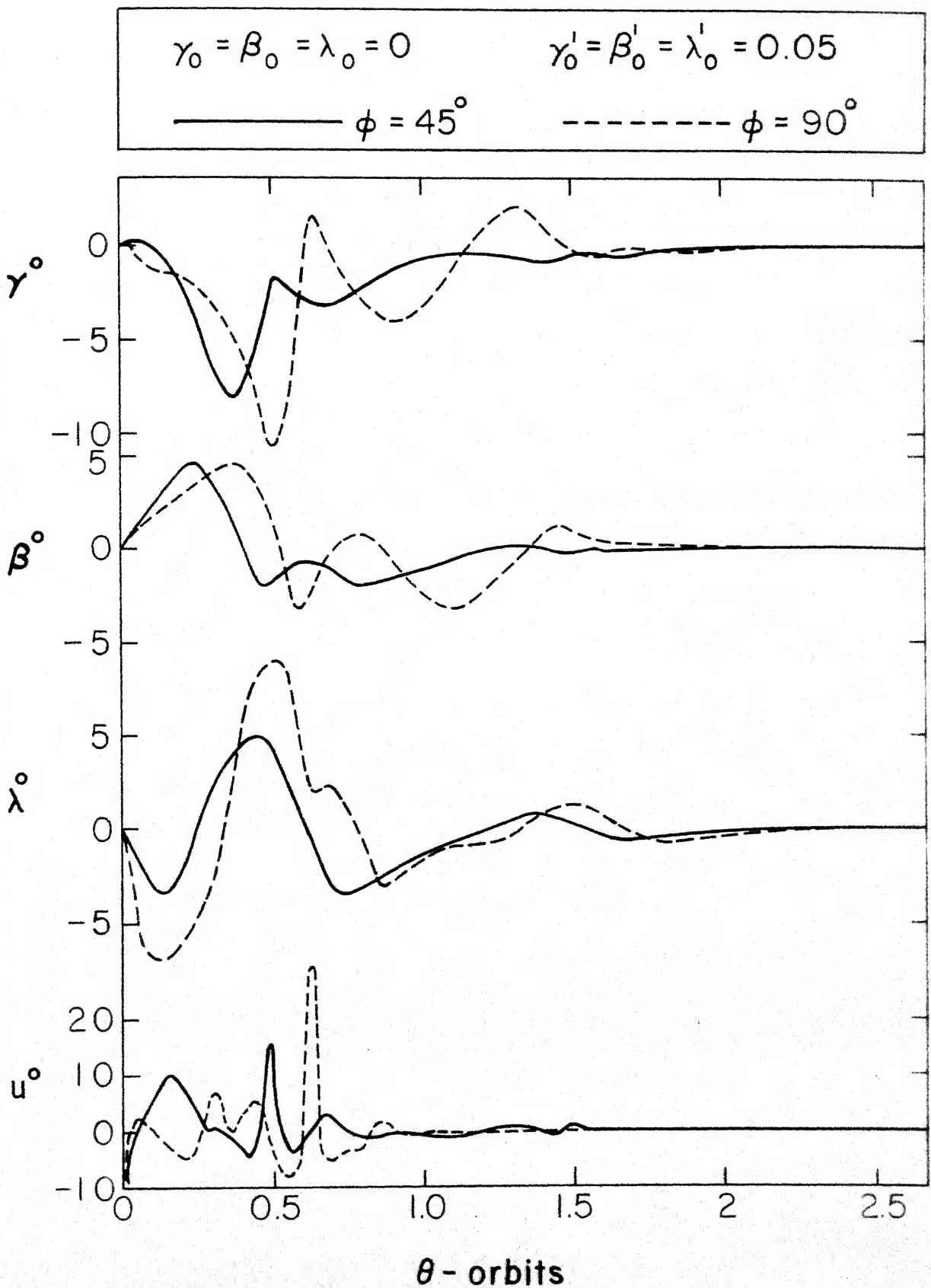


Fig. 3-6 Attitude response and control history subsequent to initial impulsive disturbance, $\phi = 45^\circ, 90^\circ$

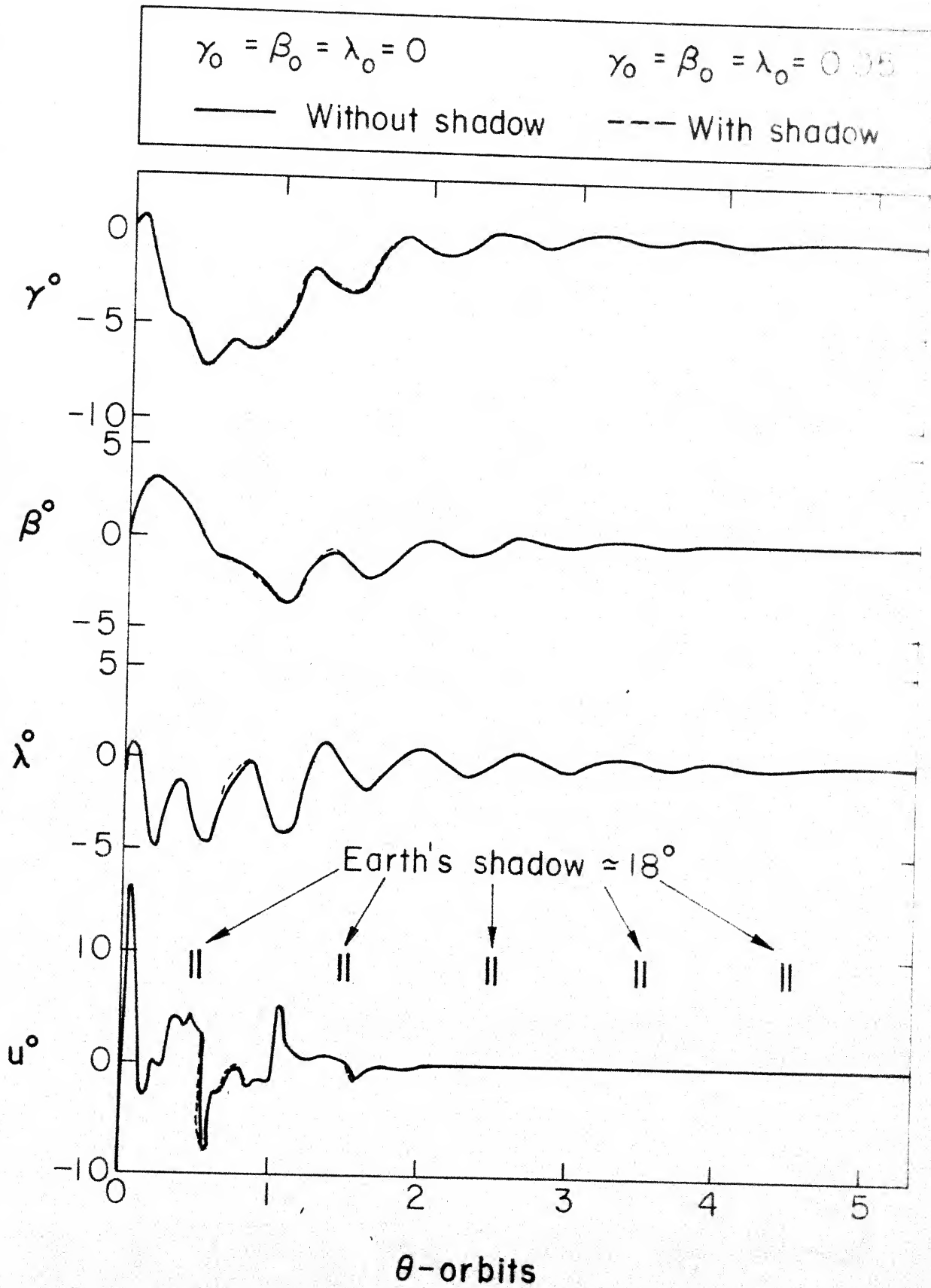


Fig. 3.7 Attitude response and control history subsequent to initial impulsive disturbance, $\phi = 0$

variations of ϕ in the latter range of ϕ (Figures 3.3 and 3.4). The analysis thus suggests that a judiciously selected gain scheduling scheme may be introduced to achieve suboptimal control resulting in reduced gain computations.

In the present analysis, the yaw control is achieved entirely through the coupling between the roll and yaw motions as the controller location λ_p was taken to be zero. With a suitable selection of λ_p , a better distribution of the control action between the roll and yaw motions would be possible with the prospect of an improved overall performance. In general, the control surface rotation axis may be skewed at any angle relative to the spacecraft axes x, y, z . Its best orientation would depend on the orbital inclination from the ecliptic.

3.5 Concluding Remarks

The significant conclusions based on the analysis may be summarized as follows :

- (i) A solar pressure attitude control system for the simultaneous roll, yaw and pitch control of earth-pointing spacecraft has been developed. The controller design minimizes the hardware requirements as it involves only two control surfaces which may be rotated differentially by a common drive mechanism.

- (ii) The hardware reduction is associated with the implementation of time-varying periodic gains which need to be continuously updated as the sun-line rotates during the year. However, effective suboptimal control may be achieved by adopting a judicious gain scheduling scheme which involves updating the gains only a few times per year.
- (iii) The controller, even with moderately sized solar surfaces, is found to be capable of maintaining the spacecraft attitude against severe external disturbances as well as destabilizing gravitational torques.
- (iv) The control system promises asymptotically stable operation throughout the year.
- (v) The influence of the earth's shadow on the performance is found to be negligible for spacecraft in geostationary orbits.
- (vi) The performance of the system is likely to improve through optimal orientation of the control surface location relative to the spacecraft body.

4. PITCH STABILIZATION OF SPACECRAFT IN AN INERTIALLY-FIXED ATTITUDE

The analyses so far have dealt with the problem of achieving an earth-pointing spacecraft attitude by means of solar radiation pressure. However, its utilization for attaining a space-oriented satellite attitude has remained unexplored. On the other hand, there are long-life spacecraft missions, such as those involving astronomical observations, which demand stabilization along inertially-fixed orientations. It therefore appears interesting to extend the solar pressure control technique for inertial attitude stabilization. If successful, it would represent an inexpensive method of attitude control for an important class of space applications.

This chapter examines the potential of the two-surface solar controller for stabilizing the pitch attitude of an unsymmetrical satellite along an inertially-fixed orientation. A control strategy involving a nominal control to counter the gravitational torque and a feedback control to impart stability to the system is developed. An essentially analytical approach leads to control laws that are easy to implement. The stability properties of the system are established for all times of the year. The influence of the important system parameters and the earth's shadow on the system performance is analyzed.

4.1 Problem Formulation and Control Synthesis

Figure 4.1 shows the geometry of the orbital and attitude motion of an unsymmetrical satellite with its center of mass S moving in a circular orbit about the earth's center O . The inertial coordinate system X, Y, Z is selected such that the Y -axis lies at an angle α_e from the line of nodes, YZ represents the plane of the orbit and the X -axis is along the orbit normal. The body-fixed principal axis y points in Y direction when the spacecraft has the desired inertially-fixed pitch orientation. The orbital angle θ is measured from the Y -axis. The angle α represents the inertial pitch attitude of the spacecraft measured from the line of nodes. The controller configuration is assumed to be the same as in Chapter 2 for maintaining an earth-pointing attitude.

The equation of pitch motion may be readily obtained by replacing θ by $(\theta + \alpha_e)$ and λ by $(\alpha - \alpha_e - \theta)$ in Equation (2.13) as

$$\alpha'' + 3K \sin(\alpha - \alpha_e - \theta) \cos(\alpha - \alpha_e - \theta) = C \sigma \{ |\sin(\zeta + \alpha - \alpha_e + \delta_1)| \sin(\zeta + \alpha - \alpha_e + \delta_1) \cos \delta_1 - |\sin(\zeta + \alpha - \alpha_e + \delta_2)| \sin(\zeta + \alpha - \alpha_e + \delta_2) \cos \delta_2 \} \quad (4.1)$$

where the solar parameter C , characterizing the controller size, is defined as

$$C = 2\rho p A \epsilon / \Omega^2 I_x \quad (4.2a)$$

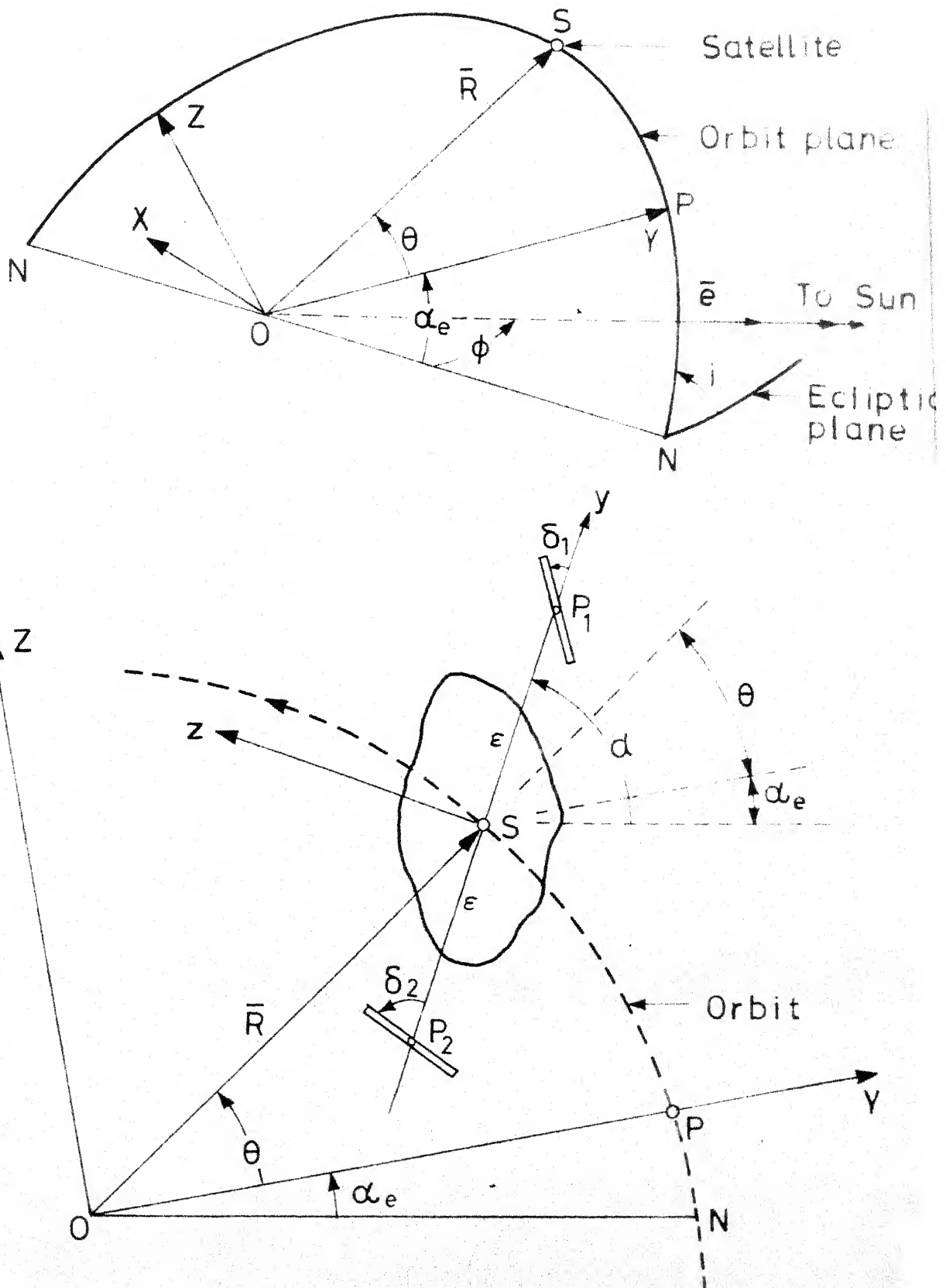


Fig. 4-1 Geometry of orbital and attitude motion

and the quantities σ and ζ are given by

$$\sigma(\phi) = 1 - \sin^2 \phi \sin^2 i \quad (4.2b)$$

$$\zeta(\phi) = \alpha_e - \arctan(\tan \phi \cos i) \quad (4.2c)$$

In absence of the controller, $\alpha = \alpha_e + \theta$ satisfies Equation (4.1). Physically, this corresponds to gravitational stabilization in an earth-pointing attitude. Inertial stabilization in a fixed attitude would require $\alpha = \alpha_e$ to be an identical solution of the pitch equation. Setting $\alpha = \alpha_e$ in Equation (4.1), the nominal controls required to counter the gravity torque are governed by

$$\begin{aligned} |\sin(\zeta + \delta_{10})| \sin(\zeta + \delta_{10}) \cos \delta_{10} - |\sin(\zeta + \delta_{20})| \\ \sin(\zeta + \delta_{20}) \cos \delta_{20} = -(3K/2C\sigma) \sin 2\theta \end{aligned} \quad (4.3)$$

The two unknowns $\delta_{10}(\theta)$, $\delta_{20}(\theta)$, however, cannot be determined from this single relation and a degree of arbitrariness remains as to their choice. A convenient constraint would be to permit them equal and opposite rotations about some mean position δ_e , i.e., let

$$\delta_{10}(\theta) = \delta_e + \delta_o(\theta) \quad (4.4a)$$

$$\delta_{20}(\theta) = \delta_e - \delta_o(\theta) \quad (4.4b)$$

Substituting in Equation (4.3), the nominal control $\delta_o(\theta)$ is then obtained from

$$\begin{aligned}
& |\sin(\zeta + \delta_e + \delta_o)| \sin(\zeta + \delta_e + \delta_o) \cos(\delta_e + \delta_o) \\
& - |\sin(\zeta + \delta_e - \delta_o)| \sin(\zeta + \delta_e - \delta_o) \cos(\delta_e - \delta_o) \\
& = -(3K/2C\sigma) \sin 2\theta
\end{aligned} \tag{4.5}$$

The transcendental nature of Equation (4.5) indicates that, in general, continuous onboard numerical computation must be performed to solve for $\delta_o(\theta)$. On the other hand, an analytical solution would be much easier to implement. It is apparent that $\delta_o = 0$ represents the solution when the right hand side of Equation (4.5) is zero, as would be the case for a satellite with symmetry about the pitch axis. When conditions exist such that $|K/C\sigma| \ll 1$ throughout the year, the solution $\delta_o(\theta)$ would be expected to remain small. Noting that $|K| \leq 1$ and $\sigma \geq \cos^2 i$, the requirement can be met for most satellites with a fairly moderate controller size, except in orbits with too large an inclination from the ecliptic. As an example, for a satellite in the geostationary orbit having $I_x = 250 \text{ Kg-m}^2$, $K = 0.5$ and a controller with $A = 0.25 \text{ m}^2$, $\epsilon = 3\text{m}$, $|K/C\sigma|_{\max} = 0.114 \ll 1$. For small $\delta_o(\theta)$, therefore, the left hand side of Equation (4.5) may be expanded in powers of δ_o and only the linear terms retained. This results in the approximate solution

$$\delta_o(\theta) = -(3K/4C\sigma D) \sin 2\theta \tag{4.6}$$

where

$$\begin{aligned}
D = & |\sin(\zeta + \delta_e)| \{ 2 \cos \delta_e \cos(\zeta + \delta_e) \\
& - \sin \delta_e \sin(\zeta + \delta_e) \}
\end{aligned} \tag{4.7}$$

The analytical approach would be justified provided the quantity D does not become too small at any time of the year. The obvious solution lies in suitably updating the mean position δ_e as ζ varies slowly, i.e., let $\delta_e = \delta_e(\zeta)$. Best results would be obtained by upgrading δ_e such that it maximizes $|D|$ for a given ζ . The variation of the optimal δ_e with ζ is indicated in Figure 4.2a. The relationship is not only periodic with a half-year period but is also practically linear, making the selection of the optimum δ_e quite simple. The figure also shows the variation of the associated $|D|$ which remains within the limits $1 \leq |D| \leq 1.16$. This establishes the validity of the analytical solution for all times. Its accuracy was assessed by comparison with the exact solution obtained by numerically solving Equation (4.5) for several parameter combinations. Excellent agreement was found as reflected by the typical plots shown in Figure 4.2b.

It should be pointed out here that various other choices of the relation $\delta_e = \delta_e(\zeta)$ would also result in sufficiently large values of $|D|$. For example, δ_e may be assigned a constant value over a range of ζ (i.e., ϕ) and then updated to a new constant value over the next range of ζ . This would amount to replacing the optimum curve in Figure 4.2a by a stepped function.

Although the nominal control opposes the disturbing gravitational torque, it does not stabilize the satellite

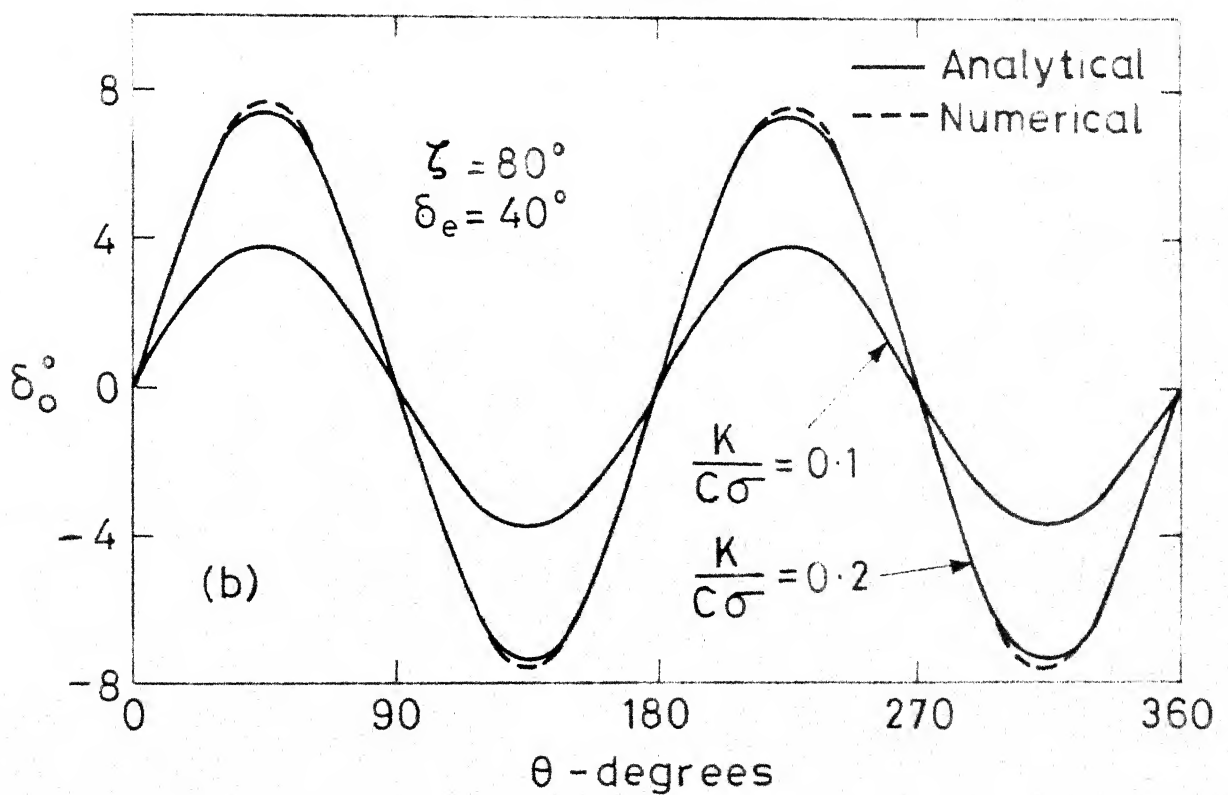
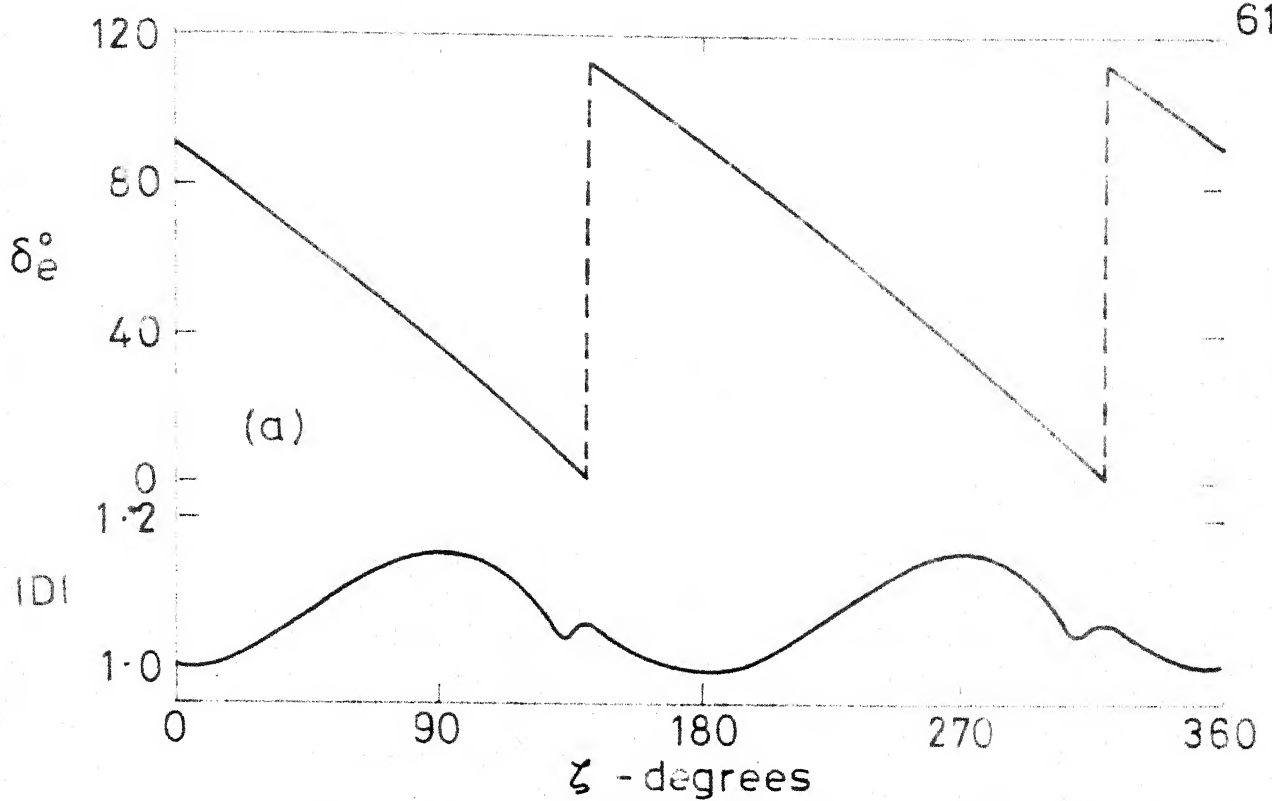


Fig. 4.2 (a) Variation of optimal δ_e and $|D|$ with ζ
 (b) Typical comparison of the approximate and exact nominal control $\delta_o(\theta)$

against initial errors or disturbances such as might arise from micrometeorite impacts. A suitable feedback control system is hence required. Letting $\tilde{\delta}$ denote the additional feedback controlled rotations to be provided, the total control surface rotations become

$$\delta_1 = \delta_e + \delta_o + \tilde{\delta} \quad (4.8a)$$

$$\delta_2 = \delta_e - \delta_o - \tilde{\delta} \quad (4.8b)$$

For the general case of an arbitrarily large $\delta_o(\theta)$, the equation of motion in the neighbourhood of the desired inertially-fixed orientation α_e may be obtained by letting $\alpha = \alpha_e + \tilde{\alpha}$, substituting Equations (4.8) in Equation (4.1), and linearizing in $\tilde{\alpha}$ and $\tilde{\delta}$. Subsequent to considerable algebraic manipulations, with due regard to Equation (4.5), this results in

$$\tilde{\alpha}'' + \{3K \cos 2\theta - C\sigma f_1(\theta)\}\tilde{\alpha} - \{C\sigma f_2(\theta)\}\tilde{\delta} = 0 \quad (4.9)$$

where

$$\begin{aligned} f_1(\theta) = 2\{ & |\sin(\zeta + \delta_e + \delta_o)| \cos(\zeta + \delta_e + \delta_o) \cos(\delta_e + \delta_o) \\ & - |\sin(\zeta + \delta_e - \delta_o)| \cos(\zeta + \delta_e - \delta_o) \cos(\delta_e - \delta_o)\} \end{aligned} \quad (4.10a)$$

$$\begin{aligned} f_2(\theta) = f_1(\theta) - \{ & |\sin(\zeta + \delta_e + \delta_o)| \sin(\zeta + \delta_e + \delta_o) \sin(\delta_e + \delta_o) \\ & - |\sin(\zeta + \delta_e - \delta_o)| \sin(\zeta + \delta_e - \delta_o) \sin(\delta_e - \delta_o)\} \end{aligned} \quad (4.10b)$$

Equation (4.9) represents a linear controlled system with complicated time-varying coefficients dependent on the nominal control $\delta_0(\theta)$. The low order of the system, however, suggests the possibility of analytically synthesizing a suitable feedback control law.

The problem simplifies considerably if attention is restricted to the case of small $K/C\sigma$ values leading to small $\delta_0(\theta)$. One may then expand the coefficients of $\tilde{\alpha}$ and $\tilde{\delta}$ in Equation (4.9) and retain only the first order terms in δ_0 to obtain

$$\tilde{\alpha}'' + (3K \cos 2\theta - 2C\sigma E\delta_0)\tilde{\alpha} - (2C\sigma D)\tilde{\delta} = 0 \quad (4.11)$$

where

$$E = \{ 2 \cos \delta_e \cos 2(\zeta + \delta_e) - \sin \delta_e \sin 2(\zeta + \delta_e) \} \operatorname{sgn} \{ \sin(\zeta + \delta_e) \} \quad (4.12)$$

Substituting the analytical solution (4.6) for $\delta_0(\theta)$, the governing equation takes the form

$$\tilde{\alpha}'' + \{ 3K(1+E^2/4D^2)^{\frac{1}{2}} \cos(2\theta - v) \} \tilde{\alpha} - (2C\sigma D)\tilde{\delta} = 0 \quad (4.13)$$

where

$$v = \arctan (E/2D) \quad (4.14)$$

In absence of the feedback control $\tilde{\delta}$, the attitude motion near the nominal orientation is governed by an undamped second order differential equation with a periodic coefficient. The control law for $\tilde{\delta}$ should be so chosen that it introduces

corrective restoring and damping effects into the system. A logical choice which is simple to realize would be a piecewise linear control law of the form

$$\tilde{\delta} = - (\mu \tilde{\alpha}' + \nu \tilde{\alpha}) \operatorname{sgn} D \quad (4.15)$$

where μ , ν represent constant system gains.

4.2 Stability Analysis

The usefulness of the proposed control law would be established provided it leads to asymptotically stable system operation for a wide choice of the controller gains.

Substituting Equation (4.15) in Equation (4.13), and shifting the independent variable from θ to $(\theta - \nu/2)$ for convenience, the dynamics of the controlled pitch motion is governed by

$$\tilde{\alpha}'' + \tilde{\mu} \tilde{\alpha}' + (\tilde{\nu} + q \cos 2\theta) \tilde{\alpha} = 0 \quad (4.16)$$

where the parameters $\tilde{\mu}$, $\tilde{\nu}$ and q are defined as :

$$\tilde{\mu} = 2C \sigma |D| \mu \quad (4.17a)$$

$$\tilde{\nu} = 2C \sigma |D| \nu \quad (4.17b)$$

$$q = 3K(1+E^2/4D^2)^{\frac{1}{2}} \quad (4.17c)$$

Equation (4.16) represents a linear differential equation with a time-varying periodic coefficient. Floquet theory³¹ may therefore be applied to investigate the stability properties as a function of the parameters $\tilde{\mu}$, $\tilde{\nu}$ and q . The

method involves the examination of the characteristic multipliers of the system. In absence of a closed form solution, their determination requires numerical integration of Equation (4.16) twice over the period π for every combination of $\tilde{\mu}$, $\tilde{\nu}$ and q . Considerable saving of computational work occurs if one eliminates the first derivative term through the transformation

$$\tilde{\alpha} = x e^{-\tilde{\mu}\theta/2} \quad (4.18)$$

which converts Equation (4.16) to

$$x'' + (h + q \cos 2\theta)x = 0 \quad (4.19)$$

where

$$h = \tilde{\nu} - \tilde{\mu}^2/4 \quad (4.20)$$

Equation (4.19) is the classical Mathieu equation whose stability properties are well known. In the h, q plane, the stable and unstable regions occur alternately with transition curves associated with periodic solutions of period π and 2π separating them. For a chosen value of q , a sequence of values of h separating the stable and unstable regions is obtained. These in turn map into parabolas in the $\tilde{\mu}, \tilde{\nu}$ plane (Figures 4.3 and 4.4) in accordance with Equation (4.20). As the solution x can at best exhibit ordinary stability, the asymptotic stability of α requires that $\tilde{\mu}$, and hence the gain μ , must be positive. The entire region of stability for x thus corresponds to asymptotic stability of α .

To determine the regions of asymptotic stability of α which overlap the instability regions of x , consider the solution x of Equation (4.19) which has the form

$$x = C_1 e^{\gamma_1 \theta} p_1(\theta) + C_2 e^{\gamma_2 \theta} p_2(\theta) \quad (4.21)$$

where $p_1(\theta)$, $p_2(\theta)$ are periodic functions of period π , C_1 and C_2 represent arbitrary constants and γ_1 , γ_2 are the characteristic exponents of the system. The real parts of γ_1 , γ_2 may be obtained from the characteristic multipliers ρ_1 , ρ_2 as

$$r_i = \ln |\rho_i| / \pi, \quad i = 1, 2 \quad (4.22)$$

Substituting Equation (4.21) in Equation (4.18), it is apparent that in the instability region for x , where at least one of the $r_i > 0$, $\tilde{\alpha} \rightarrow 0$ as $\theta \rightarrow \infty$ provided $\tilde{\mu}/2$ exceeds r_{\max} , the greater of the r_i .

With the selected value of q , a number of values of h lying in the unstable regions of x in the h, q plane were identified. In conjunction with numerical integration of Equation (4.19), Floquet theory was used to determine the characteristic multipliers and the real parts of the characteristic exponents. Proceeding to the $\tilde{\mu}$, $\tilde{\nu}$ plane, this results in parabolic contours of constant r_{\max} filling the instability regions of x . The asymptotic stability region for $\tilde{\alpha}$, overlapping the instability region of x , is then identified by requiring that $\tilde{\mu}/2 > r_{\max}$.

The stability investigation was carried out for several values of q and the resulting information is presented in Figures 4.3 and 4.4 in the form of stability charts in the \tilde{u}, \tilde{v} plane with q as a parameter. The stability charts may be thought of as cross-sections of a three-dimensional \tilde{u}, \tilde{v}, q space depicting the stability behaviour. Note also that, in view of the symmetry properties of the Mathieu equation, the same charts result for both positive and negative values of q . As anticipated, the instability regions increase with an increase in q .

Proper interpretation of the stability results requires a consideration of Equation (4.17) which indicate that the parameters \tilde{u}, \tilde{v} and q acquire different values at different times of the year. Also, the nature of their slow variation depends on the upgrading policy $\delta_e = \delta_e(\zeta)$ through the quantities D and E . For a given satellite and controller (constant K, C, μ, ν), the system representative point therefore moves during the year in the \tilde{u}, \tilde{v} plane and the stability-instability regions also change as q varies. A safe design would be achieved when the controller parameters C, μ, ν are such that the representative point remains within the stable region which is common for all the q values encountered during the year. Fortunately, the stability-instability pattern varies with q in such a manner that the desired common region can be readily identified by considering the stability chart

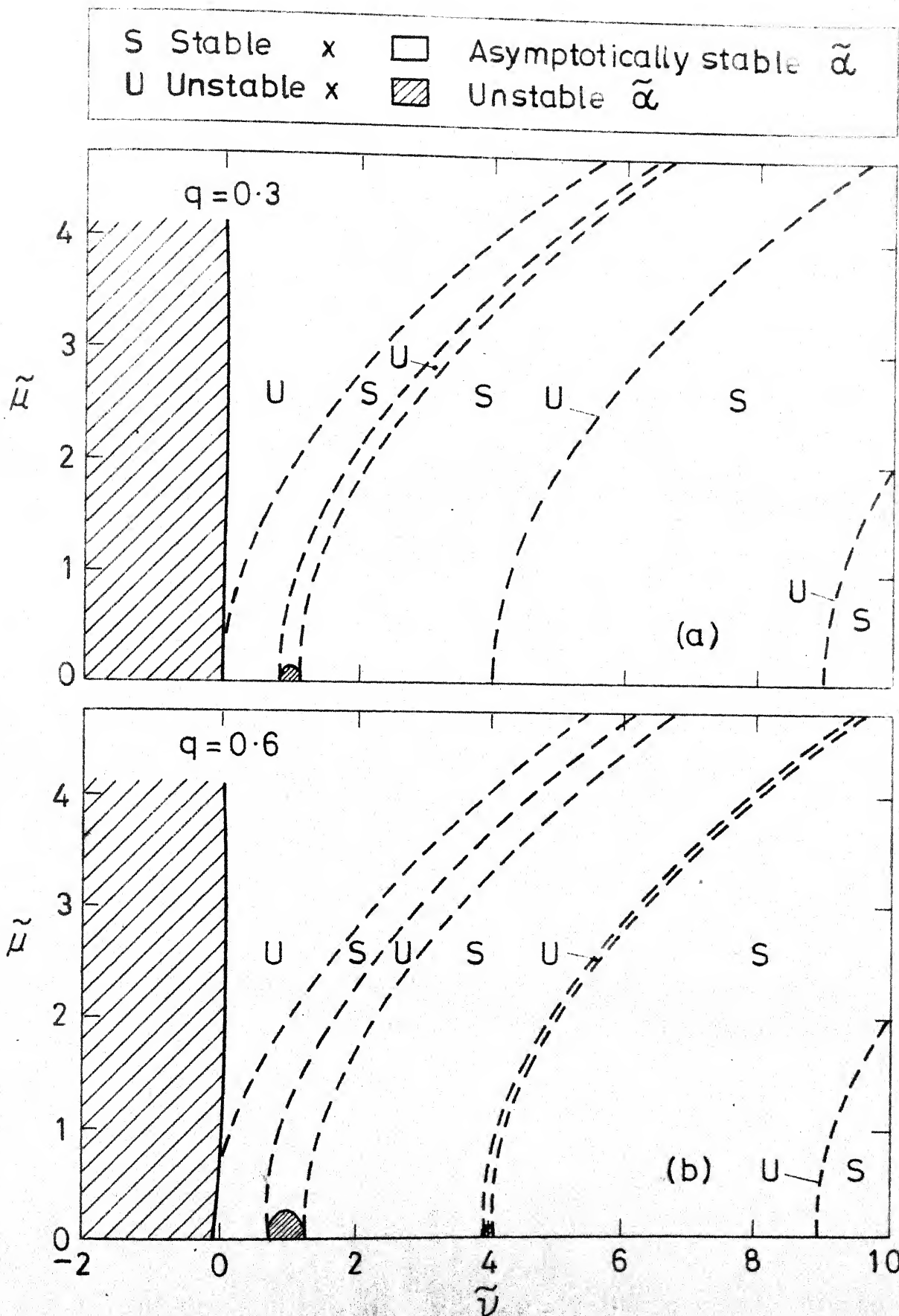


Fig. 4.3 Stability charts for (a) $q=0.3$, (b) $q=0.6$

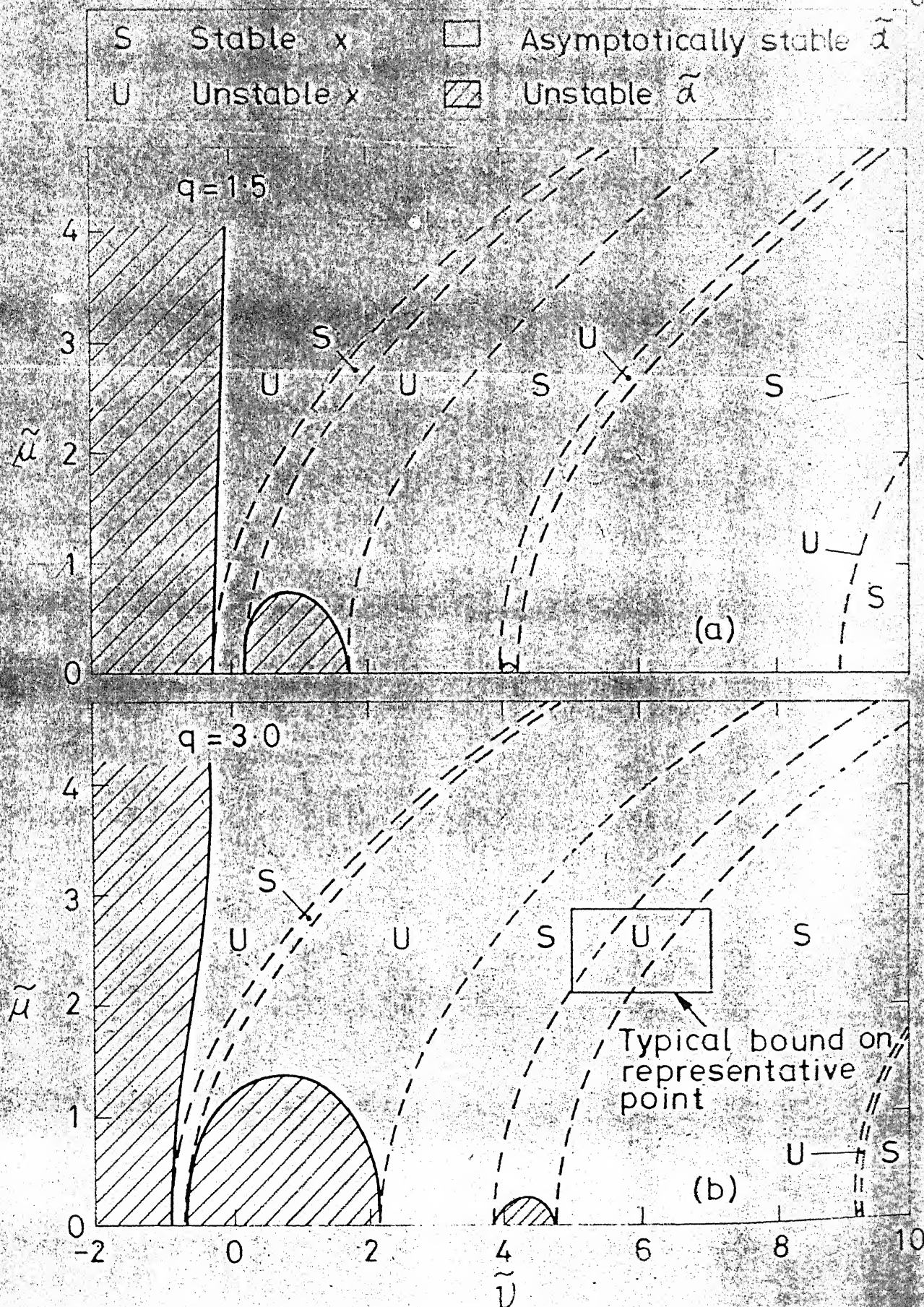


Fig. 4-4 (a) Stability chart for $q = 1.5$
 (b) Stability chart for $q = 3.0$ showing the
 rectangular bound on the representative
 point for $i = 23.5^\circ$, $C = 5$, $\mu = 0.25$, $\nu = 0.6$

for the worst time of the year corresponding to the maximum value of q .

For example, in conjunction with the strategy $\delta_e = \delta_e(\zeta)$ developed presently (Figure 4.2a), a loose bound on the traverse of the representative point is easily obtained as the rectangle defined by

$$2C\mu \cos^2 i < \tilde{\mu} < 2.32 C\mu \quad (4.23a)$$

$$2C\nu \cos^2 i < \tilde{\nu} < 2.32 C\nu \quad (4.23b)$$

Also, the greatest q value is found to be

$$q_{\max} = 3.034 K \quad (4.24)$$

For a satellite representing the most adverse situation of the greatest gravity-gradient torque, $|K| = 1$ which gives $q_{\max} \approx 3$. Consequently, any selection of C, μ and ν such that the rectangle described by Equation (4.23) lies in the stable region of Figure 4.4b would lead to stable operation throughout the year. A typical bound for a satellite in the equatorial orbit ($i = 23.5^\circ$) with $C = 5$, $\mu = 0.25$, $\nu = 0.6$ is indicated in Figure 4.4b. It is apparent that a wide choice of these parameters is possible even under such conditions. With a reduction in K , the q_{\max} value reduces and the allowable range of the design parameters increases further.

4.3 System Performance

An estimate of the pitch damping rates the controller is

capable of may be obtained from the system 'time constant'.

In the region of stable x , the envelope of $\tilde{\alpha}$ would decay exponentially with the time constant

$$\tau = 2/\tilde{\mu} = 1/\mu C|D|. \quad (4.25)$$

It is interesting to note that the maximization of $|D|$, which earlier led to a smaller nominal control $\delta_0(\theta)$, results in quicker damping of the transients. The damping rates also improve with increased controller size and velocity gain.

When the system operates at a point lying in the region of unstable x , the time constant increases somewhat to

$$\tau = 1/(\tilde{\mu}/2 - r_{\max}) = 1/(\mu C|D| - r_{\max}) \quad (4.26)$$

In any of these regions, the greatest value of r_{\max} equals half the height of the instability region for $\tilde{\alpha}$, which is fairly small and reduces further with an increase in \tilde{v} . Therefore, in general, the increase in the time constant would be quite insignificant for larger $\tilde{\mu}$ and/or \tilde{v} .

The attitude response was evaluated by numerically integrating the nonlinear pitch equation (4.1) in conjunction with the control laws (4.6 and 4.15) and the shadow criterion (Appendix C) for various combinations of the system parameters. Initial conditions representing initial misalignments as well as the effect of impulsive disturbances were simulated. In orbits lying entirely outside the earth's shadow, perfect inertial

stabilization was achieved subsequent to the damping of the initial disturbance in a fraction of an orbit. When the satellite encounters the earth's shadow during its orbit, a small attitude deviation following each passage through the shadow region was observed. The magnitude and duration of the error were generally very small, and were found to be strongly dependent on the magnitude of the gravity torque and the length of the shadow period.

Figure 4.5 presents the system response under the most severe earth's shadow condition which corresponds to the coincidence of the sun-line with the line of nodes ($\phi = 0, \pi$). The associated control histories are also indicated. The parameters represent a satellite in the geostationary orbit with $I_x = 250 \text{ Kg-m}^2$ and the controller dimensions $A = 0.25 \text{ m}^2$, $c = 3\text{m}$. It is apparent that the controller effectively removes the initial pointing error of 20° in less than half an orbit. The earth's shadow effect leads to a periodic pointing error arising once per orbit. The maximum attitude deviation is found to be about 1° for the case of $K = 0.5$ (Figure 4.5a). When the worst possible combination of the greatest gravity torque ($K = 1$) and the longest shadow period is considered, the error amplitude increases to about 2° (Figure 4.5b). The controller, even under such adverse conditions, is able to reorient the spacecraft quite quickly on emergence from the shadow. The

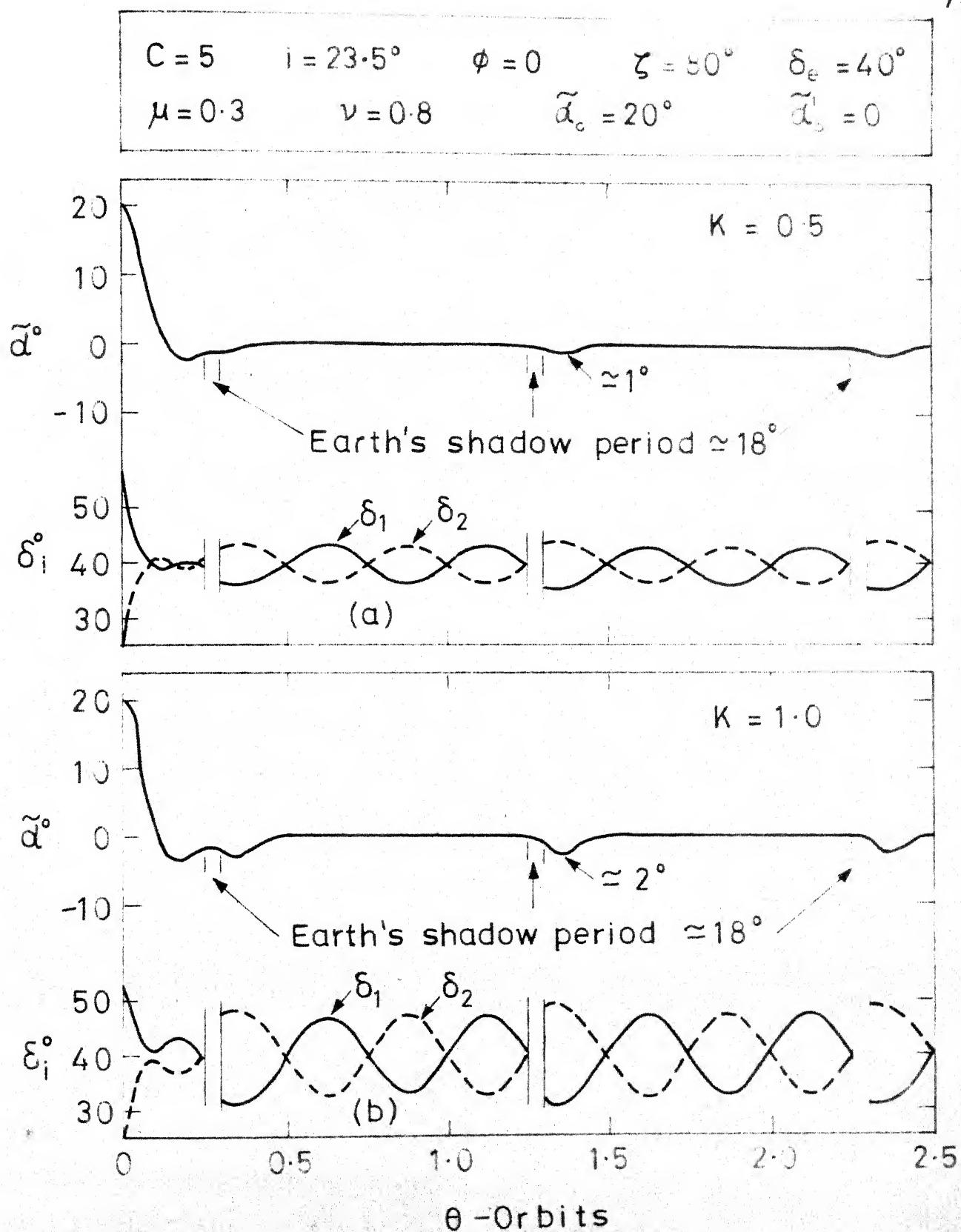


Fig. 4.5 Typical system response (a) $K = 0.5$,
(b) $K = 1.0$

performance may be further improved through an increase in the controller size and an optimum selection of the system gains. It may also be pointed out here that most orbits at the geostationary altitude would either be entirely free from the earth's shadow or encounter relatively small shadow periods. Consequently, the shadow induced error would be significant only during a small fraction of the satellite's life-time.

4.4 Concluding Remarks

The conclusions based on the present study may be summarized as follows :

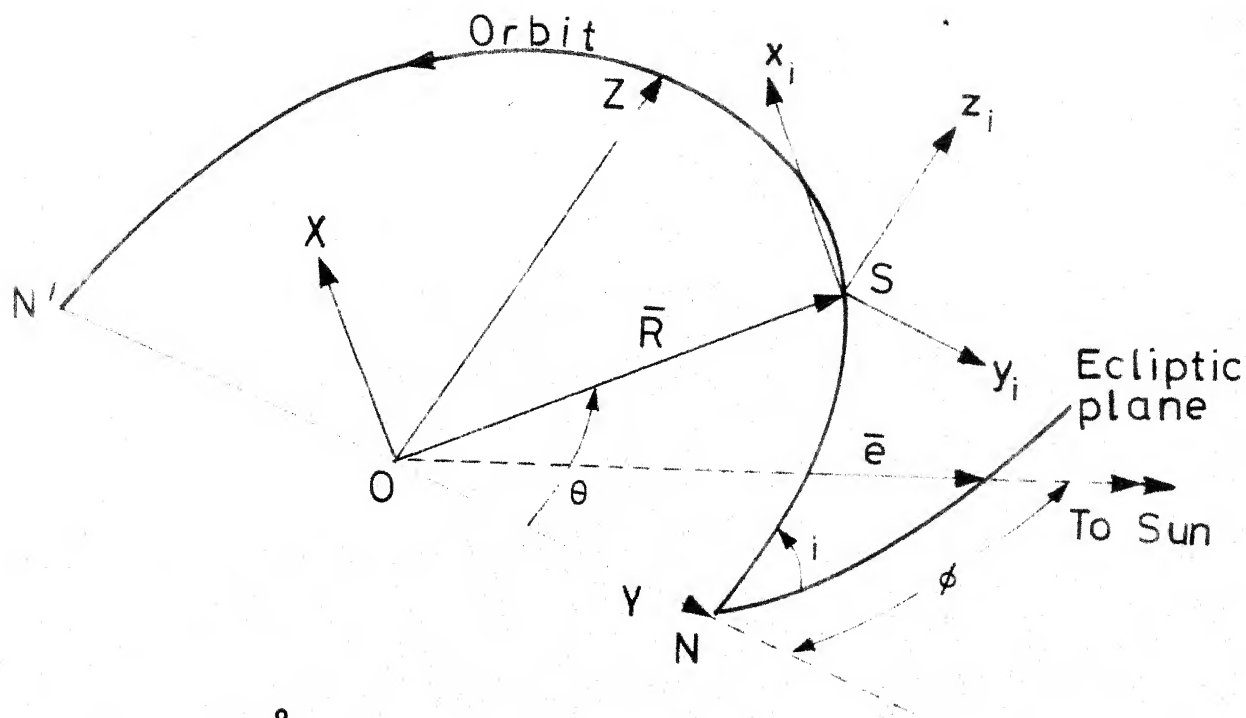
- (i) The feasibility of attaining an inertially-fixed pitch attitude of a high altitude satellite by means of solar radiation pressure has been demonstrated.
- (ii) The analytical solution developed for the nominal control is very accurate and renders the control law simple to realize. The approximate solution remains valid for a variety of the updating strategies for the mean position δ_e .
- (iii) Asymptotically stable behaviour of the system throughout the year over a wide range of the system gains is particularly attractive from the design point of view.
- (iv) The system performance, even under the most severe gravitational torque and earth shadow conditions, appears to be acceptable for a variety of missions. It may be further improved through an optimal selection of the controller gains.

5. STABILIZATION OF SPACECRAFT SYMMETRY AXIS ALONG AN INERTIALLY-FIXED ATTITUDE

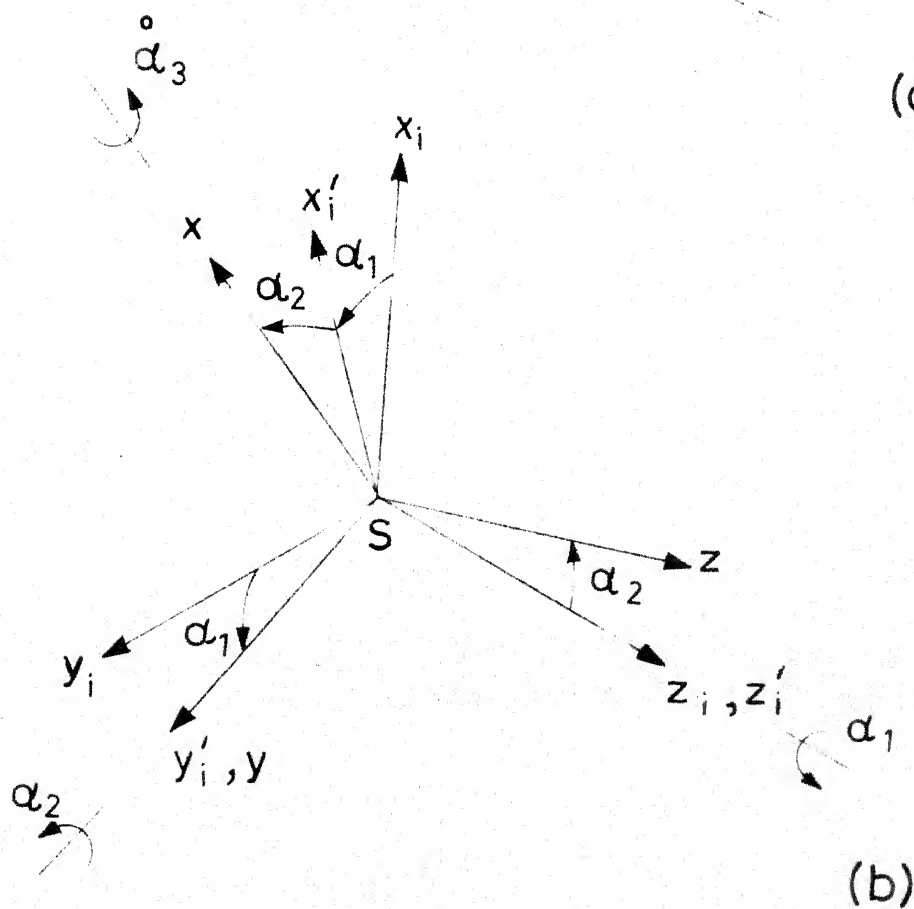
The previous investigation clearly establishes the feasibility of inertially-fixed pitch stabilization by means of the two-surface solar controller. This chapter extends the approach to the problem of imparting any inertially-fixed orientation to the symmetry axis of an axisymmetric spacecraft. For this more complex problem, a numerical approach is followed throughout. The two-dimensional character of the system necessitates the use of independent nominal rotations of the two control surfaces. Their differential rotation, however, may still be employed as the feedback control. An optimal linear feedback control strategy is synthesized through the minimization of a quadratic performance index which assures asymptotic stability for the system. The possibility of simplifying the software implementation through the use of suboptimal control policies is also explored. The effectiveness of the control system in stabilizing the spacecraft along arbitrary inertial orientations is evaluated through simulations of the governing nonlinear equations of motion.

5.1 Formulation of the Problem

Figure 5.1a shows the geometry of the orbital motion of an axisymmetric satellite with its center of mass S moving in a circular orbit about the earth's center O . x_i, y_i, z_i represent



(a)



(b)

Fig. 5-1 (a) Geometry of orbital motion
(b) Geometry of attitude motion

a system of coordinates parallel to the inertial frame X, Y, Z but with its origin at S . Two sequential finite rotations, α_1 about the z_i -axis and α_2 about the y_i' -axis are employed to bring the x_i, y_i, z_i frame in coincidence with the principal axis system x, y, z . Relative to the x, y, z coordinates, the spacecraft spins about its symmetry axis (x -axis) with an angular velocity $\dot{\alpha}_3$. The angles α_1 and α_2 completely specify the attitude of the satellite symmetry axis in inertial space. Figure 5.2 shows the two-surface solar controller configuration with the control surfaces located along the symmetry axis of the spacecraft. The control surfaces are permitted rotations δ_1 and δ_2 , measured from the xz -plane, about the x -axis.

Presently, the Eulerian formulation is used to derive the equations of attitude motion in the gravity-gradient field. The Euler dynamical equations for the axisymmetric spacecraft may be written as :

$$\dot{\omega}_x = (M_{gx} + M_{sx})/I_x \quad (5.1a)$$

$$\dot{\omega}_y - (1 - I) \omega_z \omega_x = (M_{gy} + M_{sy})/I_y \quad (5.1b)$$

$$\dot{\omega}_z + (1 - I) \omega_x \omega_y = (M_{gz} + M_{sz})/I_z \quad (5.1c)$$

where M_{gk}, M_{sk} ($k = x, y, z$) represent the components of the gravitational and radiation torques along x, y, z axes, respectively. The angular velocity components are easily expressed as :

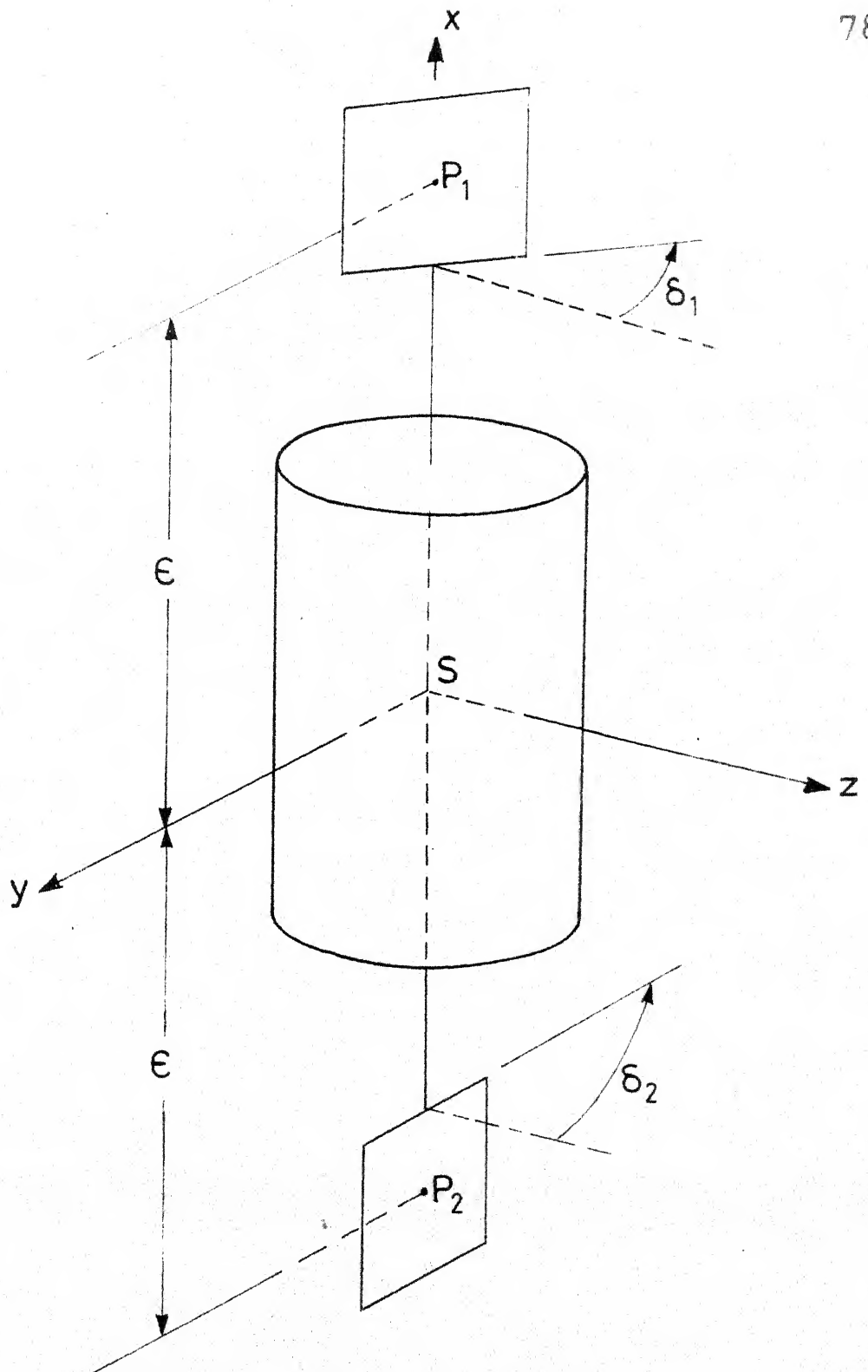


Fig. 5.2 Solar controller configuration

$$\omega_x = - \dot{\alpha}_1 \sin \alpha_2 + \dot{\alpha}_3 \quad (5.2a)$$

$$\omega_y = \dot{\alpha}_2 \quad (5.2b)$$

$$\omega_z = \dot{\alpha}_1 \cos \alpha_2 \quad (5.2c)$$

The derivation of the gravitational torque components is quite lengthy but straightforward. With the usual first approximation including terms upto the order of (satellite dimension/R)², they are given by³⁰:

$$M_{gx} = 0 \quad (5.3a)$$

$$M_{gy} = - 3 \Omega^2 (1 - I) I_y r_x r_z \quad (5.3b)$$

$$M_{gz} = 3 \Omega^2 (1 - I) I_y r_x r_y \quad (5.3c)$$

where

$$r_x = (\sin \alpha_1 \cos \alpha_2) \cos \theta - (\sin \alpha_2) \sin \theta \quad (5.4a)$$

$$r_y = (\cos \alpha_1) \cos \theta \quad (5.4b)$$

$$r_z = (\sin \alpha_1 \sin \alpha_2) \cos \theta + (\cos \alpha_2) \sin \theta \quad (5.4c)$$

Following the procedure adopted in earlier chapters, the solar control torque components are easily found to be :

$$M_{sx} = 0 \quad (5.5a)$$

$$M_{sy} = 2 \rho p A \epsilon h_1(\delta_1, \delta_2) \quad (5.5b)$$

$$M_{sz} = 2 \rho p A \epsilon h_2(\delta_1, \delta_2) \quad (5.5c)$$

where

$$h_1(\delta_1, \delta_2) = |\cos \xi_1| \cos \xi_1 \cos \delta_1 - |\cos \xi_2| \cos \xi_2 \cos \delta_2 \quad (5.6a)$$

$$h_2(\delta_1, \delta_2) = |\cos \xi_1| \cos \xi_1 \sin \delta_1 - |\cos \xi_2| \cos \xi_2 \sin \delta_2 \quad (5.6b)$$

Here, the angles of incidence ξ_i are given by

$$\cos \xi_i = -e_y \sin \delta_i + e_z \cos \delta_i, \quad (i = 1, 2) \quad (5.7)$$

and the satellite - sun unit vector components take the form :

$$e_x = -\sin \phi (\sin i \cos \alpha_1 \cos \alpha_2 + \cos i \sin \alpha_2) + \cos \phi (\sin \alpha_1 \cos \alpha_2) \quad (5.8a)$$

$$e_y = \sin \phi (\sin i \sin \alpha_1) + \cos \phi (\cos \alpha_1) \quad (5.8b)$$

$$e_z = -\sin \phi (\sin i \cos \alpha_1 \sin \alpha_2 - \cos i \cos \alpha_2) + \cos \phi (\sin \alpha_1 \sin \alpha_2) \quad (5.8c)$$

Substituting Equations (5.2), (5.3) and (5.5) in the Euler dynamical relations (5.1), the desired equations governing α_1 , α_2 and α_3 degrees of freedom are obtained as :

$$\frac{d}{dt}(-\dot{\alpha}_1 \sin \alpha_2 + \dot{\alpha}_3) = 0 \quad (5.9a)$$

$$\begin{aligned} \ddot{\alpha}_2 - (1 - I) \dot{\alpha}_1 \cos \alpha_2 (-\dot{\alpha}_1 \sin \alpha_2 + \dot{\alpha}_3) = \\ = -3 \Omega^2 (1 - I) r_x r_z + (2 \rho p A \epsilon / I_y) h_1(\delta_1, \delta_2) \end{aligned} \quad (5.9b)$$

$$\begin{aligned} & \ddot{\alpha}_1 \cos \alpha_2 + \dot{\alpha}_1 \dot{\alpha}_2 \cos \alpha_2 + (1-I)(-\dot{\alpha}_1 \sin \alpha_2 + \dot{\alpha}_3) \dot{\alpha}_2 \\ & = 3 \Omega^2 (1-I) r_x r_y + (2 \rho p A \epsilon / I_y) h_2(\delta_1, \delta_2) \end{aligned} \quad (5.9c)$$

Since the torque components in the α_3 degree of freedom are zero, it represents a cyclic coordinate. The associated first integral of motion given by

$$-\alpha_1' \sin \alpha_2 + \alpha_3' = k \text{ (constant)} \quad (5.10)$$

may be used to eliminate α_3' from the remaining equations of motion. The parameter k represents a nondimensional measure of the nominal spin rate of the spacecraft about its symmetry axis. For a nonspinning satellite, however, it would be zero. The equations describing the attitude motion of the symmetry axis finally take the nondimensional form :

$$\begin{aligned} & \alpha_1'' \cos \alpha_2 - \alpha_1' \alpha_2' \sin \alpha_2 + (1-I)k \alpha_2' - 3(1-I)r_x r_y \\ & = C h_2(\delta_1, \delta_2) \end{aligned} \quad (5.11a)$$

$$\alpha_2'' - (1-I)k \alpha_1' \cos \alpha_2 + 3(1-I)r_x r_z = C h_1(\delta_1, \delta_2) \quad (5.11b)$$

where the solar parameter C is defined as

$$C = 2 \rho p A \epsilon / I_y \Omega^2 \quad (5.12)$$

The governing equations represent a fourth order, coupled, nonlinear, nonautonomous, system of differential equations. The manner in which the control surface rotations δ_1 and δ_2 appear in the equations of motion is also quite complicated which makes the control synthesis problem quite difficult.

5.2 Control Synthesis

It is apparent from the equations of motion (5.11) that in absence of the controller and any external disturbances, $\alpha_1 = \alpha_2 = 0$ represents an equilibrium configuration for the satellite. This, however, represents a specific case of an inertially-fixed symmetry axis attitude with the symmetry axis normal to the orbit plane. An arbitrary inertially-fixed orientation, $\alpha_1 = \alpha_{1e}$, $\alpha_2 = \alpha_{2e}$, in general, would correspond to a nonequilibrium orientation in the gravity-gradient field. If the solar surfaces are so operated that the radiation torque exactly balances the gravitational torques, it should be possible to stabilize the symmetry axis along any orientation in space. The required nominal controls $\delta_{10}(\theta)$ and $\delta_{20}(\theta)$ would have to be such that $\alpha_1 = \alpha_{1e}$, $\alpha_2 = \alpha_{2e}$ represents an identical solution of Equation (5.11). This leads to :

$$h_1(\delta_{10}, \delta_{20}) = [3(1-I)/C] r_{xe}(\theta) r_{ze}(\theta) \quad (5.13a)$$

$$h_2(\delta_{10}, \delta_{20}) = -[3(1-I)/C] r_{xe}(\theta) r_{ye}(\theta) \quad (5.13b)$$

where

$$r_{xe}(\theta) = (\sin \alpha_{1e} \cos \alpha_{2e}) \cos \theta - (\sin \alpha_{2e}) \sin \theta \quad (5.14a)$$

$$r_{ye}(\theta) = (\cos \alpha_{1e}) \cos \theta \quad (5.14b)$$

$$r_{ze}(\theta) = (\sin \alpha_{1e} \sin \alpha_{2e}) \cos \theta + (\cos \alpha_{2e}) \sin \theta \quad (5.14c)$$

These two nonlinear algebraic equations may be solved for the nominal controls $\delta_{10}(\theta)$ and $\delta_{20}(\theta)$. In view of the periodic

nature of the right hand side, the nominal controls would be periodic functions of period π .

In addition, the solar controller would have to stabilize the spacecraft against disturbances such as due to initial misalignments and micrometeorite impacts. Incorporation of suitable feedback controls, in addition to nominal controls, would therefore be required. For small amplitude motion near the nominal orientation, the governing nonlinear equations may be simplified through linearization. Substituting

$\alpha_1 = \alpha_{1e} + \tilde{\alpha}_1$, $\alpha_2 = \alpha_{2e} + \tilde{\alpha}_2$, $\delta_1 = \delta_{10} + \tilde{\delta}_1$, $\delta_2 = \delta_{20} + \tilde{\delta}_2$, and linearizing in $\tilde{\alpha}_1$, $\tilde{\alpha}_2$, $\tilde{\delta}_1$ and $\tilde{\delta}_2$, Equations (5.11) become :

$$\tilde{\alpha}_1'' + a_1 \tilde{\alpha}_1' + a_2 \tilde{\alpha}_1 + a_3 \tilde{\alpha}_2 + a_4 \tilde{\delta}_1 + a_5 \tilde{\delta}_2 = 0 \quad (5.15a)$$

$$\tilde{\alpha}_2'' + b_1 \tilde{\alpha}_1' + b_2 \tilde{\alpha}_1 + b_3 \tilde{\alpha}_2 + b_4 \tilde{\delta}_1 + b_5 \tilde{\delta}_2 = 0 \quad (5.15b)$$

Here, a_i , b_i ($i = 1, 5$) represent very lengthy functions of θ, ϕ , α_{1e} , α_{2e} , $\delta_{10}(\theta)$, $\delta_{20}(\theta)$ and the system parameters.

Their full forms are presented in Appendix B.

Although independent control laws governing $\tilde{\delta}_1$ and $\tilde{\delta}_2$ may be synthesized, it would not be necessary for attitude stabilization in view of the coupling between the $\tilde{\alpha}_1$ and $\tilde{\alpha}_2$ motions. On the other hand, specifying a suitable constraint between $\tilde{\delta}_1$ and $\tilde{\delta}_2$ would reduce the problem to one with a single control variable leading to considerable software simplifications.

A careful examination of the functions a_4 and a_5 provides significant guidance as to the choice of the constraint. Equation (5.13) reveals that there exist values of θ near which δ_{10} and δ_{20} are nearly equal irrespective of the values of I and C . Whenever the controller size is large (large C) or the spacecraft is near spherical ($I \approx 1$), it indicates the nominal controls δ_{10} and δ_{20} to be quite close to each other for all θ . Equations (B-4, B-5, B-9 and B-10) show that a_4 and a_5 (and similarly b_4 and b_5) would then tend to become negative of each other. Consequently, to generate larger feedback control torques, $\tilde{\delta}_1$ and $\tilde{\delta}_2$ should have opposite signs. For convenience, they are presently constrained to be of the same magnitude also, i.e., $\tilde{\delta}_1 = -\tilde{\delta}_2$.

Letting $x_1 = \tilde{\alpha}_1$, $x_2 = \tilde{\alpha}_1'$, $x_3 = \tilde{\alpha}_2$, $x_4 = \tilde{\alpha}_2'$, $u = \tilde{\delta}_1 = -\tilde{\delta}_2$, Equations (5.15) may be expressed in the state variable form as

$$\bar{x}'(\theta) = A(\theta) \bar{x}(\theta) + B(\theta) \bar{u}(\theta) \quad (5.16)$$

where A and B matrices are given by

$$A(\theta) = \begin{bmatrix} 0 & 1 & 0 & 0 \\ -a_2 & 0 & -a_3 & -a_1 \\ 0 & 0 & 0 & 1 \\ -b_2 & -b_1 & -b_3 & 0 \end{bmatrix} \quad \text{and} \quad B(\theta) = \begin{bmatrix} 0 \\ a_5 - a_4 \\ 0 \\ b_5 - b_4 \end{bmatrix} \quad (5.17)$$

Note that the elements of A and B matrices are periodic functions of the orbital time θ with the period π .

In order to obtain a feedback control law which assures asymptotically stable operation³³ of the system, we consider the minimization of the quadratic performance index

$$J = (1/2) \int_0^{\theta_f \rightarrow \infty} [\bar{x}^T(\theta) Q(\theta) \bar{x}(\theta) + \bar{u}^T(\theta) W(\theta) \bar{u}(\theta)] d\theta \quad (5.18)$$

where $Q(\theta)$ and $W(\theta)$ represent positive semidefinite and positive definite weighting matrices, respectively. The control law minimizing this performance index is well known to be³⁴

$$\bar{u}(\theta) = F(\theta) \bar{x}(\theta) \quad (5.19)$$

with the gain matrix $F(\theta)$ given by

$$F(\theta) = -W^{-1}(\theta) B^T(\theta) K(\theta) \quad (5.20)$$

Here, $K(\theta)$ represents the solution of the matrix - Riccati equation

$$\begin{aligned} K'(\theta) = & -K(\theta) A(\theta) - A^T(\theta) K(\theta) - Q(\theta) \\ & + K(\theta) B(\theta) W^{-1}(\theta) B^T(\theta) K(\theta) \end{aligned} \quad (5.21)$$

with the boundary condition $K(\theta_f \rightarrow \infty) = 0$.

5.3 Computational Procedure

The performance of the proposed control system is studied through a response analysis of the system. A specific

satellite and controller configuration with the following specifications is selected for the computations :

$$I_x = 167 \text{ Kg-m}^2 \quad I_y = I_z = 500 \text{ Kg-m}^2$$

$$A = 1 \text{ m}^2 \quad \epsilon = 3 \text{ m} \quad i = 23.5^\circ$$

This leads to the inertia parameter $I \approx 1/3$ and the solar parameter $C \approx 10$ for a geostationary orbit. The computational procedure may be summarized as follows :

- (i) The appropriate value for the solar aspect angle ϕ , determining the time of the year, is selected.
- (ii) Equations (5.13) are solved numerically to determine the nominal controls $\delta_{10}(\theta)$ and $\delta_{20}(\theta)$. In view of its transcendental nature, the solutions obtained are not unique but depend on the initial guess. The pair of nominal controls need to be computed only for the range $0 \leq \theta \leq \pi$ as they repeat after every half orbit.
- (iii) The next step is to choose weighting matrices $Q(\theta)$ and $W(\theta)$. In the present analysis equal weights are assigned to attitude errors, their derivatives and the control.
- (iv) The matrix-Riccati equation (5.21) is solved backward with boundary condition $K(\theta_f \rightarrow \infty) = 0$. In practice, $\theta_f = 10$ orbits was found to be sufficiently large for the solution $K(\theta)$ to reach a steady state periodic character with period π .

(v) The feedback gain matrix

$$F(\theta) = [F_{\alpha_1} \quad F_{\alpha_1'} \quad F_{\alpha_2} \quad F_{\alpha_2'}] \quad (5.22)$$

is then computed in accordance with Equation (5.20).

(vi) The full nonlinear equations of motion (5.11) are finally simulated in conjunction with the nominal and the feedback control laws synthesized via the linearized analysis. The total control surface rotations required during simulation are given by

$$\delta_1(\theta) = \delta_{10}(\theta) + u(\theta) \quad (5.23a)$$

$$\delta_2(\theta) = \delta_{20}(\theta) - u(\theta) \quad (5.23b)$$

The earth's shadow criterion (Appendix C) is incorporated during the simulation.

(vii) For different values of ϕ , steps (ii) to (vii) are repeated to assess the system performance at different times of the year. Note that replacing ϕ by $\phi + \pi$ simply leads to an interchange of the nominal control histories $\delta_{10}(\theta)$ and $\delta_{20}(\theta)$. Simultaneously, if u is changed to $-u$, the governing equations (5.11) remain the same. Hence, the controller behaviour need be studied explicitly only over the half-year interval, $0 \leq \phi \leq \pi$

5.4 Results and Discussion

Figures 5.3 and 5.4 show the nature of the periodic time-varying gains for the system. They also indicate the effect of the solar aspect angle ϕ spanning an entire half-year period.

Typical responses of the system to initial position and impulsive disturbances are shown in Figure 5.5 for the case of $\phi = 45^\circ$. Figure 5.5a represents a situation when the satellite symmetry axis is misaligned from the desired inertially-fixed orientation by 10° in both α_1 and α_2 . The controller is able to restore the desired alignment in about one orbit. The associated feedback control u (Figure 5.5a) and the nominal controls (Figure 5.5c) are also indicated. Once the transients are removed, the nominal control surface rotations continue to counter the gravitational torques and the desired fixed inertial orientation is precisely maintained. The response to an initial impulsive disturbance, such as might be caused by micrometeorite impacts, is shown in Figure 5.5b.

The response of the system to the same disturbances occurring at different times of the year, $\phi = 90^\circ$ and $\phi = 135^\circ$, is presented in Figures 5.6 and 5.7. Note that the overall quality of the response remains essentially the same and only some local variations in the response character are observed. The system behaviour was found to be quite similar when inertial stabilization along other orientations was considered (Figure 5.8).

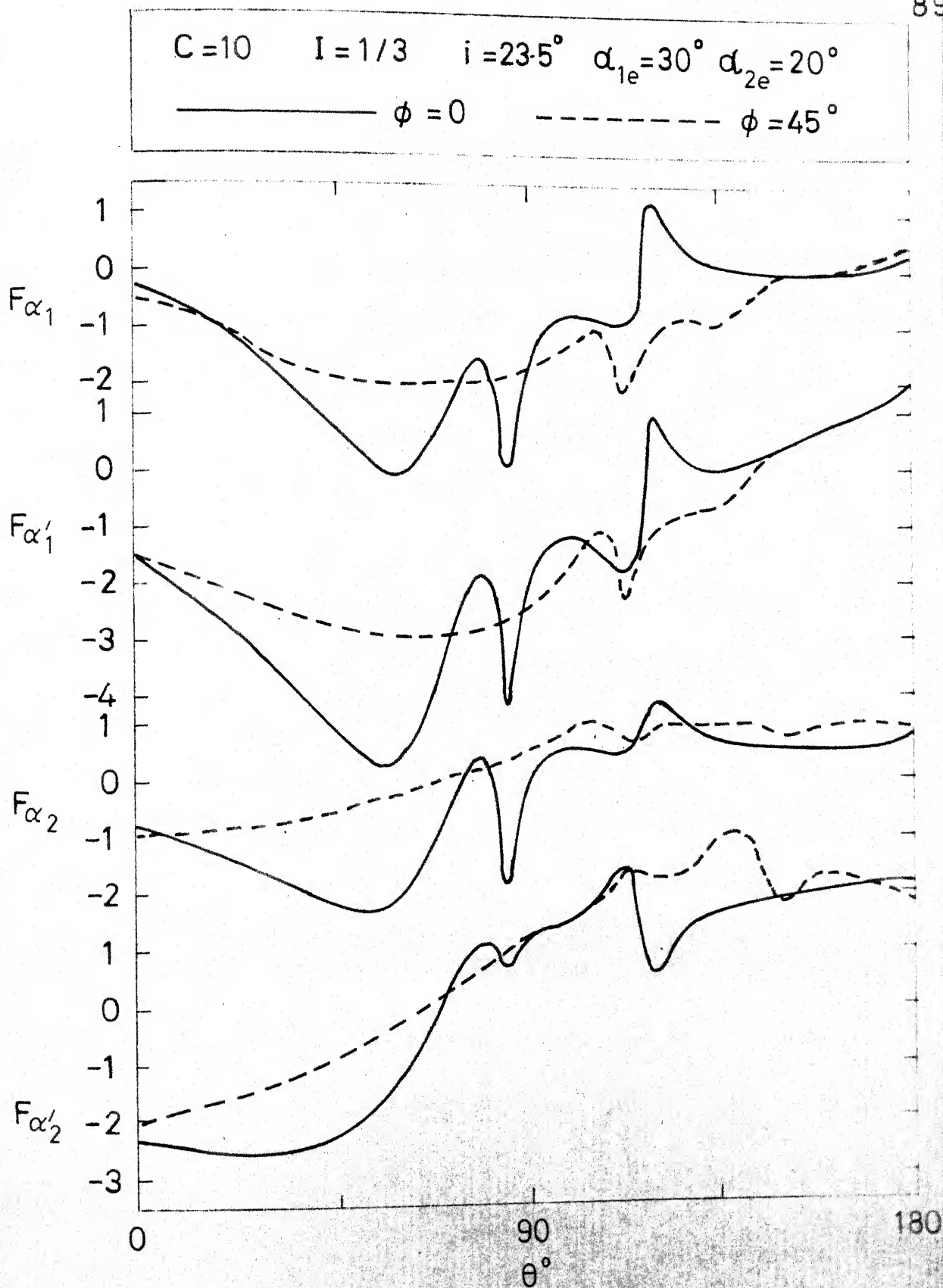


Fig. 5.3 Typical system gain histories for $\phi=0$

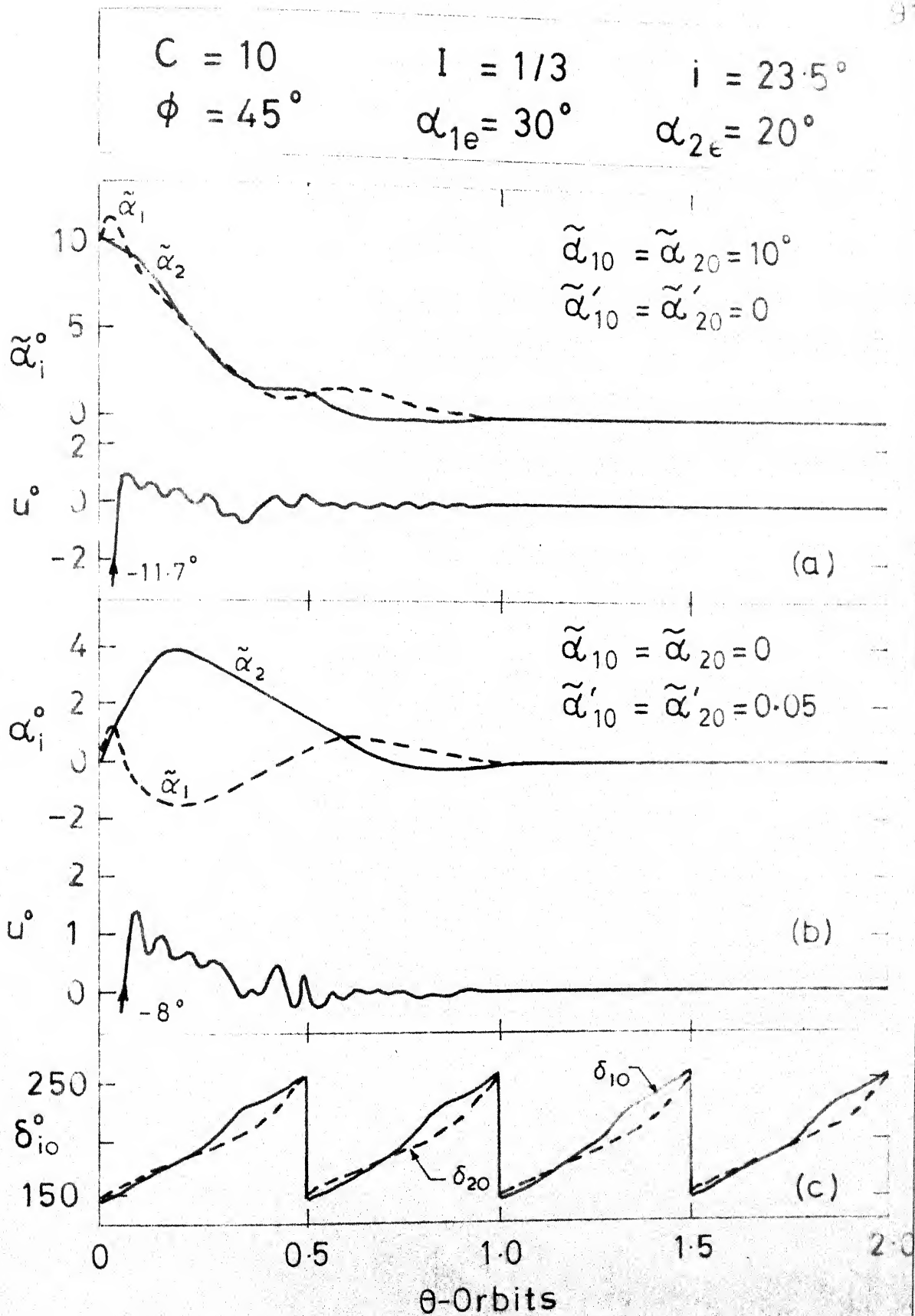


Fig.5-5 Attitude responses and control histories for stabilization along

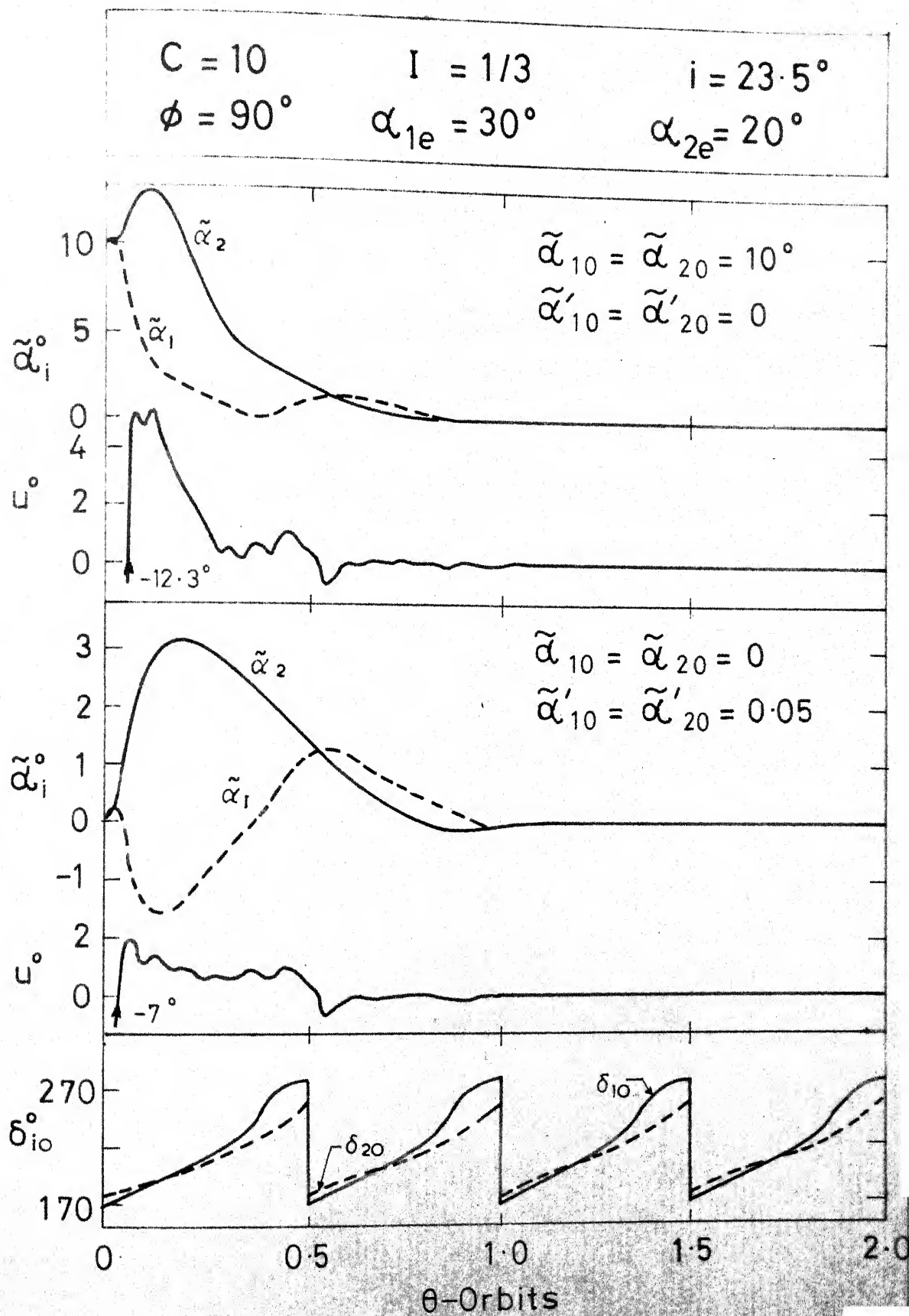


Fig. 5-6 Attitude responses and control histories for stabilization along

$$C = 10$$

$$I = 1/3$$

$$i = 23.5^\circ$$

$$\phi = 135^\circ$$

$$\alpha_{1e} = 30^\circ$$

$$\alpha_{2e} = 20^\circ$$

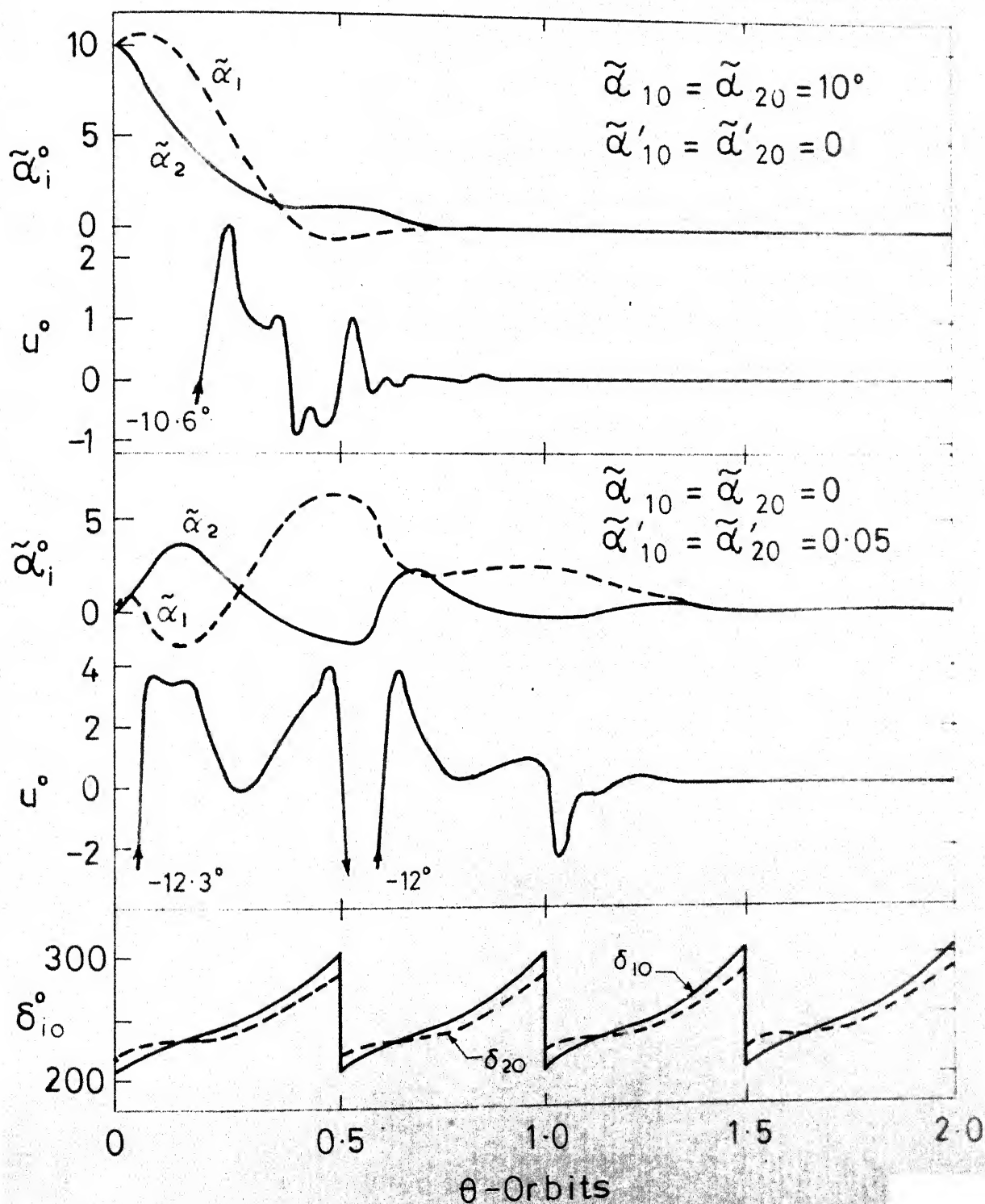


Fig. 5.7 Attitude responses and control histories for stabilization along

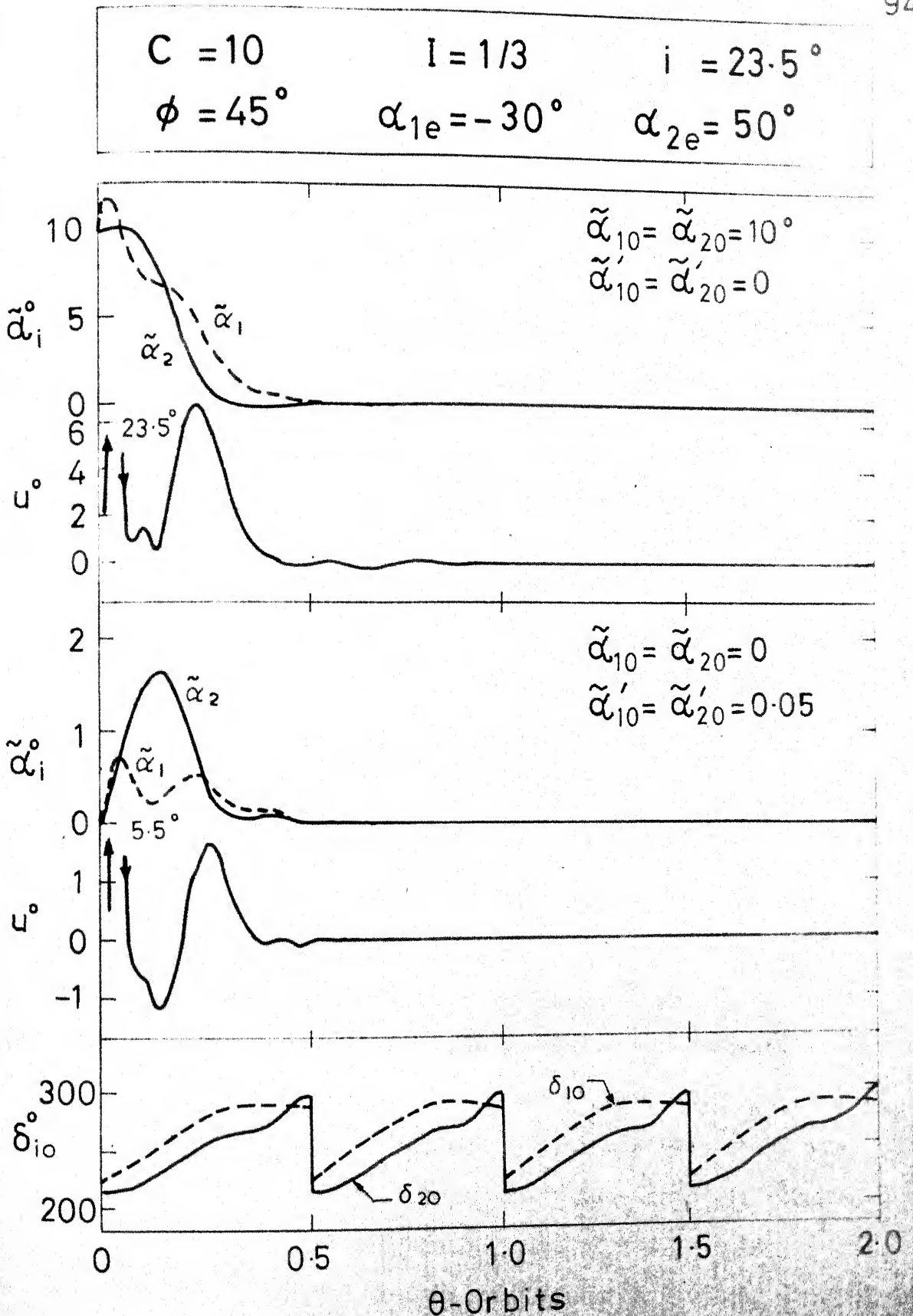


Fig. 5.8 Attitude responses and control histories for stabilization along $\alpha_{1e} = -30^\circ$, $\alpha_{2e} = 50^\circ$ ($\phi = 45^\circ$)

The results presented so far correspond to those periods of the year when the geostationary orbit does not encounter the earth's shadow. The worst case of the shadow occurs when $\phi = 0$ or 180° , i.e., the earth-sun line coincides with the line of nodes. Figure 5.9 represents the system response in this situation. Subsequent to the damping of the initial disturbance effect, the periodic loss of solar control leads to a steady-state attitude variation from the desired inertially-fixed orientation. The error amplitudes are found to be less than 3° under the most severe shadow encounter. Preliminary results indicate that through suitable changes in the relative weights Q and W , the shadow induced errors may be reduced further.

A comment concerning the numerical implementation of the feedback gains and nominal controls during the integration would be significant here. Since both the system gains and the nominal controls are periodic functions, Fourier coefficients were fitted to them for convenience of repeated generation. Fourier series truncated after seven sine and cosine terms ~~was~~ first used for both. Although the transients damped out effectively, a steady state attitude error ($\leq 5^\circ$) remained due to the imperfect cancellation of the gravity torque. The nominal controls were then improved through linear interpolation over steps of 0.5° . This led to a practically perfect pointing.

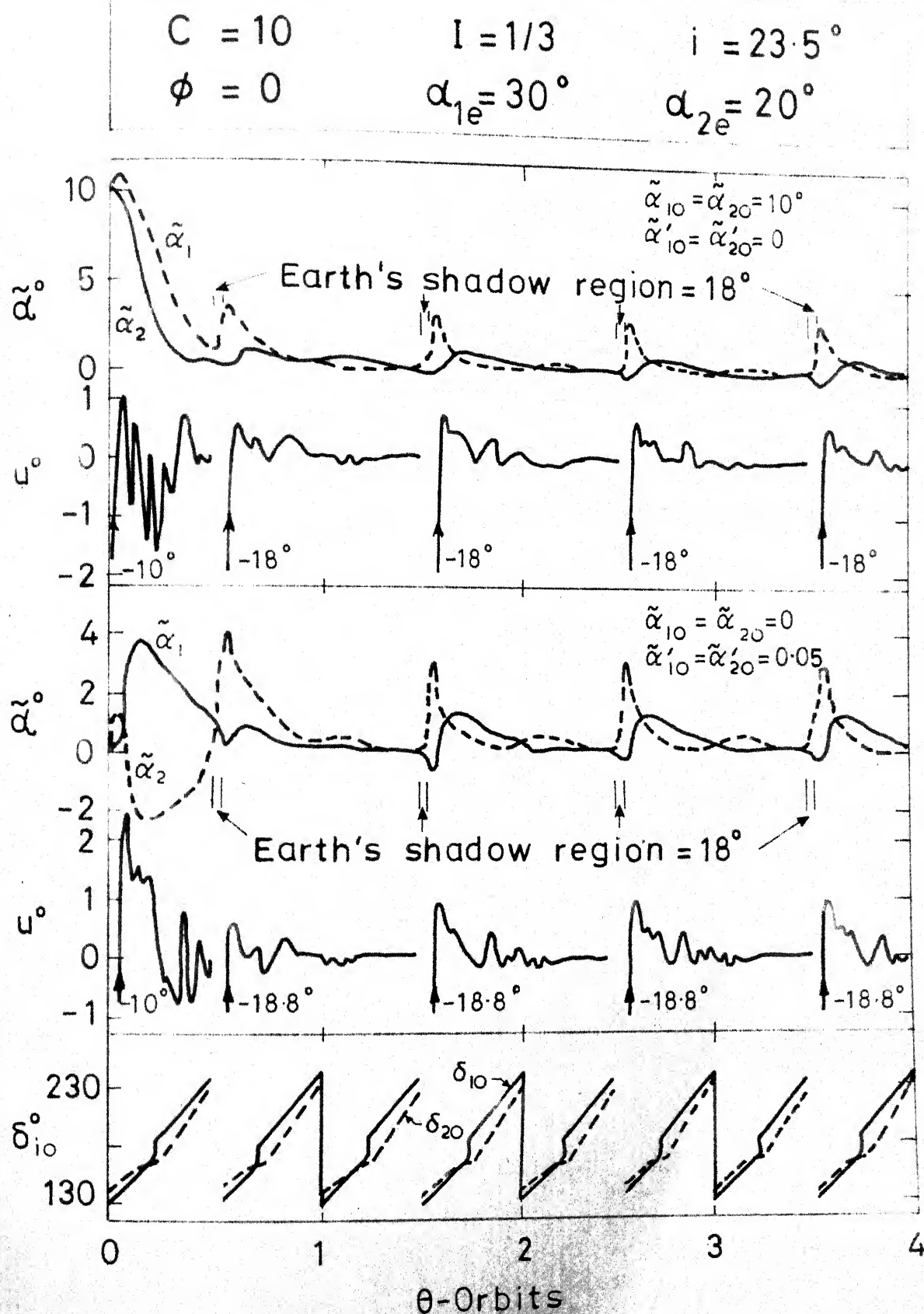


Fig. 5-9 Attitude responses and control histories for stabilization along $\alpha_{1e} = 30^\circ$, $\alpha_{2e} = 20^\circ$, showing the

The present control policy is valid for a particular time of the year. Therefore, continuous updating of the nominal as well as the feedback controls would be required as the sun position ϕ changes. This would involve a significant amount of computation. Considerable simplifications in the software implementation would result if the controls developed for a particular value of ϕ could be used over a range of ϕ . This would represent a suboptimal control policy. Numerous simulations performed in this light showed that the nominal controls are quite sensitive to ϕ and require a more or less continuous generation. On the other hand, the feedback gains remain effective over a large range of ϕ . Figures 5.10, 5.11 and 5.12 show the system performance for $\phi = 30^\circ, 60^\circ, 90^\circ$ where the gain histories computed for $\phi = 45^\circ$ have been used. It is apparent that a particular gain history remains effective over a very large period of the year. Hence, a schedule involving only a few gain computations in a year would be necessary. It is interesting to compare the suboptimal response for $\phi = 90^\circ$ (Figure 5.12) with the optimal response for the same case presented earlier (Figure 5.6). As anticipated, the suboptimal case results in a slower rate of damping. The performance deterioration, however, is not excessive.

$$C = 10$$

$$\phi = 30^\circ$$

$$I = 1/3$$

$$\alpha_{1e} = 30^\circ$$

$$i = 23.5^\circ$$

$$\alpha_{2e} = 20^\circ$$

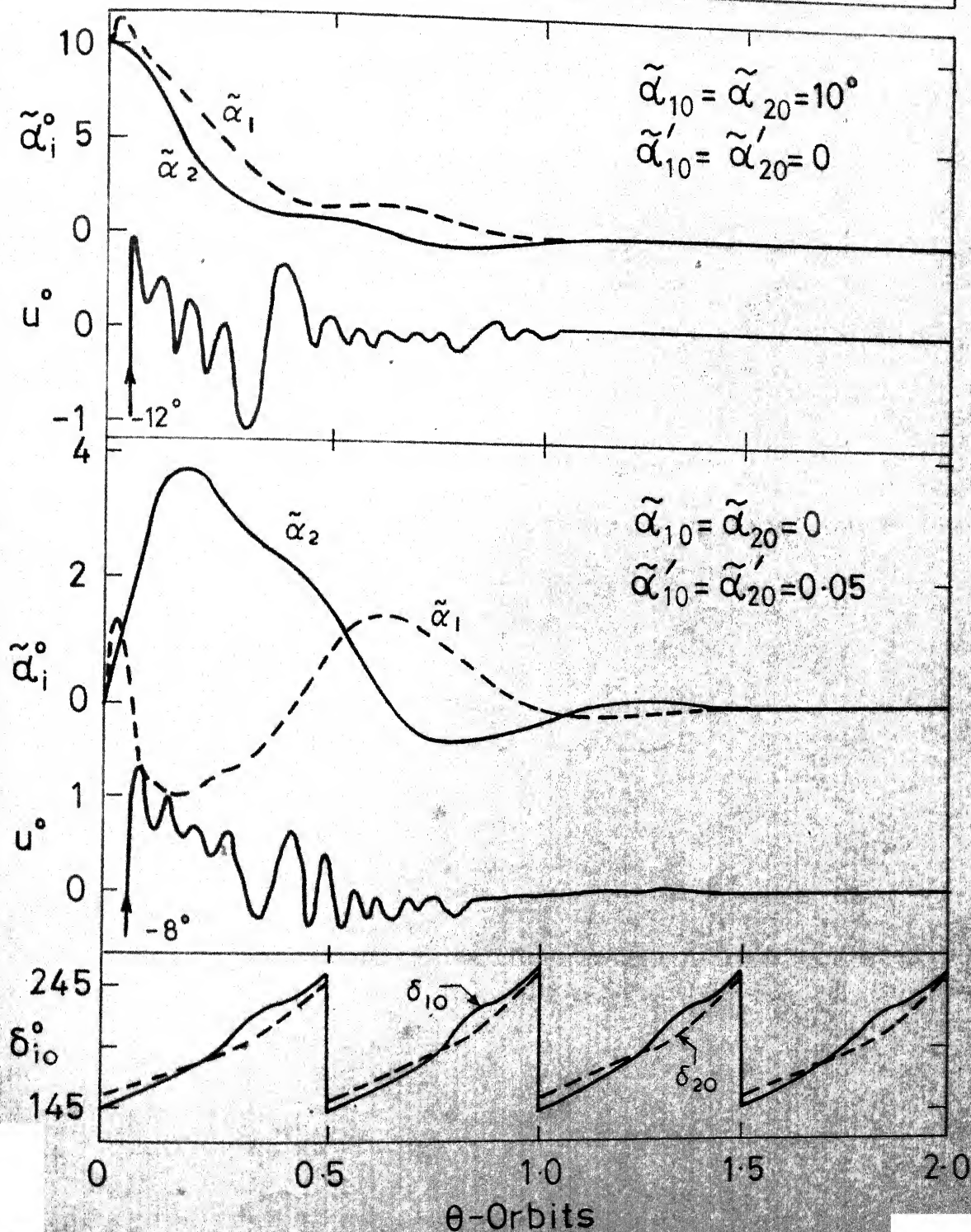


Fig. 5.10 Suboptimal system response for $\phi = 30^\circ$ obtained using feedback gains corresponding to $\phi = 45^\circ$

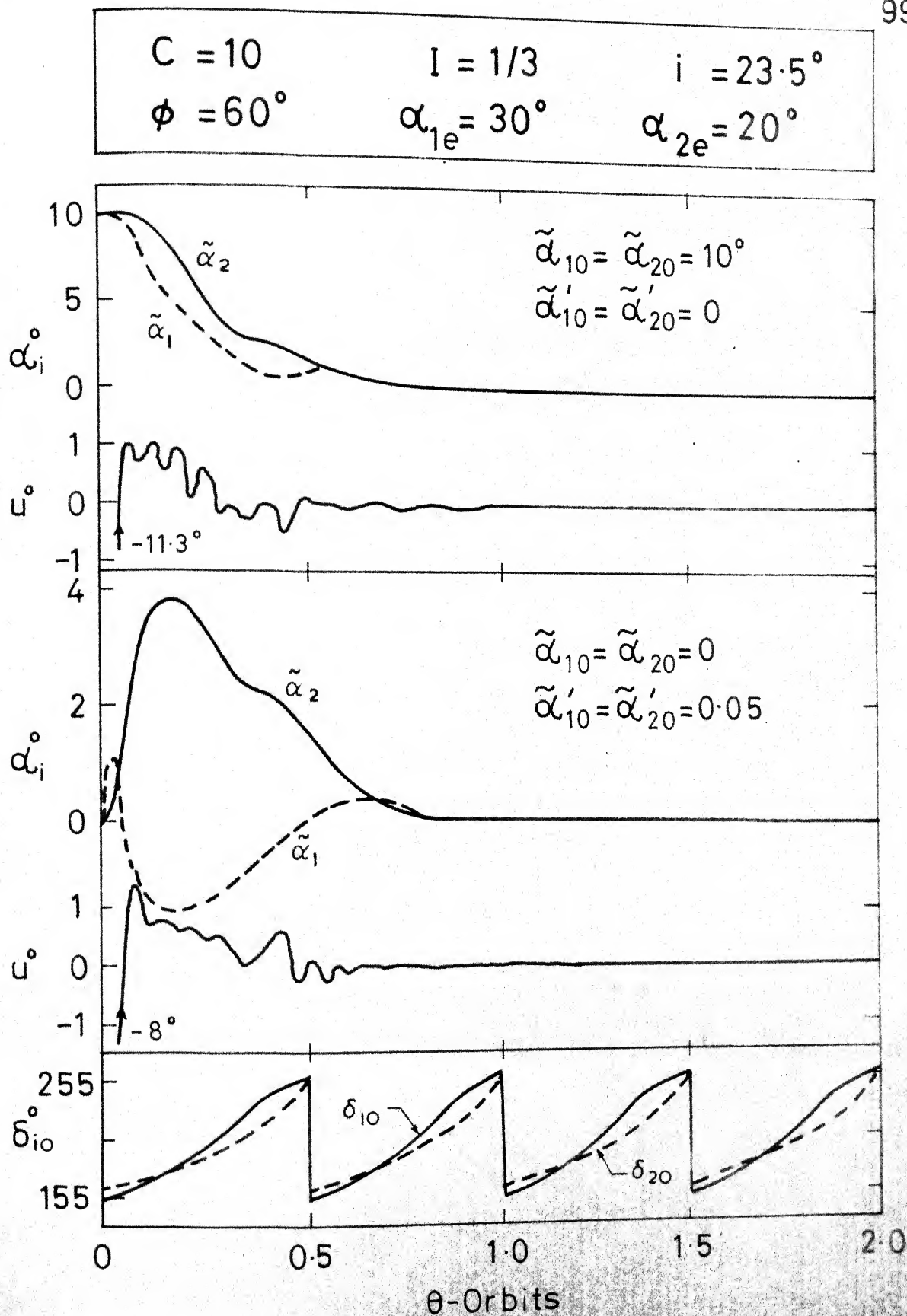


Fig. 5.11 Suboptimal system response for $\phi = 60^\circ$ obtained using feedback gains corresponding to $\phi = 45^\circ$

$$C = 10$$

$$\phi = 90^\circ$$

$$I = 1/3$$

$$a_{1e} = 30^\circ$$

$$i = 23.5^\circ$$

$$a_{2e} = 20^\circ$$

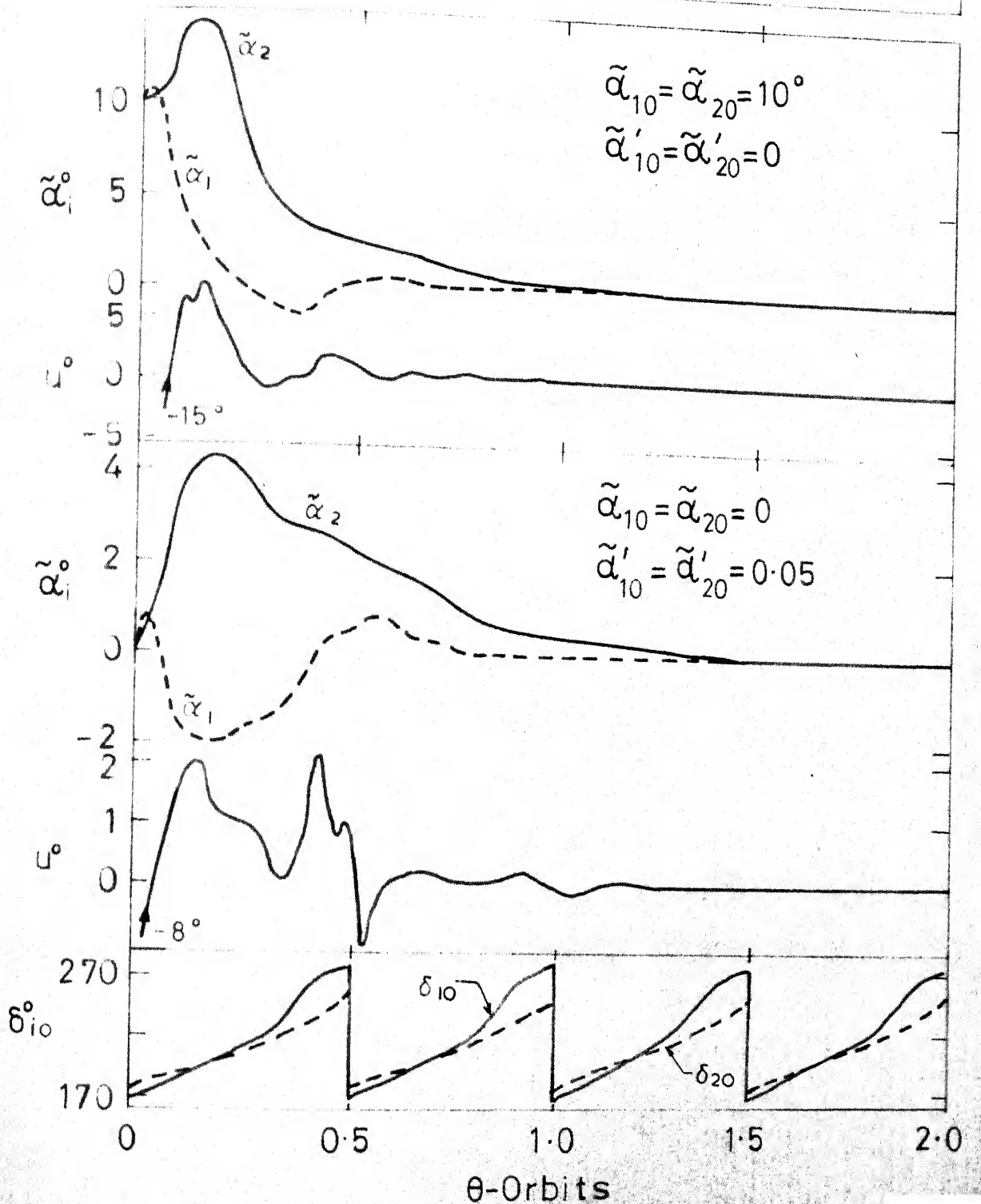


Fig. 5.12 Suboptimal system response for $\phi = 90^\circ$ obtained using feedback gains corresponding to $\phi = 45^\circ$

5.5 Concluding Remarks

The conclusions based on the investigation may be summarized as follows :

- (i) The potential of a simple two-surface solar controller for orienting the symmetry axis of a nonspinning spacecraft along any inertially - fixed direction in presence of gravitational torques is investigated.
- (ii) A control law consisting of nominal and feedback control surface rotations has been developed. The nominal controls counter the continuous gravity-gradient disturbances and the feedback controls impart asymptotic stability to the system.
- (iii) Accurate attitude pointing requires that the nominal controls be updated more or less continuously with the time of the year. However, the feedback gain scheduling need be done only a few times in a year.
- (iv) The control system continues to have a stable operation even when the spacecraft passes through the earth's shadow. In shadowed orbits, small pointing errors occur which depend on the duration of the shadow passage.

6. LARGE-ANGLE ATTITUDE MANEUVERS OF SPACECRAFT SYMMETRY AXIS

The analyses presented so far have considered the solar controller design from the viewpoint of maintaining the spacecraft attitude either in earth-pointing or along inertially-fixed orientations. It would be of interest to examine the feasibility of carrying out arbitrary large-angle attitude maneuvers of the spacecraft by means of the two-surface solar controller. Such a capability would add versatility to the system and make it possible to fulfil diverse mission requirements. This chapter presents the development of control laws for accomplishing large attitude changes of the symmetry axis of a nonspinning spacecraft in the presence of gravitational torques.

6.1 Problem Formulation and Control Synthesis

The same spacecraft and controller configurations as presented in Chapter 5 for inertial stabilization are considered here. The governing equations of attitude motion, for convenience, are restated as

$$\alpha_1'' \cos \alpha_2 - \alpha_1' \alpha_2' \sin \alpha_2 - 3(1-I)r_x r_y = C h_2(\delta_1, \delta_2) \quad (6.1a)$$

$$\alpha_2'' + 3(1-I)r_x r_z = C h_1(\delta_1, \delta_2) \quad (6.1b)$$

where all symbols have the same meaning as before. To recapitulate, these equations present an exceedingly complicated, non-linear, nonautonomous system of differential equations. Furthermore, they do not possess an equilibrium position and therefore appropriate nominal controls are required to obtain any fixed-inertial orientation.

The objective of the controller is to drive the symmetry axis from an initial attitude $(\alpha_{10}, \alpha'_{10}, \alpha_{20}, \alpha'_{20})$ to the desired final attitude $(\alpha_{1f}, \alpha'_{1f}, \alpha_{2f}, \alpha'_{2f})$. It would, of course, be desirable to achieve the transition in the minimum possible time. In general, the optimal control would require independent time-histories for $\delta_1(\theta)$ and $\delta_2(\theta)$. However, as pointed out earlier, system mechanization would be simpler by considering equal and opposite rotations, i.e., $\delta_1(\theta) = -\delta_2(\theta)$.

For convenience, the governing equations may be rewritten in the state variable notation. Letting $x_1 = \alpha_1$, $x_2 = \alpha'_1$, $x_3 = \alpha_2$, $x_4 = \alpha'_2$, and $u = \delta_1 = -\delta_2$, they take the form

$$\dot{\bar{x}}'(\theta) = \bar{F}(\bar{x}(\theta), u(\theta), \theta) \quad (6.2)$$

where

$$\bar{x}(\theta) = [x_1 \ x_2 \ x_3 \ x_4]^T \quad (6.3a)$$

$$\bar{f}(\bar{x}, u, \theta) = [f_1 \ f_2 \ f_3 \ f_4]^T \quad (6.3b)$$

and the components of \bar{f} are :

$$f_1 = x_2 \quad (6.4a)$$

$$f_2 = \{x_2 \ x_4 \ \sin x_3 + 3(1-I)r_x \ r_y \\ + 3(|\cos \xi_1| \cos \xi_1 + |\cos \xi_2| \cos \xi_2) \sin u\} \sec x_3 \quad (6.4b)$$

$$f_3 = x_4 \quad (6.4c)$$

$$f_4 = -3(1-I) \ r_x \ r_z \\ + 3(|\cos \xi_1| \cos \xi_1 - |\cos \xi_2| \cos \xi_2) \cos u \quad (6.4d)$$

The quantities r_x , r_y , r_z , $\cos \xi_1$ and $\cos \xi_2$ are given by :

$$r_x = (\sin x_1 \cos x_3) \cos \theta - (\sin x_3) \sin \theta \quad (6.5a)$$

$$r_y = (\cos x_1) \cos \theta \quad (6.5b)$$

$$r_z = (\sin x_1 \sin x_3) \cos \theta + (\cos x_3) \sin \theta \quad (6.5c)$$

$$\cos \xi_1 = -e_y \sin u + e_z \cos u \quad (6.6a)$$

$$\cos \xi_2 = e_y \sin u + e_z \cos u \quad (6.6b)$$

where the components of \bar{e} have the form

$$\begin{aligned} e_x = & -\sin \phi (\sin i \cos x_1 \cos x_3 + \cos i \sin x_3) \\ & + \cos \phi (\sin x_1 \cos x_3) \end{aligned} \quad (6.7a)$$

$$e_y = \sin \phi (\sin i \sin x_1) + \cos \phi (\cos x_1) \quad (6.7b)$$

$$\begin{aligned} e_z = & -\sin \phi (\sin i \cos x_1 \sin x_3 - \cos i \cos x_3) \\ & + \cos \phi (\sin x_1 \sin x_3) \end{aligned} \quad (6.7c)$$

The problem may be formulated as that of finding $u(\theta)$ which takes the system from the given initial state to the desired final state in minimum time. The resulting two point boundary value problem may be solved by techniques such as quasilinearization or variation of extremals. These, however, become impractical in the present situation as the optimality condition,

$$\partial H / \partial u = 0 \quad (6.8)$$

where H is the system Hamiltonian, cannot be solved analytically for the control u in terms of the state and costate variables.

Alternatively, gradient techniques may be used which bypass the problem of solving the optimality condition (6.8)

for the control u . However, the approach requires a knowledge of boundary conditions on the costate variables at the terminal time. One way of achieving this would be to add a penalty function representing a measure of the terminal state error to the cost function and letting the final state be free³⁶. Another approach is to require the satisfaction of suitably chosen terminal constraints on the states. The latter method has been presently selected to obtain the optimal control.

The control problem is therefore stated as :

Find the control $u(\theta)$ which minimizes the cost function

$$J = \int_0^{\theta_f} (1) d\theta \quad (6.9)$$

for the system

$$\bar{x}'(\theta) = \bar{f}(\bar{x}(\theta), u(\theta), \theta) \quad (6.10)$$

with the initial state

$$\bar{x}(0) = [\alpha_{10} \quad \alpha'_{10} \quad \alpha_{20} \quad \alpha'_{20}]^T \quad (6.11)$$

and the terminal constraints

$$\bar{\psi}(\bar{x}(\theta_f)) = [\psi_1 \quad \psi_2 \quad \psi_3 \quad \psi_4]^T = \bar{0} \quad (6.12)$$

where

$$\psi_1 = (1/2) (x_1(\theta_f) - \alpha_{1f})^2 \quad (6.13a)$$

$$\psi_2 = (1/2) (x_2(\theta_f) - \alpha'_{1f})^2 \quad (6.13b)$$

$$\psi_3 = (1/2) (x_3(\theta_f) - \alpha_{2f})^2 \quad (6.13c)$$

$$\psi_4 = (1/2) (x_4(\theta_f) - \alpha'_{2f})^2 \quad (6.13d)$$

6.2 Gradient Technique

The desired control may be determined by the approach developed by Bryson and Denham³⁷. The essence of the method as adapted to the present problem is briefly described below.

Consider the cost functional

$$J = \phi(\bar{x}(\theta_f), \theta_f) + \int_0^{\theta_f} L(\bar{x}(\theta), u(\theta), \theta) d\theta \quad (6.14)$$

for the system

$$\bar{x}'(\theta) = \bar{f}(\bar{x}(\theta), u(\theta), \theta) \quad (6.15)$$

After augmenting the functional J in the usual manner to include the differential equation constraints (6.15), through the use of Lagrange multipliers $\bar{\lambda}(\theta)$, the differential change dJ due to the differential change $d\theta_f$ and the variation $\delta u(\theta)$, may be expressed as

$$dJ = [L + \bar{\lambda}^T \bar{f} + (\partial \phi / \partial \theta)]_{\theta_f} d\theta_f + \int_0^{\theta_f} [(\partial L / \partial u) + \bar{\lambda}^T (\partial \bar{f} / \partial u)] \delta u d\theta \quad (6.16)$$

where $\bar{\lambda}(\theta)$ is given by

$$\bar{\lambda}' = -(\partial L / \partial \bar{x})^T - [\partial \bar{f} / \partial \bar{x}]^T \bar{\lambda} \quad (6.17a)$$

with the boundary conditions

$$\bar{\lambda}(\theta_f) = (\partial\phi/\partial\bar{x})_{\theta_f}^T \quad (6.17b)$$

Now consider the functional

$$J_o = \int_0^{\theta_f} (1) d\theta \quad (6.18)$$

for the system (6.15). Putting $\phi = 0$, $L = 1$ and letting $\bar{p}(\theta)$ represent the Lagrange multipliers, the differential dJ_o is obtained from Equations (6.16) and (6.17) as

$$dJ_o = [1 + \bar{p}^T \bar{f}]_{\theta_f} d\theta_f + \int_0^{\theta_f} \bar{p}^T (\partial \bar{f} / \partial u) \delta u d\theta \quad (6.19)$$

with

$$\bar{p}' = - [\partial \bar{f} / \partial \bar{x}]^T \bar{p} \quad (6.20a)$$

$$\bar{p}(\theta_f) = \bar{0} \quad (6.20b)$$

Obviously, Equation (6.20) has the solution $\bar{p}(\theta) = \bar{0}$. Hence, Equation (6.19) simply becomes

$$dJ_o = d\theta_f \quad (6.21)$$

Next consider the functionals

$$J_i = \psi_i(\bar{x}(\theta_f)), \quad i = 1, 2, 3, 4 \quad (6.22)$$

for the same system (6.15). With $\phi = \psi_i$, $L = 0$ and \bar{R}_i

representing the multiplier vector, one obtains from Equations (6.16) and (6.17),

$$dJ_i = [(\partial\psi_i/\partial\bar{x})\bar{f}]_{\theta_f} d\theta_f + \int_0^{\theta_f} \bar{R}_i^T (\partial\bar{f}/\partial u) \delta u d\theta \quad (6.23)$$

with

$$\bar{R}_i' = -[\partial\bar{f}/\partial\bar{x}]^T \bar{R}_i \quad (6.24a)$$

$$\bar{R}_i(\theta_f) = (\partial\psi_i/\partial\bar{x})_{\theta_f}^T \quad (6.24b)$$

Note that dJ_i simply equals $d\psi_i$. Consequently, a change $d\psi_i$ in the terminal constraint depends on $d\theta_f$ and δu according to

$$d\psi_i = [(\partial\psi_i/\partial\bar{x})\bar{f}]_{\theta_f} d\theta_f + \int_0^{\theta_f} \bar{R}_i^T (\partial\bar{f}/\partial u) \delta u d\theta \quad (6.25)$$

Equations (6.24) and (6.25) for $i = 1$ to 4, may be written in matrix notation as

$$R' = -[\partial\bar{f}/\partial\bar{x}]^T R \quad (6.26a)$$

$$R(\theta_f) = [\partial\bar{\psi}/\partial\bar{x}]_{\theta_f}^T \quad (6.26b)$$

and

$$d\bar{\psi} = \{ [\partial\bar{\psi}/\partial\bar{x}] \bar{f} \}_{\theta_f} d\theta_f + \int_0^{\theta_f} R^T (\partial\bar{f}/\partial u) \delta u d\theta \quad (6.27)$$

where

$$R = [\bar{R}_1 \mid \bar{R}_2 \mid \bar{R}_3 \mid \bar{R}_4] \quad (6.28a)$$

$$\bar{\psi} = (\psi_1 \quad \psi_2 \quad \psi_3 \quad \psi_4)^T \quad (6.28b)$$

It is apparent that any nominal choice of θ_f and $u(\theta)$ for the system (6.15) would result in a terminal error $\bar{\psi}(\bar{x}(\theta_f))$. Corrections $d\theta_f$ and $\delta u(\theta)$ are now sought which change $\bar{\psi}(\bar{x}(\theta_f))$ in the direction of satisfying the constraints $\bar{\psi}(\bar{x}(\theta_f)) = \bar{0}$ and reduce dJ_0 . One way of doing this would be to minimize dJ_0 subject to the constraints (6.27) where $d\bar{\psi}$ represents the desired change in the terminal error (say $d\bar{\psi} = -\epsilon \bar{\psi}(\bar{x}(\theta_f))$, $0 < \epsilon \leq 1$). Note that dJ_0 as well as the constraint equation are linear in $d\theta_f$ and $\delta u(\theta)$. To ensure that their optimal choices are small enough for linear perturbation theory to be valid, quadratic penalty functions in $d\theta_f$ and $\delta u(\theta)$ are added to dJ_0 to obtain

$$d\tilde{J}_0 = dJ_0 + (1/2)b (d\theta_f)^2 + (1/2) \int_0^{\theta_f} W(\theta) (\delta u)^2 d\theta \quad (6.29)$$

where b is an arbitrary positive constant and $W(\theta)$ is a positive definite quantity.

The augmented functional then becomes

$$\begin{aligned} d\tilde{J} = & d\theta_f + (1/2)b (d\theta_f)^2 + (1/2) \int_0^{\theta_f} W(\theta) (\delta u)^2 d\theta \\ & + \bar{v}^T \left\{ \left[\frac{d\bar{\psi}}{d\bar{x}} \right] \bar{f} \right\}_{\theta_f} d\theta_f + \int_0^{\theta_f} R^T(\theta) \bar{f} / \partial u \delta u d\theta - d\bar{\psi} \} \end{aligned} \quad (6.30)$$

where $\bar{\mathbf{v}}$ represents the Lagrange multiplier vector. Neglecting the change in the coefficients, the differential of $d\tilde{J}$ may be written as

$$d(d\tilde{J}) = \left\{ 1 + \bar{\mathbf{v}}^T \left[\frac{\partial \bar{\psi}}{\partial \bar{x}} \right] \bar{\mathbf{f}} + b \frac{d\theta_f}{d\theta} \right\}_{\theta_f} d(d\theta_f) + \int_0^{\theta_f} \left[\left(\frac{\partial \bar{\mathbf{f}}}{\partial u} \right)^T \mathbf{R} \bar{\mathbf{v}} + W \delta u \right] d(\delta u) d\theta \quad (6.31)$$

Hence, a minimum occurs when :

$$d\theta_f = - (1/b) \left\{ 1 + \bar{\mathbf{v}}^T \left[\frac{\partial \bar{\psi}}{\partial \bar{x}} \right] \bar{\mathbf{f}} \right\}_{\theta_f} \quad (6.32)$$

$$\delta u(\theta) = - (1/W) \left\{ \left(\frac{\partial \bar{\mathbf{f}}}{\partial u} \right)^T \mathbf{R} \bar{\mathbf{v}} \right\} \quad (6.33)$$

Substituting Equations (6.32) and (6.33) in Equation (6.27), the undetermined constraints $\bar{\mathbf{v}}$ may be obtained from

$$d\bar{\psi} = - (1/b) \left\{ \left(\frac{d\bar{\psi}}{d\theta} \right) \left[\left(\frac{d\bar{\psi}}{d\theta} \right)^T \bar{\mathbf{v}} + 1 \right] \right\}_{\theta_f} - \mathbf{I}_{\psi\psi} \bar{\mathbf{v}} \quad (6.34)$$

where

$$\mathbf{I}_{\psi\psi} = \int_0^{\theta_f} \left[\mathbf{R}^T \left(\frac{\partial \bar{\mathbf{f}}}{\partial u} \right) W^{-1} \left(\frac{\partial \bar{\mathbf{f}}}{\partial u} \right)^T \mathbf{R} \right] d\theta \quad (6.35)$$

The solution for $\bar{\mathbf{v}}$ is found to be

$$\bar{\mathbf{v}} = - \left[\mathbf{I}_{\psi\psi} + (1/b) \left(\frac{d\bar{\psi}}{d\theta} \right)_{\theta_f} \left(\frac{d\bar{\psi}}{d\theta} \right)_{\theta_f}^T \right]^{-1} \times \left\{ d\bar{\psi} + (1/b) \left(\frac{d\bar{\psi}}{d\theta} \right)_{\theta_f} \right\}_{\theta_f} \quad (6.36)$$

The expected change in J_0 is then obtained by substituting Equation (6.32) in Equation (6.21) as

$$dJ_0 = - (1/b) \{ 1 + \bar{\psi}^T [\partial \bar{\psi} / \partial \bar{x}] \bar{f} \}_{\theta_f} \quad (6.37)$$

When sufficient number of corrections $d\theta_f$ and $\delta u(\theta)$ have been applied iteratively, one would expect that $d\bar{\psi} \rightarrow \bar{0}$ and $dJ_0 \rightarrow 0$, which represent the optimal solution. It may, of course, be easily shown that the corrections $d\theta_f$ and $\delta u(\theta)$ tend to zero as the optimal solution is approached. These, in turn, may be interpreted as the satisfaction of the transversality condition ($H|_{\theta_f} = 0$) and the optimality condition ($\partial H / \partial u = 0$) associated with the original time-optimal control problem with given initial and final states.

6.3 Computational Procedure

The computational procedure may be summarized in the following steps :

- (i) Estimate a terminal time $\theta_f = (\theta_f)_0$, control history $u(\theta) = u_0(\theta)$.
- (ii) Integrate the system equations (6.10) with the specified initial conditions (6.11). Record $\bar{x}(\theta)$, $\bar{\psi}(\bar{x}(\theta_f))$ and $(d\bar{\psi}/d\theta)_{\theta_f}$.
- (iii) Integrate Equations (6.26a) backward with the boundary conditions (6.26b), compute the integral $I_{\bar{\psi}\psi}$ from Equation (6.35), and store the history $(\partial \bar{f} / \partial u)^T R$.

- (iv) Select desired $d\bar{\Psi} = -\epsilon \bar{\Psi}(\bar{x}(\theta_f))$, $0 < \epsilon \leq 1$.
- (v) Calculate \bar{v} from Equation (6.36).
- (vi) Compute $d\theta_f$ and $\delta u(\theta)$ from Equations (6.32) and (6.33).
- (vii) Stop if $\bar{\Psi}(\bar{x}(\theta_f)) = 0$ and $d\theta_f = 0$ are satisfied to a desired accuracy. Otherwise, update θ_f and $u(\theta)$ according to

$$\theta_f \Big|_{\text{new}} = \theta_f \Big|_{\text{old}} + d\theta_f \quad (6.38a)$$

$$u(\theta) \Big|_{\text{new}} = u(\theta) \Big|_{\text{old}} + \delta u(\theta) \quad (6.38b)$$

and go back to step (ii).

6.4 Results and Discussion

A computer program incorporating the gradient method was developed. Some computational simplifications were found possible without seriously affecting the convergence process. The integral $I_{\psi\psi}$ was evaluated by assuming the integrand to be piecewise constant. The updated θ_f values were rounded off to the nearest integral multiple of the step size of the integration (0.5°). This makes the storage, updating and retrieval of $u(\theta)$ easily programable.

The weightages W and b , and the parameter ϵ may be varied during the iterative process to improve the convergence. Presently, however, constant values $W = b = 500$ and $\epsilon = 0.5$ were taken which gave convergence to the desired

accuracy ($\psi_i \leq 0.005$, $i = 1$ to 4 and $|\delta \theta_f| \leq 0.005$) in about 15 - 20 iterations in most cases.

The optimal control problem was solved for various attitude maneuvers over a range of parameters. Typical results representing the case of $\phi = 45^\circ$, $i = 23.5^\circ$, $I = 1/3$ and $C = 10$ are presented and discussed below. Throughout, the initial and desired terminal attitude rates are taken to be zero ($\alpha'_{10} = \alpha'_{20} = 0$ and $\alpha'_{1f} = \alpha'_{2f} = 0$).

Figure 6.1 shows the convergence process for the maneuver $\alpha_{10} = -10^\circ$, $\alpha_{20} = -10^\circ$ to $\alpha_{1f} = 25^\circ$, $\alpha_{2f} = 30^\circ$ in the α_1, α_2 space. As is characteristic of the gradient method, the rate of convergence is fast in the beginning and slows down considerably as the optimum is approached. The figure also shows the initial guess and the optimal time history of the control $u(\theta)$. The initial guess of ramp form for $u(\theta)$ physically represents equal and opposite rotations of the control surfaces at a constant rate.

It appears interesting to examine the effect of different initial guesses for $u_0(\theta)$ on the optimal solution. Figure 6.2 shows the results obtained with different ramps selected as $u_0(\theta)$ with the same guess $(\theta_f)_0 = 90^\circ$. It turns out that different optimal controls $u_{opt}(\theta)$ are obtained for each case. The corresponding trajectories in the α_1, α_2 space and the control times $(\theta_f)_{opt}$ are also distinct. This may be interpreted as convergence to local stationary solutions in the neighbourhood

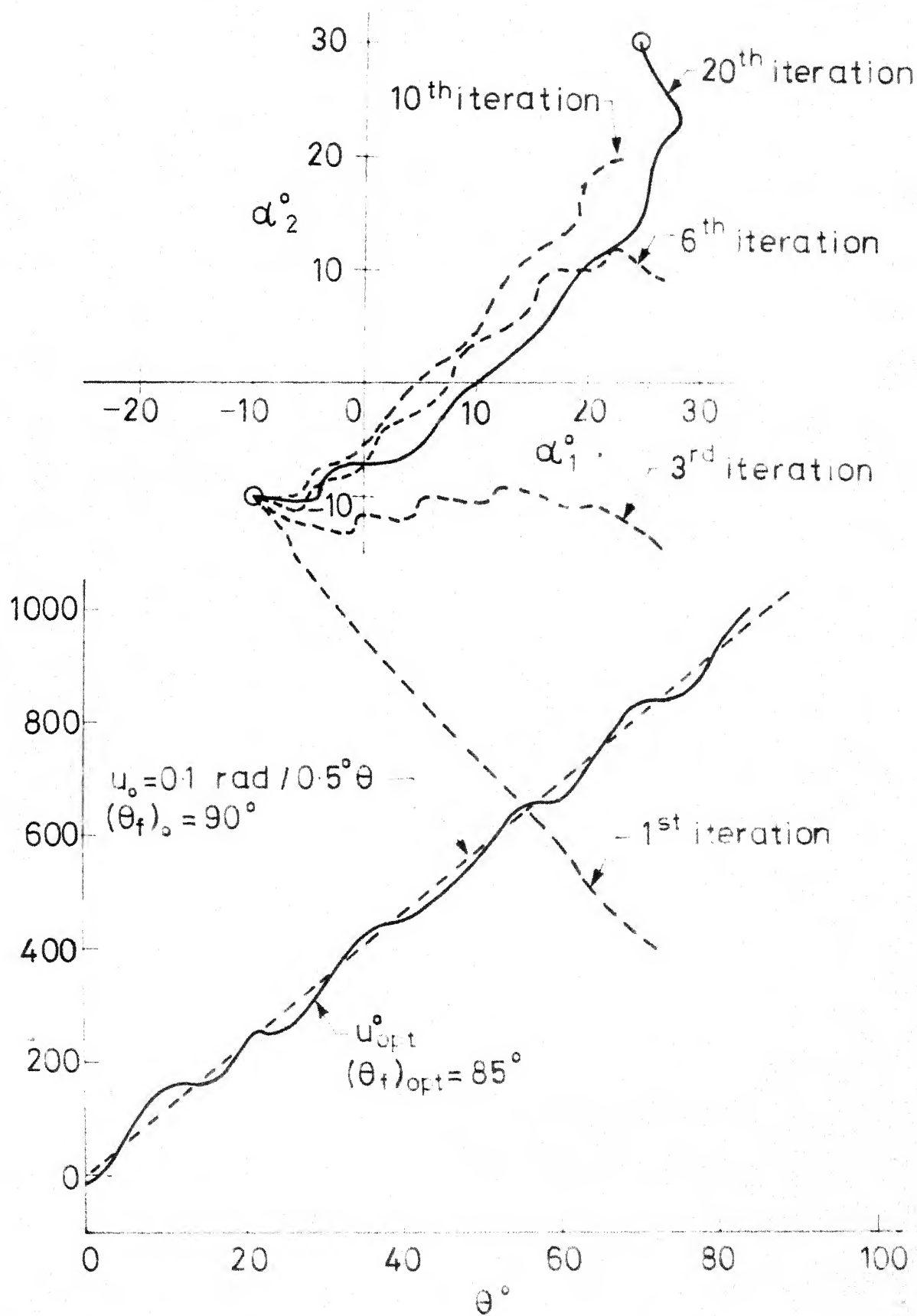


Fig. 6.1 Typical convergence to the optimal solution for the maneuver $\alpha_{10} = -10^\circ$,

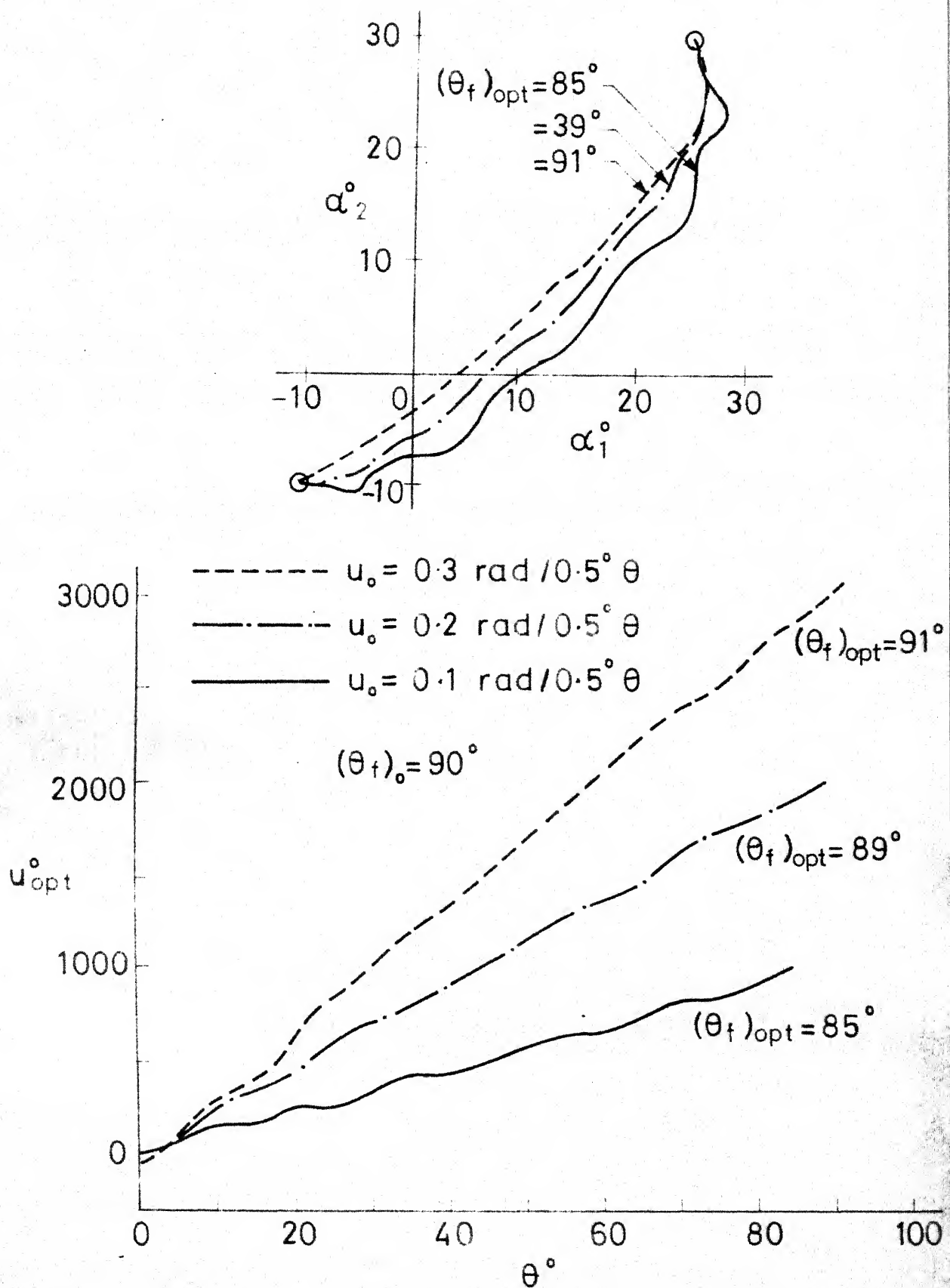


Fig. 6.2 Optimal trajectories and control histories obtained with different ramp type initial guesses for the control

of the initial guesses. Another result with an initial guess of rather different character, $u_0(\theta) = 0$, is shown in Figure 6.3.

The influence of the guess $(\theta_f)_0$ on the solution is indicated in Figure 6.4 for the case of a different maneuver. With the control guess $u_0(\theta)$ held the same, the convergence to optimal solutions with $(\theta_f)_{\text{opt}}$ in the neighbourhood of $(\theta_f)_0$ is observed.

The above results clearly indicate the convergence of the solution to local optima near the initial guesses $u_0(\theta)$ and $(\theta_f)_0$. Also, it appears that the problem is characterized by numerous locally optimal solutions. This may be attributed to the highly nonlinear, transcendental nature of the system equations. Nevertheless, the approach is quite useful as it enables one to determine a control $u(\theta)$ which can accomplish the desired attitude maneuver in inertial space. The transfer times obtained are also reasonably small and remain within a moderate range despite different starting conditions $u_0(\theta)$ and $(\theta_f)_0$.

The open-loop control obtained for a specified maneuver would drive the spacecraft symmetry axis very close to its desired inertial orientation. The satellite attitude, however, would deviate from this condition due to the residual terminal error and the gravitational torques. Attitude stabilization

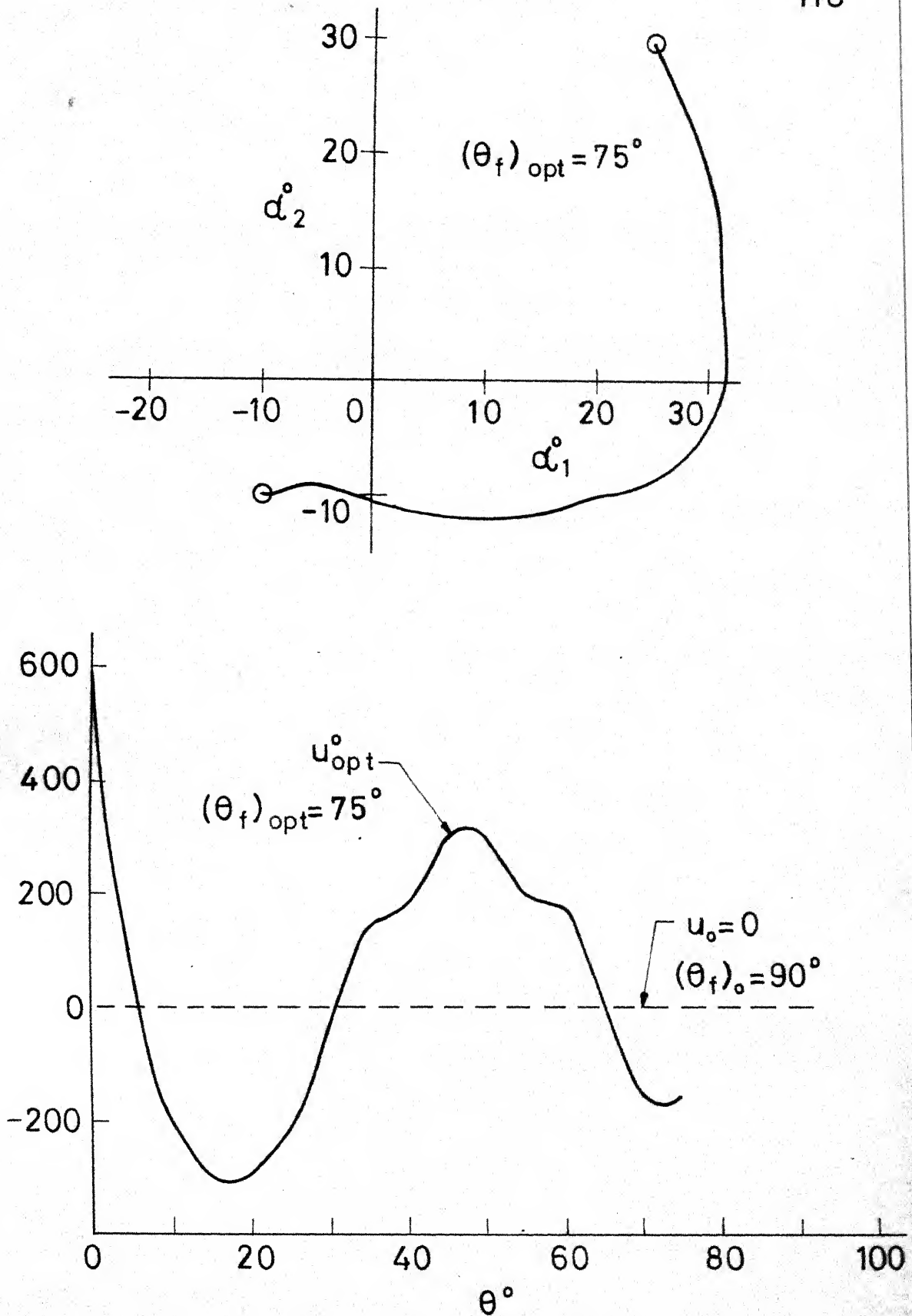


Fig.6.3 Optimal trajectory and control history obtained with the initial guess $u_o(\theta) = 0$

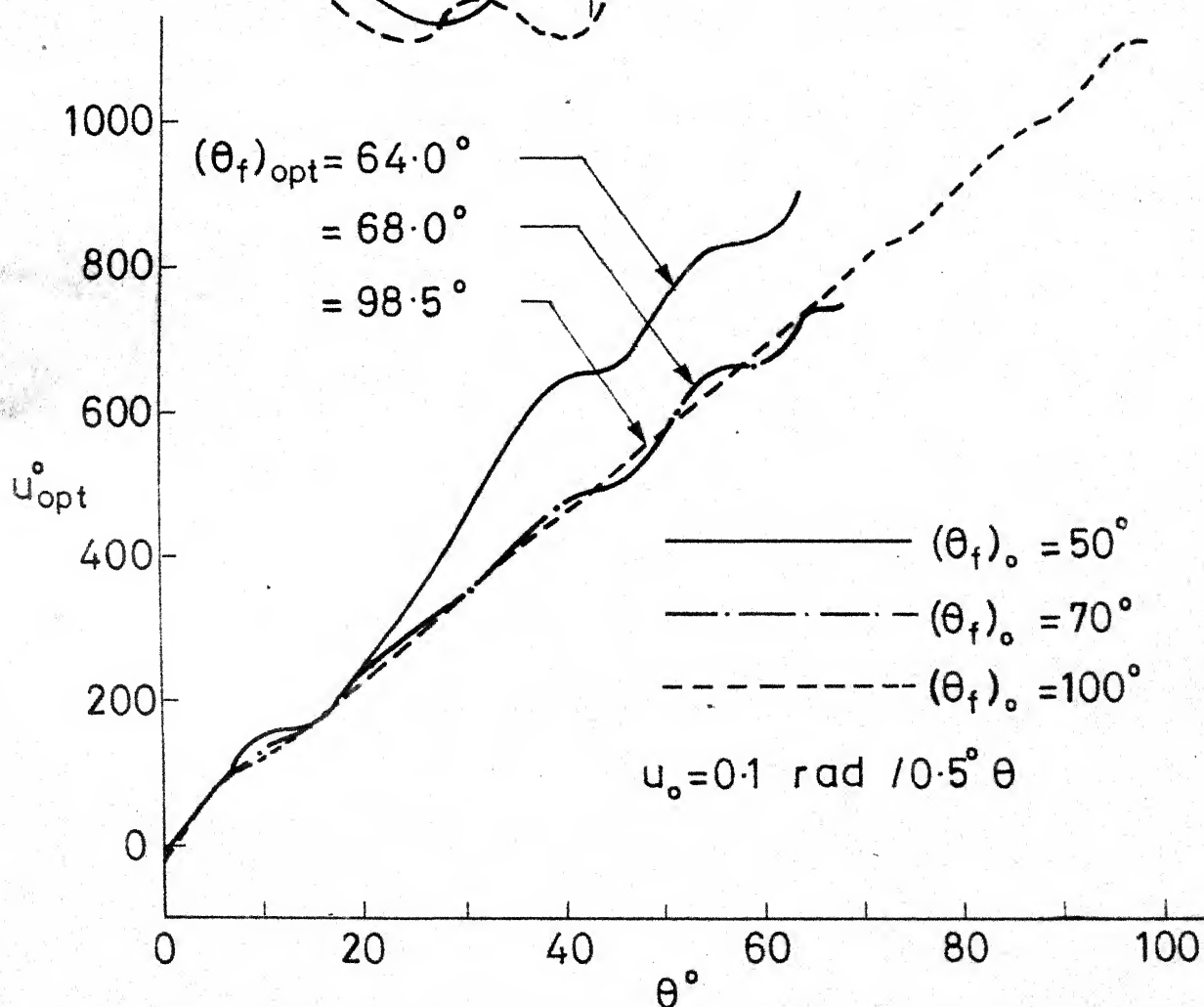
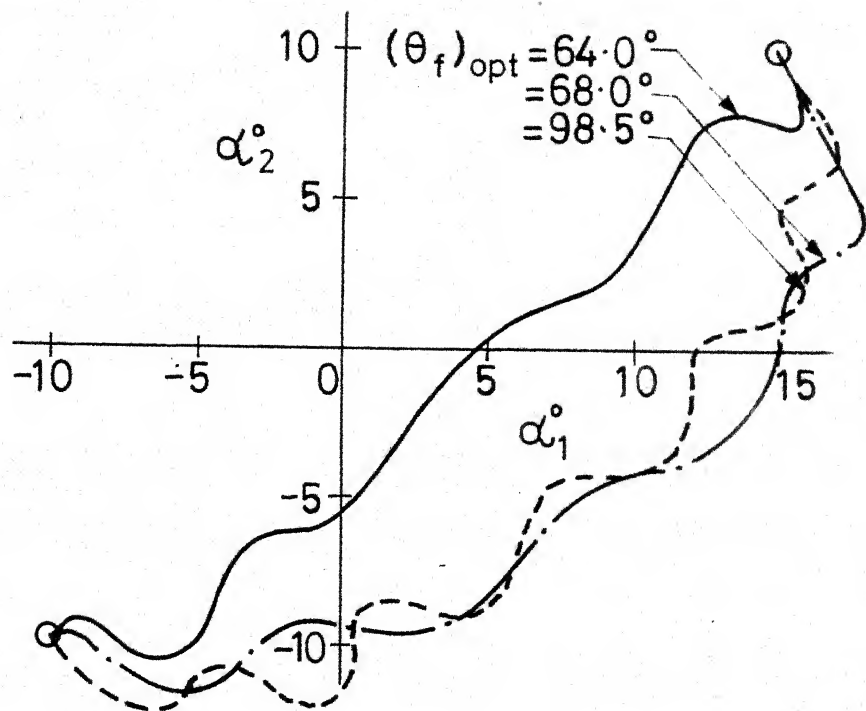


Fig. 6.4 Optimal trajectories and control histories obtained with different initial guesses for the final time

in the desired orientation would then be necessary. This may be achieved by applying the nominal and feedback control strategies developed in Chapter 5. As an example Figure 6.5 shows the attitude transition from $\alpha_{10} = -10^\circ$, $\alpha_{20} = -10^\circ$ to $\alpha_{1f} = 25^\circ$, $\alpha_{2f} = 30^\circ$. The optimal open-loop control was obtained with $u_o(\theta) = 0.2 \text{ rad}/0.5^\circ \theta$ and $(\theta_f)_o = 90^\circ$ (Figure 6.2). A smooth transition from the given initial orientation to the neighbourhood of the desired final pointing is achieved by the open-loop control in 89° of the orbit. The nominal and feedback controls then stabilize the spacecraft along the desired inertially-fixed orientation. The individual control surface rotations during the entire maneuver are :

$$\text{for } 0 \leq \theta < 89^\circ \quad \delta_1(\theta) = u_{\text{opt}}(\theta) \quad (6.39a)$$

$$\delta_2(\theta) = -u_{\text{opt}}(\theta) \quad (6.39b)$$

$$\text{for } \theta \geq 89^\circ \quad \delta_1(\theta) = \delta_{10}(\theta) + u_{\text{fb}}(\theta) \quad (6.40a)$$

$$\delta_2(\theta) = \delta_{20}(\theta) - u_{\text{fb}}(\theta) \quad (6.40b)$$

where $u_{\text{fb}}(\theta)$ here denotes the feedback control $u(\theta)$ of Chapter 5.

The case of yet another arbitrary maneuver ($\alpha_{10} = -10^\circ$, $\alpha_{20} = -10^\circ$ to $\alpha_{1f} = 15^\circ$, $\alpha_{2f} = 10^\circ$) involving the use of optimal large-angle transfer and inertially-fixed stabilization

$$\begin{array}{llll} \alpha_{10} = -10^\circ & \alpha'_{10} = 0 & \alpha_{20} = -10^\circ & \alpha'_{20} = 0 \\ \alpha_{1f} = 25^\circ & \alpha'_{1f} = 0 & \alpha_{2f} = 30^\circ & \alpha'_{2f} = 0 \end{array}$$

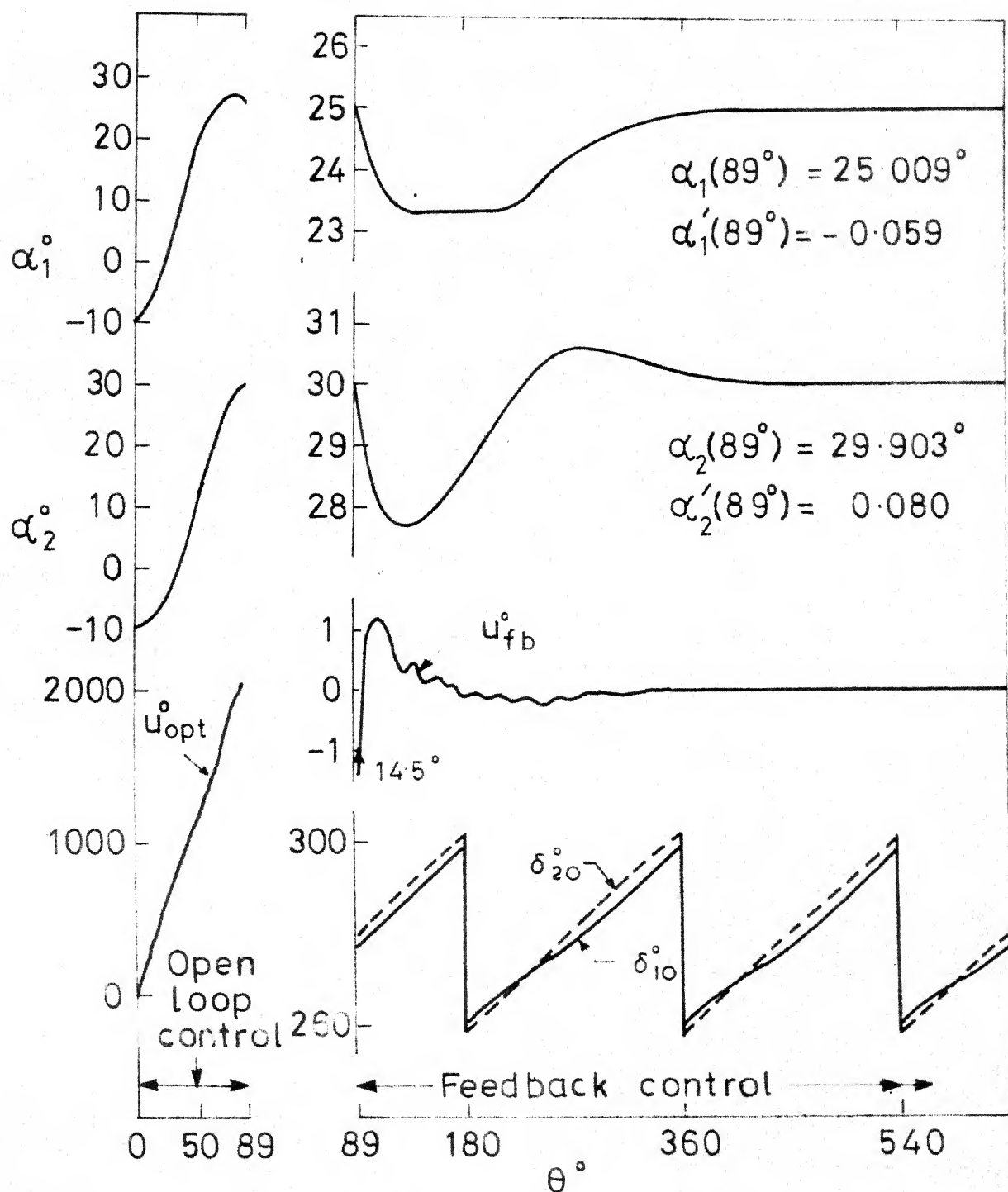


Fig. 6.5 System response and control required for large-angle maneuver followed by inertially-fixed attitude stabilization

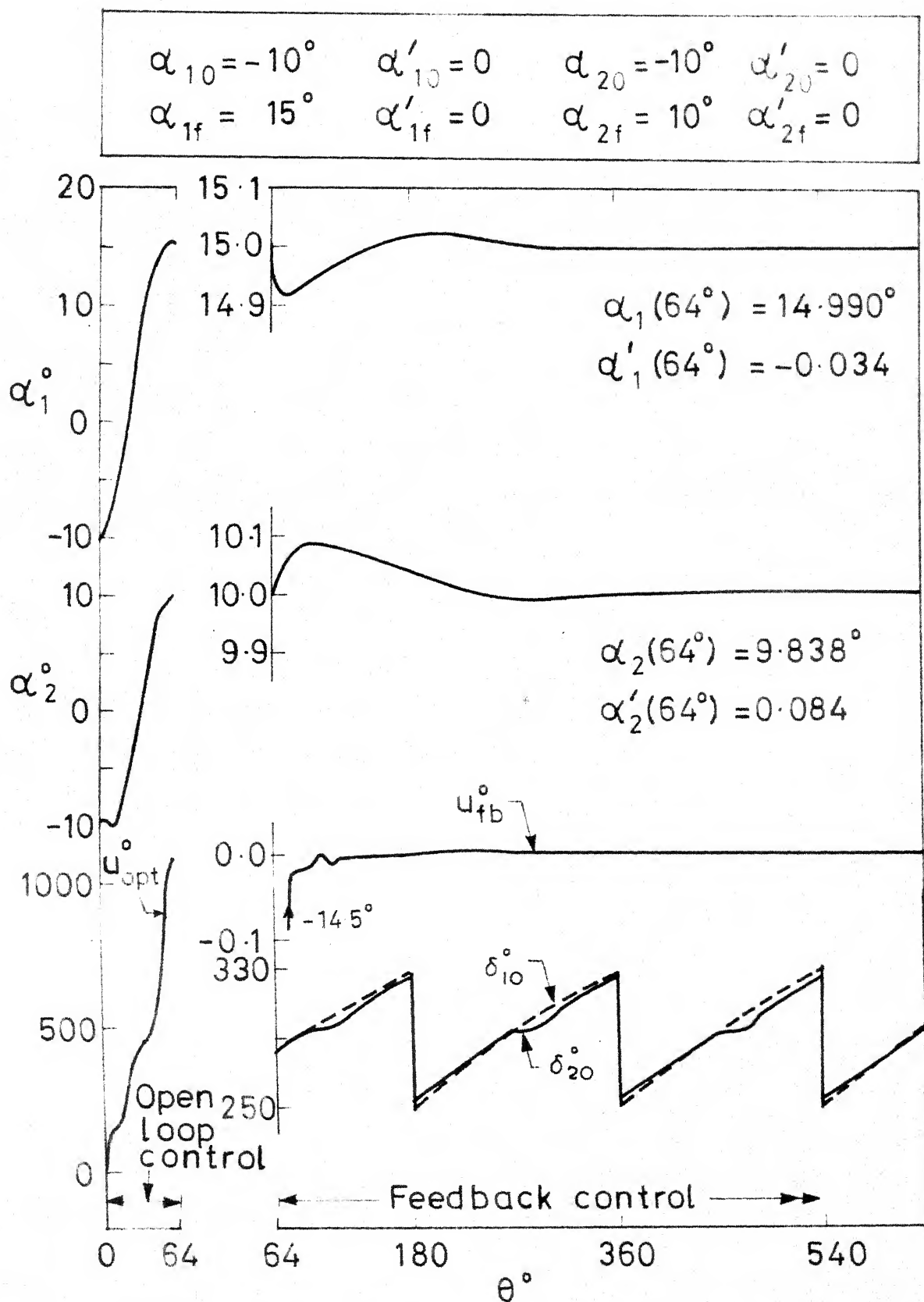


Fig. 6.6 System response and control required for large-angle maneuver followed by inertially-fixed attitude stabilization

strategies is indicated in Figure 6.6. The $u_{\text{opt}}(\theta)$ was computed with $u_o(\theta) = 0.1 \text{ rad}/0.5^\circ \theta$ and $(\theta_f)_o = 50^\circ$ (Figure 6.4).

6.5 Concluding Remarks

- (i) The feasibility of employing a simple two-surface solar controller for achieving arbitrary large-angle attitude maneuvers of the symmetry axis of a nonspinning spacecraft has been established.
- (ii) An open-loop control strategy for the differential control surface rotation is obtained employing the gradient procedure. The control law minimizes the time required for a specified attitude transition.
- (iii) The numerical procedure was found to converge to different solutions depending on the initial guesses for the control and the terminal time. With a moderately sized controller, the optimal solutions lead to control times of a fraction of an orbit for any desired maneuver.
- (iv) After completion of the large-angle maneuver the same controller may be used, in the nominal and feedback control mode, to stabilize the spacecraft along the final inertially-fixed orientation.
- (v) The proposed controller adds versatility to the system as it makes it possible to achieve different inertially-fixed attitudes.

7. CLOSING COMMENTS

7.1 Summary of the Conclusions

The conclusions based on the preceding investigation may be summarized as follows :

- (i) The feasibility of employing a two-surface solar controller, representing the minimum hardware configuration, for earth-pointing as well as inertially-fixed attitude stabilization has been established.
- (ii) Feedback control laws directly governing the control surface rotations are synthesized. The resulting control systems promise asymptotically stable operation throughout the year.
- (iii) The implementation of the controller for pitch control in both earth-pointing and inertially-fixed modes of stabilization is particularly simple. For multidimensional attitude control, implementation of time-varying gains is involved. Considerable computational simplifications may be achieved through the use of suboptimal control policies.
- (iv) The control systems, using moderately sized controllers, are found to be capable of stabilizing the spacecraft even along gravitationally unstable orientations. Time constants of the order of a few orbital degrees are possible and may be reduced further through the use of increased gains.

- (v) The effectiveness of the controller in maintaining inertially-fixed attitudes for a nonspinning spacecraft in the gravity-gradient field suggests new applications for the concept of solar pressure control.
- (vi) An open-loop control law for achieving arbitrary large-angle attitude maneuvers is established. This capability makes the system more versatile and opens the possibility of designing satellites for diverse missions.
- (vii) Due to the loss of solar control during encounters with the earth's shadow, small attitude deviations are observed. On emergence from the shadow, however, the controller is able to reorient the satellite precisely along the desired orientation.
- (viii) An analysis accounting for the possibility of one of the control surfaces being shadowed by the spacecraft would be highly dependent on the relative shapes and sizes of the satellite and the controller. Preliminary results suggest the effect to be of little consequence for earth-pointing applications and during inertial stabilization along orientations that are not too close to the sun-line.
- (ix) Attitude control systems have been presented for spacecraft in circular orbits. Through minor modifications of the control policies, solar controllers applicable to satellites in elliptic orbits may be developed.

- (x) The concept of solar pressure control does not involve any mass expulsion schemes and/or active elements requiring large power consumption. The semipassive character of the control systems promises increased lifetimes for the spacecraft.

7.2 Recommendations for Future Work

On the basis of the present study, the following recommendations are made for future work :

- (i) A systematic study may be carried out to determine the best orientation of the rotation axis of the two-surface controller relative to the spacecraft body. The analysis would likely involve optimizing the control torque components averaged over the year as a function of the orbital inclination.
- (ii) The inertial orientation problem may be extended to three-axis control through the use of three rotatable control surfaces.
- (iii) The concept of nominal control may be applied to counter the continuous disturbance due to radiation pressure arising for spacecraft with a nonzero offset between the centers of mass and pressure.
- (iv) The possibility of modifying the approach for solar control of spacecraft having a limited attitude determination capabilities could be explored.

- (v) Utilization of solar radiation pressure for attitude control has so far been limited to rigid spacecraft. On the other hand, increasingly flexible configurations are being contemplated to meet the challenges of the future. Feasibility of the concept of solar control for flexible spacecraft represents an exciting area for future investigations.
- (vi) The development of solar controllers for achieving controlled variations of the orbital elements and orbital transfers represents another field with important challenging problems.

12. Harrington, J.C., "The Dynamics of Spinning-Solar Pressure - Stabilized Satellite with Precession Damping," CSR-TR-66-6, June 1966, MIT Centre for Space Research.
13. Falcovitz, J., "Attitude Control of a Spinning Sun-Orbiting Spacecraft by Means of Grated Solar Sail," CSR-TR-66-17, December 1966, MIT Centre for Space Research.
14. Crocker, M.C. II, "Attitude Control of a Sun-Pointing Spinning Spacecraft by Means of Solar Radiation Pressure," Journal of Spacecraft and Rockets, Vol. 7, No.3, March 1970, pp.357-359.
15. Pande, K.C., "Attitude Control of Spinning Spacecraft by Radiation Pressure," Journal of Spacecraft and Rockets, Vol. 13, No.12, December 1976, pp.765-768.
16. Mallach, E.G., "Solar Pressure Damping of the Librations of a Gravity Oriented Satellite," AIAA Student Journal, Vol. 4, No.4 December 1966, pp.143-147.
17. Modi, V.J. and Flanagan, R.C., "Librational Damping of a Gravity Oriented System using Solar Radiation Pressure," The Aeronautical Journal of the Royal Aeronautical Society, Vol. 75, No. 728, August 1971, pp.560-564.
18. Modi, V.J. and Tschann, C., "On the Attitude and Librational Control of a Satellite using Solar Radiation Pressure," Proceedings of the XXI International Astronautical Congress, Edited by L.G. Napolitano, North-Holland Publishing Co., Amsterdam, The Netherlands, 1971, pp.84-100.
9. Modi, V.J. and Tschann, C., "The Solar Radiation Damping of a Gravity Oriented Satellite using WKB Method," Israel Journal of Technology, Vol. 11, 1973, pp.53-61.
19. Modi, V.J. and Kumar, K., "Coupled Librational Dynamics and Attitude Control of Satellites in Presence of Solar Radiation Pressure," Astronautical Research 1971, Proceedings of the XII Congress of the International Astronautical Federation, Editor-in-chief: L.G. Napolitano, D. Reidel Publishing Company, Dordrecht-Holland, 1973, pp.37-52.
- Modi, V.J. and Kumar, K., "Attitude Control of Satellites using the Solar Radiation Pressure," Journal of Spacecraft and Rockets, Vol. 9, No.9, September 1972, pp.711-713.

22. Modi, V.J. and Pande, K.C., "Solar Pressure Control of a Dual-Spin Satellite," Journal of Spacecraft and Rockets, Vol. 10, No.6, June 1973, pp.355-361.
23. Modi, V.J. and Pande, K.C., "A Bang-Bang Solar Pressure Attitude Control System," Journal of Astronautical Sciences, Vol. XXII, No.1, July-September 1974, pp.1-20.
24. Pande, K.C., Davies, M.S., and Modi, V.J., "Time Optimal Pitch Control of Satellites using Solar Radiation Pressure," Journal of Spacecraft and Rockets, Vol. 11, No.8, August 1974, pp.601-603.
25. Modi, V.J. and Pande, K.C., "Magnetic-Solar Hybrid Attitude Control of Satellites in Near-Equatorial Orbits," Journal of Spacecraft and Rockets, Vol. 11, No.12, December 1974, pp.845-851.
26. Modi, V.J. and Pande, K.C., "Aerodynamic-Solar Hybrid Attitude Control of Near-Earth Satellites," Journal of Astronautical Sciences, Vol. XXII, No.1, July-September 1974, pp.36-54.
27. Scull, J.R., "Guidance and Control of the Mariner Planetary Spacecraft," Technical Report 32-924, Jet Propulsion Laboratory, Pasadena, Calif.; also published in Peaceful uses of Automation in Outerspace, pp.97-108, Plenum Press, 1966.
28. Scull, J.R., "Mariner IV - Revisited - or the Tale of the Ancient Mariner," XX Int. Astronautical Cong., Argentina, 1969, pp.747-758.
29. Renner, U., "Attitude Control by Solar Sailing - A Promising Experiment with OTS-2," European Space Agency, Vol. 3, No.1, 1979, pp.35-40.
30. Plummer, H.C., An Introductory Treatise on Dynamical Astronomy, Dover Publications, New York, 1960.
31. Cesari, L., Asymptotic Behaviour and Stability Problems in Ordinary Differential Equations, Academic Press, New York, 1963, pp.55-59.
32. Ehricke, K.A., Principles of Guided Missile Design, Princeton, N.J., D. Van Nostrand, 1960, pp.241-256.
33. Lapidus, L. and Luus, R., Optimal Control of Engineering Processes. Blaisdell Publishing Company, Massachusetts, 1967, pp.346-353.

34. Kirk, D.E., Optimal Control Theory: an Introduction,
Prentice-Hall Inc., Englewood Cliffs, New Jersey, 1970,
pp.209-218.
35. Kane, T.R., "Attitude Stability of Earth-Pointing
Satellites," AIAA Journal, Vol. 3, No.4, April 1965,
pp.726-731.
36. Kelley, H.J., "Method of Gradients," Optimization
Techniques with Applications to Aerospace Systems, Ed:
G. Leitmann, Academic Press Inc., New York, 1962.
37. Bryson, A.E. and Ho, Y.C., Applied Optimal Control,
Blaisdell Publishing Company, Massachusetts, 1969,
pp.225-228.

APPENDIX A

The components of the earth-sun unit vector \bar{e} in the satellite principal axis system are given by :

$$e_x = \sin \phi [- \sin i \cos \gamma \cos \beta + \cos i (\sin \theta \sin \gamma \cos \beta - \cos \theta \sin \beta)] \\ + \cos \phi [\sin \theta \sin \beta + \cos \theta \sin \gamma \cos \beta] \quad (A-1)$$

$$e_y = \sin \phi [\sin i (\sin \gamma \cos \lambda - \cos \gamma \sin \beta \sin \lambda) \\ + \cos i \{ \sin \theta (\cos \gamma \cos \lambda + \sin \gamma \sin \beta \sin \lambda) \\ + \cos \theta (\cos \beta \sin \lambda) \}] \\ + \cos \phi [- \sin \theta (\cos \beta \sin \lambda) \\ + \cos \theta (\cos \gamma \cos \lambda + \sin \gamma \sin \beta \sin \lambda)] \quad (A-2)$$

$$e_z = \sin \phi [- \sin i (\sin \gamma \sin \lambda + \cos \gamma \sin \beta \cos \lambda) \\ + \cos i \{ \sin \theta (\sin \gamma \sin \beta \cos \lambda - \cos \gamma \sin \lambda) \\ + \cos \theta (\cos \beta \cos \lambda) \}] \\ + \cos \phi [- \sin \theta (\cos \beta \cos \lambda) \\ + \cos \theta (\sin \gamma \sin \beta \cos \lambda - \cos \gamma \sin \lambda)] \quad (A-3)$$

The functions f_γ , f_β , f_λ appearing in Equations (3.11) are given by :

$$\begin{aligned}
 f_\gamma = & [(I_x - I_y \sin^2 \lambda - I_z \cos^2 \lambda) \cos \gamma \cos 2\beta \\
 & - (I_y \cos^2 \lambda + I_z \sin^2 \lambda) \cos \gamma \\
 & - (I_y - I_z) \sin \gamma \sin \beta \sin 2\lambda] \beta' \\
 & + [(1/2) (I_y - I_z) (2 \sin \gamma \cos \beta \cos 2\lambda \\
 & - \cos \gamma \sin 2\beta \sin 2\lambda) - I_x \sin \gamma \cos \beta] \lambda' \\
 & + (1/2) (I_y - I_z) \beta'^2 \sin \beta \sin 2\lambda \\
 & - (I_x - I_y \sin^2 \lambda - I_z \cos^2 \lambda) \gamma' \beta' \sin 2\beta \\
 & + [I_x - (I_y - I_z) \cos 2\lambda] \beta' \lambda' \cos \beta \\
 & - (I_y - I_z) \gamma' \lambda' \cos^2 \beta \sin 2\lambda \\
 & - (1/2) [I_x \sin 2\gamma \cos^2 \beta + \{(I_y \sin^2 \lambda + I_z \cos^2 \lambda) \sin^2 \beta \\
 & - (I_y \cos^2 \lambda + I_z \sin^2 \lambda)\} \sin 2\gamma \\
 & + (I_y - I_z) \cos 2\gamma \sin \beta \sin 2\lambda] \\
 & - (3/4) [(2I_x - I_y - I_z) \sin 2\gamma \cos^2 \beta \\
 & - (I_y - I_z) (\sin 2\gamma \cos 2\lambda + \sin 2\gamma \sin^2 \beta \cos 2\lambda \\
 & - \cos 2\gamma \sin \beta \sin 2\lambda)] \quad (A-4)
 \end{aligned}$$

$$\begin{aligned}
f_{\beta} = & -I_x(\gamma' \cos 2\beta + \lambda' \sin \beta) \cos \gamma \\
& + (I_y - I_z)(\gamma' \sin \beta - \lambda') \sin \gamma \sin 2\lambda \\
& + [(I_y \sin^2 \lambda + I_z \cos^2 \lambda) \cos 2\beta \\
& + (I_y \cos^2 \lambda + I_z \sin^2 \lambda)] \gamma' \cos \gamma \\
& - (I_y - I_z) \lambda' \cos \gamma \sin \beta \cos 2\lambda \\
& + (1/2)(I_x - I_y \sin^2 \lambda - I_z \cos^2 \lambda)(\gamma'^2 - \cos^2 \gamma \\
& + 3 \sin^2 \gamma) \sin 2\beta \\
& + (I_y - I_z)(\beta' \lambda' - \sin 2\gamma \cos \beta) \sin 2\lambda \\
& - [I_x + (I_y - I_z) \cos 2\lambda] \gamma' \lambda' \cos \beta
\end{aligned} \tag{A-5}$$

$$\begin{aligned}
f_{\lambda} = & I_x[\gamma' (\sin \gamma + \beta') \cos \beta + \beta' \cos \gamma \sin \beta] \\
& - (1/2)(I_y - I_z)[(\beta' - \sin \gamma)^2 \\
& - (\gamma' \cos \beta + \cos \gamma \sin \beta)^2 \\
& + 3(\sin^2 \gamma \sin^2 \beta - \cos^2 \gamma)] \sin 2\lambda \\
& - (3/2)(I_y - I_z) \sin 2\gamma \sin \beta \cos 2\lambda
\end{aligned} \tag{A-6}$$

APPENDIX B

The quantities a_i , b_i ($i = 1$ to 5) appearing in Equations (5.15) are given by :

$$a_1 = (1 - I)k / \cos \alpha_{2e} \quad (B-1)$$

$$a_2 = -3(1 - I) l_1 / \cos \alpha_{2e} \\ - (2C / \cos \alpha_{2e}) [|q_1| r_1 \sin \delta_{10} - |q_2| r_2 \sin \delta_{20}] \quad (B-2)$$

$$a_3 = -3(1 - I) l_2 / \cos \alpha_{2e} \\ - (2C / \cos \alpha_{2e}) [|q_1| s_1 \sin \delta_{10} - |q_2| s_2 \sin \delta_{20}] \quad (B-3)$$

$$a_4 = -(2C / \cos \alpha_{2e}) |q_1| [t_1 \sin \delta_{10} + (q_1/2) \cos \delta_{10}] \quad (B-4)$$

$$a_5 = (2C / \cos \alpha_{2e}) |q_2| [t_2 \sin \delta_{20} + (q_2/2) \cos \delta_{20}] \quad (B-5)$$

$$b_1 = -(1 - I)k \cos \alpha_{2e} \quad (B-6)$$

$$b_2 = 3(1 - I)m_1 \\ - 2C [|q_1| r_1 \cos \delta_{10} - |q_2| r_2 \cos \delta_{20}] \quad (B-7)$$

$$b_3 = 3(1 - I)m_2 \\ - 2C [|q_1| s_1 \cos \delta_{10} - |q_2| s_2 \cos \delta_{20}] \quad (B-8)$$

$$b_4 = -2C |q_1| [t_1 \cos \delta_{10} - (q_1/2) \sin \delta_{10}] \quad (B-9)$$

$$b_5 = 2C |q_2| [t_2 \cos \delta_{20} - (q_2/2) \sin \delta_{20}] \quad (B-10)$$

where

$$l_1 = (\cos 2\alpha_{1e} \cos \alpha_{2e}) \cos^2 \theta + (1/2)(\sin \alpha_{1e} \sin \alpha_{2e}) \sin 2\theta \quad (B-11)$$

$$l_2 = -(1/2)[(\sin 2\alpha_{1e} \sin \alpha_{2e}) \cos^2 \theta + (\cos \alpha_{1e} \cos \alpha_{2e}) \sin 2\theta] \quad (B-12)$$

$$m_1 = (1/2) [(\sin 2\alpha_{1e} \sin 2\alpha_{2e}) \cos^2 \theta + (\cos \alpha_{1e} \cos 2\alpha_{2e}) \sin 2\theta] \quad (B-13)$$

$$m_2 = (\sin^2 \alpha_{1e} \cos 2\alpha_{2e}) \cos^2 \theta - (\cos 2\alpha_{2e}) \sin^2 \theta - (\sin \alpha_{1e} \sin 2\alpha_{2e}) \sin 2\theta \quad (B-14)$$

$$q_j = -(\sin \phi \sin i \sin \alpha_{1e} + \cos \phi \cos \alpha_{1e}) \sin \delta_{j0} + (-\sin \phi \sin i \cos \alpha_{1e} \sin \alpha_{2e} + \cos \phi \sin \alpha_{1e} \sin \alpha_{2e} + \sin \phi \cos i \cos \alpha_{2e}) \cos \delta_{j0} \quad (j=1,2) \quad (B-15)$$

$$r_j = -(\sin \phi \sin i \cos \alpha_{1e} - \cos \phi \sin \alpha_{1e}) \sin \delta_{j0} + (\sin \phi \sin i \sin \alpha_{1e} \sin \alpha_{2e} + \cos \phi \cos \alpha_{1e} \sin \alpha_{2e}) \cos \delta_{j0} \quad (j=1,2) \quad (B-16)$$

$$s_j = -(\sin \phi \sin i \cos \alpha_{1e} \cos \alpha_{2e} - \cos \phi \sin \alpha_{1e} \cos \alpha_{2e} + \sin \phi \cos i \sin \alpha_{2e}) \cos \delta_{j0} \quad (j=1,2) \quad (B-17)$$

$$t_j = -(\sin \phi \sin i \sin \alpha_{1e} + \cos \phi \cos \alpha_{1e}) \cos \delta_{j0} - (-\sin \phi \sin i \cos \alpha_{1e} \sin \alpha_{2e} + \cos \phi \sin \alpha_{1e} \sin \alpha_{2e} + \sin \phi \cos i \cos \alpha_{2e}) \sin \delta_{j0} \quad (j=1,2) \quad (B-18)$$

APPENDIX C

Figure C-1 shows the geometry of the earth's shadow which is assumed to be an infinite half-cylinder. The angle between the earth-sun line and the local vertical is given by

$$\cos \Psi = (1/R) \bar{R} \cdot \bar{e} \quad (C-1)$$

The vectors \bar{R} and \bar{e} may be written in terms of their components along X,Y,Z axes as

$$\bar{R} = (R \cos \theta) \bar{J} + (R \sin \theta) \bar{K} \quad (C-2)$$

$$\bar{e} = (-\sin \phi \sin i) \bar{I} + (\cos \phi) \bar{J} + (\sin \phi \cos i) \bar{K} \quad (C-3)$$

Substitution of Equations (C-2) and (C-3) in Equation (C-1) yields

$$\cos \Psi = \cos \phi \cos \theta + \sin \phi \cos i \sin \theta \quad (C-4)$$

The distance of the satellite from the earth-sun line is given by

$$R_s = R | (1 - \cos^2 \Psi)^{\frac{1}{2}} | \quad (C-5)$$

The condition for the satellite to be in the earth's shadow is then readily expressed as

$$\cos \Psi < 0 \quad \text{and} \quad R_E - R_s > 0 \quad (C-6)$$

It may be easily shown that the satellite is eclipsed by the earth for the longest period when $\phi = 0$ or 180° . The longest shadow passage for the case of a geostationary orbit occurs for about 18° of the orbit.

BIOGRAPHICAL INFORMATION

NAME : RAPUR VENKATACHALAM

PLACE AND DATE OF BIRTH : VISAKHAPATNAM (A.P.), India,
April 28, 1953

EDUCATION :

B.E. (Mech. Engg.), 1974, Andhra University Engineering College,
Waltair, India.

M.Tech. (Mech. Engg.), 1976, Indian Institute of Technology,
Kanpur, India.

PUBLICATIONS :

1. Venkatachalam, R., "Optimal Aerodynamic Attitude Control of Spinning Satellites," 1977, M.Tech. Thesis, Department of Mechanical Engineering, IIT Kanpur; also as "On Optimal Aerodynamic Attitude Control of Spacecraft," Acta Astronautica, Vol. 6, 1979, pp. 1351-1359.
2. Pande, K.C. and Venkatachalam, R., "Semipassive Pitch Attitude Control of Satellites by Solar Radiation Pressure," IEEE Transactions on Aerospace and Electronic Systems, Vol. AES-15, No.2, March 1979, pp.194-198.
3. Pande, K.C. and Venkatachalam, R., "Inertially-Fixed Pitch Stabilization of Satellites by Solar Radiation Pressure," Acta Astronautica, in press.
4. Pande, K.C. and Venkatachalam, R., "Three-Axis Solar Pressure Attitude Control of Unsymmetrical Earth-Pointing Spacecraft," presented for publication.
5. Pande, K.C. and Venkatachalam, R., "Solar Pressure Stabilization of Nonspinning Axisymmetric Spacecraft in Arbitrary Inertially-Fixed Orientations," presented for publication.
6. Venkatachalam, R. and Pande, K.C., "Optimal Large-Angle Attitude Maneuvers of Nonspinning Axisymmetric Spacecraft by Solar Radiation Pressure," presented for publication.